Mooring System Design for Wind Farm In Very Deep Water

European Wind Energy Master Thesis

By

MEGAN N. CHAN CHOW

Department of Mechanical, Maritime and Materials Engineering
DELFT UNIVERSITY OF TECHNOLOGY

Department of Marine Technology – Group of Marine Structures
NORWEGIAN UNIVERSITY OF SCIENCE AND TECHNOLOGY

For obtaining a Master of Science in Technology-Wind Energy at the Norwegian University of Science and Technology, and a Master of Science in Offshore Engineering and Dredging at Delft University of Technology.

JANUARY 2, 2019

Supervisors:
Prof. Erin Bachynski (NTNU)
Prof. Kjell Larsen (NTNU/Equinor)
Prof. Peter Wellens (TU Delft)

Preface

This master thesis is submitted as part of the requirements for obtaining an MSc. in Offshore Engineering at the Technical University of Delft (TU Delft), and an MSc. in Technology – Wind Energy at the Norwegian University of Science and Technology (NTNU). This thesis is part of EWEM, the European Wind Energy Master, Offshore Engineering Track. It is a collaboration between the Faculty of Mechanical, Maritime and Materials Engineering at TU Delft and the Department of Marine Technology – Group of Marine Structures at NTNU in Trondheim, Norway. Professor E. Bachynski was the supervisor from NTNU and was supported by Professor K. Larsen. Professor P. Wellens was the supervisor from TU Delft.

I would like to thank my professors, family, and friends for their support throughout the years and for their support during this thesis work. I would especially like to thank my supervisors Drs Bachynski, Wellens, and Larsen for their unstinting support and patience and for always answering my questions no matter how trivial or how late at night. I would also like to thank the coordinators of the EWEM programme for facilitating this distinctive programme and allowing me to partake in such a unique experience.

Abstract

Offshore floating wind turbines are one of the newest technologies in the renewable markets today. The world's first floating wind farm, the Hywind Scotland Pilot Park, was commissioned in October 2017 and has been competitive with fixed bottom offshore wind turbines. There is a global push to make more renewable energy available, but less desire to have wind turbines cluttering the coastline. Floating wind turbines enable the developer to take advantage of unused offshore space, at depths where traditional fixed bottom structures are impractical and at locations that do not spoil the vista of the coastline.

This thesis project aims to develop a working mooring system at depth of 600 m in the Norwegian North Sea, and then investigates the possibility of shared anchors in a wind park with this mooring system. The DTU 10MW reference wind turbine atop a classic spar substructure is used. First, the mooring system at 320 m is tested under decay and environmental loads. Then a chain-polyester-chain mooring line with a bridle was developed for 600 m so that the surge offset is limited to < 60 m for 3 load cases. A simplified model of the wind turbine was then developed for these three load cases. The simplified model was then used to create a wind farm arrangement with 5-6 turbines each. Each wind farm varied in layout and in the number of shared anchors.

It was found that while the mooring system designed passes the surge offset and natural frequency requirements, and the normal ULS safety class, it failed the high safety class in some cases. For shared anchors with multidirectional loads, the resultant force on the anchor is significantly less as long as the lines are distributed equally around the anchor point. The resultant force does not increase with two lines 120° apart. The footprint of a single turbine with the designed mooring is larger than the footprint of the entire Hywind Scotland Farm, so suggestions are made for improvement and further work.

NOMENCLATURE

Symbols and Units - Latin

A_w	Area of the the waterplane	[m]
f_n	Natural frequency	[Hz]
L_U	Integral length scale	[s]
S_c	Characteristic capacity of mooring line	[s]
T_d	Design tension in a mooring line	[m/s]
T_H	Horizontal tension component	[kN]
T_n	Natural period	[kN]
T_p	Peak period	[kN]
T_z	Vertical tension component	[kN]
$T_{c,dyn}$	Characteristic dynamic tension	[kN]
$T_{c,mean}$	Characteristic mean tension	[m/s]
U_z	Mean wind speed at specified height z	[m]
U_{10}	1 hour mean mean wind speed taken at 10 m height above MWL	[kN]
V_c	Current velocity	[m/s]
z	Height above MWL	[m]

Symbols and Units - Greek

η_3	Surge displacement	[m]
γ_{dyn}	Load factor for dynamic tension	[−]
γ_{mean}	Load factor for mean tension	[−]

σ_U	Variance of wind speed	$[m^2/s^2]$

Abbreviations

BEM	Blade Element Momentum
CAPEX	Capital Expenditure
CFD	Computational Fluid Dynamics
DEA	Drag Embedded Anchor
DNV	Det Norske Veritas
DoF	Degree of Freedom
DP	Dynamic Postioning
DTU	Danmarks Tekniske Universitet
EU	European Union
FOWT	Floating Offshore Wind Turbine
GBS	Gravity Based Structure
GoM	Gulf of Mexico
IEC	International Electrotechnical Commission
LC	Load Case
LCA	Life Cycle Assessment
LCOE	Levelised Cost of Energy
LF	Low Frequency
MBR	Minimum Bending Radius
MBS	Minimum Breaking Strength
MWL	Mean Water Level
NPD	Norwegian Petroleum Directorate
NREL	National Renewable Energy Laboratory
O&G	Oil and Gas

OPEX	Operating Expenditure
OS	Operating Standard
OWT	Offshore Wind Turbine
RNA	Rotor Nacelle Assembly
RP	Recommended Practice
RWT	Reference Wind Turbine
TLP	Tension Leg Platform
TSR	Tip Speed Ratio
ULS	Ultimate Limit State
WD	Water Depth
WF	Wave Frequency

TABLE OF CONTENTS

List of Tables

List of Figures

CHAPTER 1

INTRODUCTION

1.1 Background

There is a growing concern worldwide, and especially in Europe, to reduce CO_2 emissions and eliminate the need for fossil fuels. European countries are aiming for completely renewable energy to reduce dependence on foreign energy sources and wind energy is becoming increasingly competitive. Annual wind power installations in the EU have steadily increased within the past 16 years from 2.3 GW in 2000 to 12.5 GW in 2016 [38]. With a net installed capacity of 169 GW, wind energy has overtaken coal as the second largest form of power generation capacity in Europe. The offshore wind industry is increasing rapidly and 3148 MW of new gross capacity was connected to the grid in 2017. Figure 1.1 shows the rapid increase of offshore wind capacity over the years.

The demand for energy is increasing in a modernised world, along with the desire for cleaner, cheaper, and more efficient energy. This means that wind turbines and wind farms are becoming bigger, more powerful, and more numerous. The majority of wind turbines are located onshore, however this limits their size and number. As such, there is a move to place wind farms offshore where there is greater leniency regarding the noise and visual pollution of wind turbines, as well as stronger and more consistent winds with less turbulence. Currently, the majority of offshore wind turbines are located in shallow water (< 40 m) where fixed bottom monopile substructures are dominant. Fixed bottom wind offshore wind turbines have a track record of over 25 years and are a proven technology. However, shallower waters tend to be further inshore near busy ports, waterways, and beaches. Figure 1.2 shows the types of offshore foundations in Europe as of 2017 [40], where floating concepts are in the clear minority.

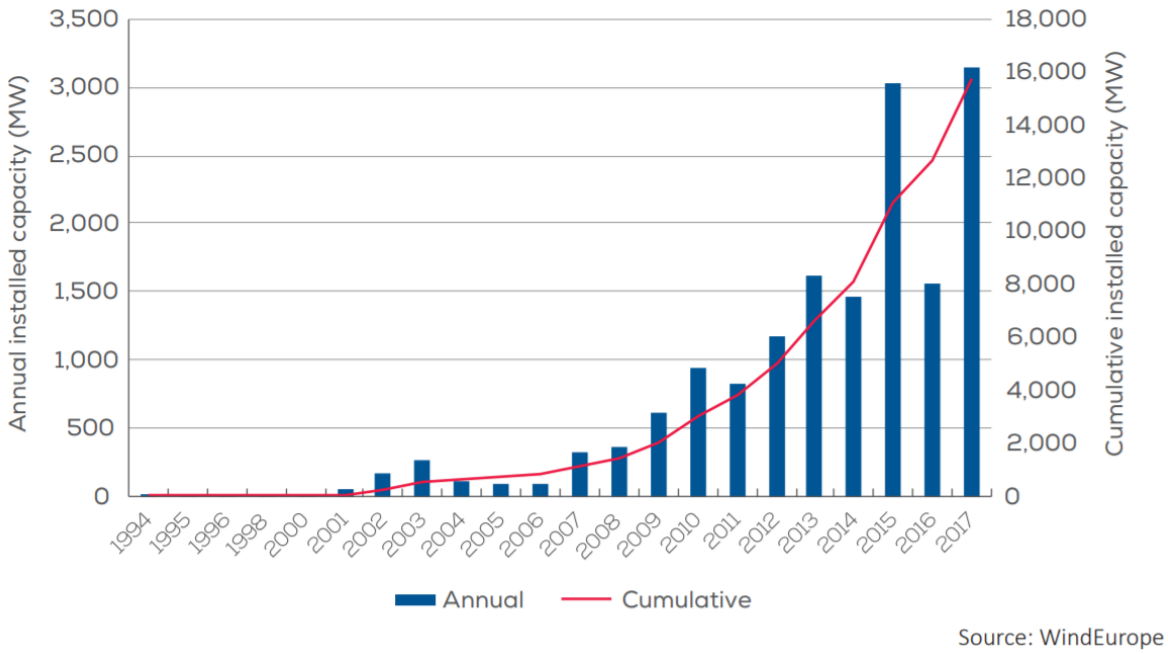

Figure 1.1: Cumulative and Annual offshore wind capacity in Europe (1994-2016) [40]

To address the lack of coastal areas with shallow waters (and the desire for offshore wind), there is increasing interest in floating wind turbines. Floating wind turbines are suitable at depths where fixed bottom structures are inconvenient and cost prohibitive (> 60 m). Equinor (formerly known as *Statoil*) has installed the first floating wind farm off the coast of Scotland, paving the way for the future of offshore wind energy and floating substructures. The Hywind Scotland Pilot park [1] consists of 5 spar-buoy type floaters (see Figure 1.3) at varying water depths between 95-129 m. For future projects, it is of interest to adapt this system to deeper waters where the mooring is critical to the feasibility of the project.

1.2 Research Motivation

The EU has agreed to a 32% renewable energy target by the year 2030 [39]; as such the offshore wind industry is moving towards deeper waters. This necessitates offshore wind turbine systems that are viable and profitable at these depths. The station-keeping system is an integral part of a floating wind turbine, therefore it is currently of interest to develop a mooring system that can capitalise on deep-water offshore real estate.

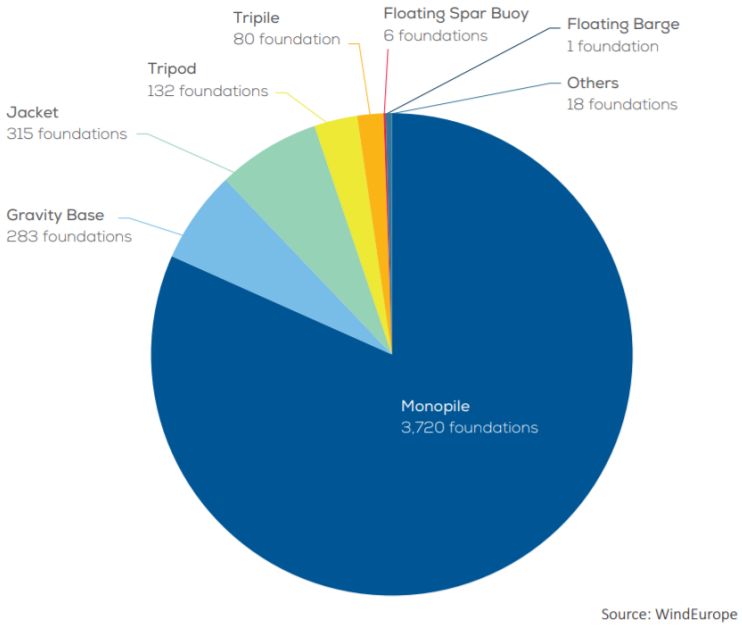

Figure 1.2: Share of substructure types (2017) [40]

1.3 Objective and Approach

The aim of this project is to design a mooring configuration for a floating offshore wind turbine (FOWT) with a spar buoy at 600 m water depth and explore the possibility of shared anchors. The mooring system must be able to pass the Ultimate Limit State (ULS) checks according to DNV regulations, and limit the offset in surge such that there is no risk of turbine collision or damage to the electrical export cables. This thesis also serves as research for similar future projects and suggestions are made for future work in Chapters 8 and 9. To support the main objective of this thesis, the following questions are also addressed:

1. Is it reasonable to use a simplified rotor model to simulate the loads on the offshore wind turbine for mooring analysis and then use this model in a park arrangement in SIMA?
2. Are shared anchors possible for wind farms in deep water and what arrangements work best in terms of line tensions, offset, and spacing?
3. How can park arrangement be maintained for larger offsets with regards to park efficiency and wake control?

While an exact location is not specified for this project, a water depth of 600 m and environmental conditions for the Norwegian North Sea are used.

Figure 1.3: Hywind Scotland Farm [36]

1.3.1 Methodology

The subsequent steps are the overall procedure used in this project:

1. A model and mooring system in SIMA at 320 m water depth was provided [41]. Decay tests in surge, heave, pitch, and yaw were performed on this model.
2. Four environmental load cases were evaluated using turbulent wind files (generated by TurbSim), with the corresponding JONSWAP wave spectrum and current profile, to determine the maximum tensions in the mooring line as well as the maximum surge offset. This was later reduced to 3 (three) load cases (discussed in Section 4.2.
3. The water depth was then increased to 600 m and subjected to the 3 load cases. A new type of mooring line and configuration was then selected and tested. After many iterations and combinations, a final configuration that produced acceptable offsets and tensions was selected.
4. This design was then tested under 3 more seed combinations for each of the three load cases in order to verify the design.
5. A simplified model at 600 m water depth was created within SIMA for use in park analysis since the software is not able to process more than one wind turbine in a single model. The model was simplified by reducing the RNA to single point mass.

6. The simplified model was then validated using 4 random wind and wave seeds for each load case.
7. The simplified model was then used in a park configuration of 3 different arrangements, with special attention paid to the loads on shared anchors.

1.4 Limitations

As always, time is a limiting factor with regards to performing analysis and research. Other limitations include (but are not limited to):

- Limited research and track record on mooring systems for floating wind turbines. Floating wind turbines are a relatively new technology in comparison to fixed bottom offshore wind turbines.
- Lack of thorough and freely available environmental data. That is, in comparison to the Gulf of Mexico (GoM) there is very little wave, wind, and current data freely available for the North Sea, so hindcast methods are used.
- Developing governing standards: There is currently only one floating wind farm in operation, therefore the track record for the mooring of floating wind turbines is not fully developed and the industry draws from the experience of O&G mooring systems.
- New software and techniques are still being developed for wind turbine analysis.
- Modelling simplifications are used, the connections and anchors are not modelled in SIMA. The wind, wave, and current are also assumed inline with each other and phase interaction of the misalignment of the wind and wave environments are not considered.
- It is assumed that the spar [41] and wind turbine model [2] supplied for this thesis is modelled correctly within SIMA.

1.5 Structure of the Report

The rest of the report is structured as follows:

- Chapter 2 explains a general overview of mooring design and analysis.
- Chapter 3 elaborates on the basis of the design of this project.
- Chapter 4 presents the environmental data used in this project.
- Chapter 5 discusses the preliminary analysis of the model in 320 m water depth.

- Chapter 6 deals with the design and analysis of a mooring system in 600 m water depth.
- Chapter 7 simplifies the model into one that can be used in SIMA for park analysis.
- Chapter 8 discusses possible arrays for shared anchor points.
- Chapter 9 concludes this thesis.

CHAPTER 2

AN OVERVIEW ON MOORING SYSTEMS

For a floating body, a mooring system is crucial to maintaining its offset within a particular radius under wind, wave, and current loads. A floating wind turbine must be able to maintain its positioning in order to sustain efficient operation, as well as for safety reasons. The orientation of a wind turbine relative to the environment is critical in its operation and therefore a mooring system should be able to provide enough restoring force to keep the system within a certain limit of offset in surge, sway, and yaw. For this, permanent mooring lines and/or dynamic positioning (DP) can be used; however, it is impractical and expensive to install DP systems on each turbine of a floating wind farm. DP systems are more suited for floating bodies that do not need to be permanently moored.

The mooring system of a non-shipshaped floating system is generally constructed of several lines arranged around the perimeter of the structure in the xy-plane near the waterline in order to address environmental forcing from all directions. The lines can be made up of chain, wire, synthetic rope, or any combination of the three. There are pros and cons to each line type which will be discussed in further detail here. A combination of line types can be used to create the optimum line for stiffness, weight, and economy. The upper ends of the mooring line are attached to the floating body via fairleads attached to the body. The lower end is attached to an anchor on the seabed which provides a fixed point for resistance.

Mooring for FOWTs draws heavily on the experience for floating platforms in the O&G industry. However, it should be noted that O&G platforms generally have high wave loads and low wind loads; for a wind turbine the opposite is true. This means that there is a larger moment arm for the loads as the wind load is considered to act at the hub height. A mooring for an oil and gas (O&G) platform will have more redundancy and higher safety factors due to higher risks

of potential loss of life. However, such redundancy is not necessary in the case of floating wind turbines [10] since the parks are unmanned. O&G structures are also generally deployed as a single structure offshore whereas wind turbines are installed as multiples in a "farm". The main loads on a wind turbine come from the wind on the rotor and the main loads on an O&G structure are a result of the wave loads and so different criteria is used in mooring line analysis for wind turbines.

2.1 Types of Mooring

This section explains the 3 most common types of moorings and their characteristics. The types are as follows:

1. Catenary Line
2. Taut Line
3. Tension Leg

2.1.1 Catenary Line Mooring

Catenary line mooring is the oldest and most widespread mooring system for offshore floating bodies [25]. By definition, a catenary is the curve which a uniform, flexible, inextensible string assumes when suspended from both ends. Therefore a catenary mooring is one in which the mooring line is suspended in a catenary shape between the hang-off point on the floater and the seabed [32]. The restoring force is provided by the lifting and lowering weight of the mooring line.

Figure 2.1[1]shows the typical schematic of a catenary layout. The mooring line touches down on the seabed before the anchor so that part of the mooring line lies on the seabed in a horizontal position. This means that the anchor system must be able to withstand a large horizontal force, but is generally not designed to withstand large vertically upward forces. The section of line on the seabed does not provide a restoring force unless lifted off. A catenary mooring system is a spread moored system where several mooring lines are uniformly arranged around the floating body. Since the mooring tension forces are created by the self weight of the line, chain is sometimes preferred due to its heavier weight. Alternatively, point masses or buoyancy modules along the line can also be used to adjust the shape of the catenary.

2.1.2 Taut Line Mooring

Similarly to the catenary mooring, a taut line system has mooring lines spaced around the floating body. However, these lines are taut, under high constant tension. The lines have low net

[1]Diagrams denoted with the *[Visio]* tag have been drawn in the Microsoft Visio programme.

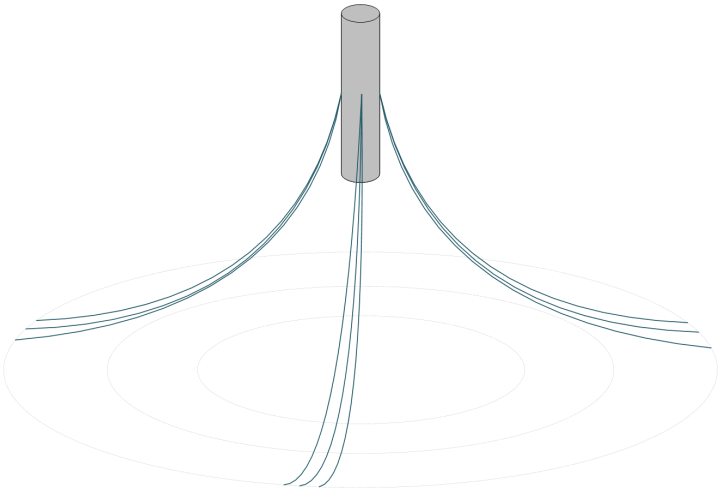

Figure 2.1: Schematic of Catenary Layout [Visio].

submerged weight and there is no catenary effect, that is, the lines remain straight and do not curve under the weight of the line. The restoring force comes from the stretch of the lines under horizontal displacement and so synthetic lines are commonly chosen for taut mooring due to their elastic spring-like properties[25]. A figure illustrating this arrangement in shown in Figure 2.2. Unlike the catenary mooring, a taut mooring line approaches the seabed at an angle and therefore the anchor must be resistant to both horizontal and vertical forces. Taut mooring lines are more suitable for ultra-deep water where the amount of line needed for catenary mooring becomes too cost-prohibitive and heavy. It is also more suited for calmer wave environments with low tidal differences since the vessel heave affects the mean tension of the lines.

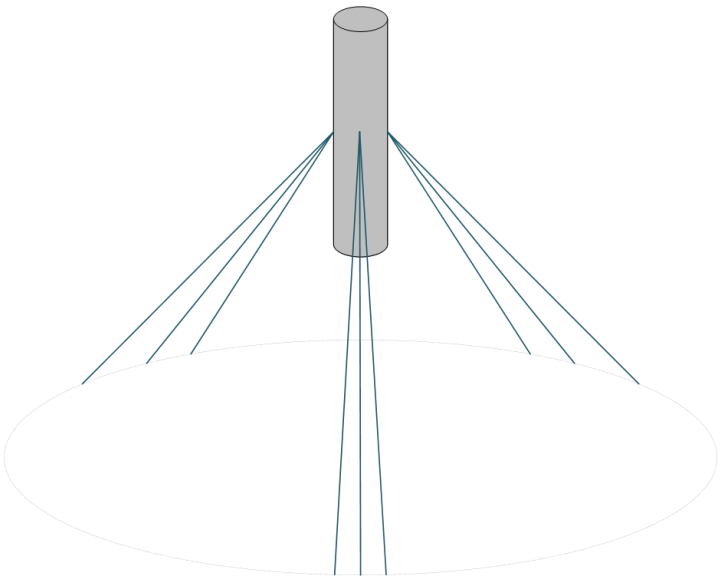

Figure 2.2: Schematic of Taut Layout [Visio]

2.1.3 Tension Leg Mooring

This mooring configuration is used for TLPs. Like the taut mooring system, the lines are in high tension. The lines in this system however are completely vertical. The buoyancy of the TLP is much higher than its weight which supplies an upward force on the tendons. The anchor system provides the downwards tension force. This means that unlike the catenary system, a tension leg system must be completely resistant to uplift failure[5]. Figure 2.3 shows the tension leg configuration.

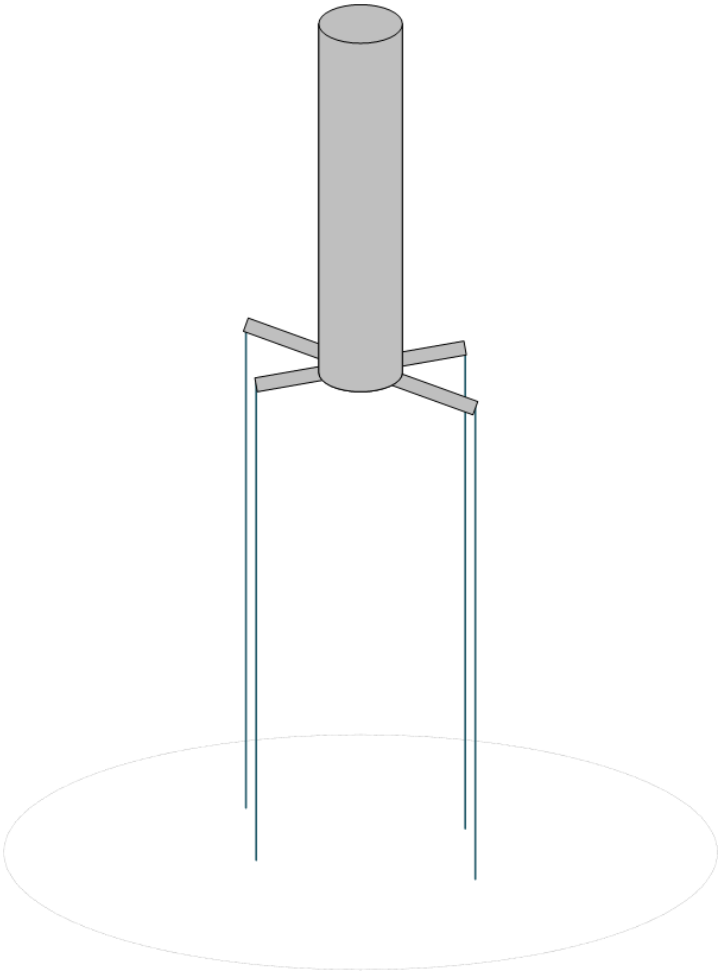

Figure 2.3: Schematic of Tension Layout [Visio].

2.2 Mooring Line Material

This section describes the 3 main materials used for mooring lines. Guidance for mooring line and material is dictated by DNVGL-OS-E301 [7].

2.2.1 Chain

Chain is made up of steel bars rolled into links and connected; the two types of chain links are stud-link and studless chain. Permanent moorings usually use studless chain, since the lack of stud reduces the weight per unit of strength and makes the line less prone to fatigue damage. However, the stud in a stud-link chain prevents the "knotting" of the chain which makes handling easier. Figure 2.4 shows the difference between stud-link and studless chain link.

Studded chain is more susceptible to a change in fatigue life since its fatigue life is sensitive to the tightening of the stud. If the stud were to become loose while in use, the fatigue life could become drastically low where it is no longer fit for purpose [7]. To avoid these complications, and for economy, studless chain is often chosen, as in this project. Additionally, it is expected that once installed, the chain will be under constant tension so there is no risk of knotting in the studless chain.

It is impractical, computationally expensive and time consuming to model each link in a chain, therefore in the SIMA[2] programme, representative weights and dimensions are used. While chain is cheaper than wire or synthetic ropes, it is heavy and the breaking strength is limited by the size of the chain links. For very deep water moorings, the amount of chain needed for catenary moorings becomes too heavy to use a purely chain line, so combinations with synthetic lines or wire ropes are used.

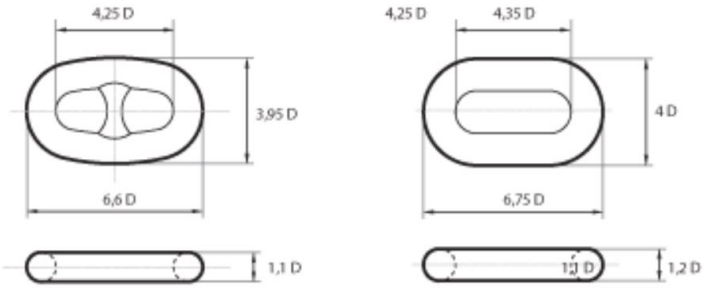

Figure 2.4: Diagram of stud-link chain (left) and studless chain (right) [5]

2.2.2 Wire

Wire ropes are made of individual wires wound around each other to form a strand, similarly to traditional fibre ropes. The flexibility and the axial stiffness of the strand is determined by the pitch of the windings. There are three main subtypes of wire ropes: single spiral strand construction, six strand-rope, and multi-strand rope. The six-strand rope is the most commonly used type of wire rope used in offshore mooring [5]. Wire ropes have lighter, more elastic characteristics than chain for the same breaking load, but are more expensive and more susceptible to corrosion.

[2]SIMA is the programme used for analysis in this project. It is further described in Section 3.7

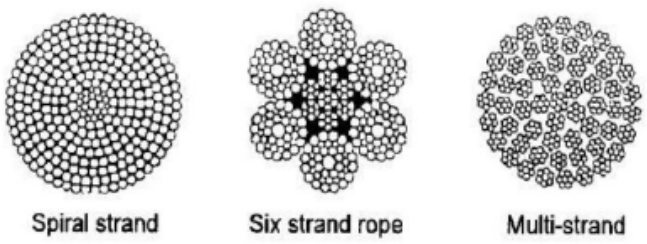

Figure 2.5: Diagram of the different arrangements of wire rope [5]

2.2.3 Synthetic Rope

Synthetic rope is the newest technology of all of these types of mooring lines. Its use has become increasingly popular with deep water mooring systems due to the light weight and high breaking strength. The elasticity of the material also lends itself to preventing excessive dynamic tensions by absorption of imposed dynamic motions [5]. Due to the light self-weight of the line, it is sometimes impractical to use synthetic rope for the complete line, especially for catenary mooring where the self weight is a main contributor to the pretension of the line. Most often, a chain-synthetic-chain arrangement is used to provided adequate self weight. The addition of point masses and floaters can also be used to adjust the self weight and shape of the line [5].

2.3 Anchor Types

Anchors are used to fix the mooring line to the seabed to keep a floating body in position. The type of anchor chosen for a particular project depends on the application and the soil/sea bottom conditions. In this case, the soil conditions are unknown so comments here are made regarding the suitability for multidirectional loading only. This project considers shared anchors for mooring wind turbines in order to reduce the amount of hardware needed and thereby lowering the CAPEX of the project. Anchor types can be broken down into two general categories:

1. Surface or gravity anchors
2. Embedded anchors

Surface or gravity anchors rely on the friction between the the anchor and seabed, along with a shallow embedment to constrain movement. These anchors are resistant to horizontal forces but are easily lifted once a vertical force is applied. They are restricted to shallow waters due to size limitations as this dictates the holding capacity.

Embedded anchors are used in applications which require more holding capacity than gravity anchors provide, such as for a large floating body like an FOWT or O&G platform. There are four main types of embedded anchors [32] [6] commonly used in offshore applications:

1. ***Piled anchors***: These can be driven piles or dynamically installed piles. They are commonly used for many offshore applications and are a proven technology. They are resistant to both horizontal and vertical forces.

2. ***Suction caissons***: These are large cylinders with the top end closed and and open bottom end, similar to an upturned bucket. Suction caissons are installed by initial penetration with self weight and then a suction at the top is used to drive the cylinder further into the seabed until all the water is removed and sides of the cylinder are fully penetrated. The mooring line is attached to the sides of the caisson at a depth that optimises its load bearing capacity. Suction caissons are designed to resist rotation under lateral loading.

3. ***Drag embedment anchors (DEA)***: DEAs are derived from conventional ship anchors and consist of a broad fluke connected to a shank. The fluke is angled to the shank by a predetermined amount and embedded into the seabed by dragging the anchor in a particular direction so that the fluke "digs into" the seabed. These anchors are suitable for catenary moorings but not for taut or tension-leg moorings since they are not resistant to vertical loads and are usually removed through application of a vertical force.

4. ***Plate anchors***: There are a variety of plate anchors suitable for different applications. They are a modified version of DEAs and consist of a plate attached to a fluke. The plate can be embedded in a variety of ways, each suited to a different purpose. They are attractive because of their low cost but are only capable of handling load in one direction.

Anchor types with axial symmetry such as piled anchors and suction caissons can be adapted to multiline loading attaching additional padeyes around the circumference [6]. Multiple padeye protrusions may reduce skin friction resistance above the attachment point. Drag embedment anchors and plate anchors are suitable mainly for unidirectional loading but can possibly be used for multidirectional loading by attachment to the anchor with a single ring. However it has not been tested and these anchors are vulnerable to out of plate bending [6]. Therefore it must be certain that the ring loads are not subjected to out of plane bending.

The Hywind Scotland Pilot Park project uses suction caissons to anchor each mooring line. This provides adequate lateral and vertical resistance for mooring stability[36].

For the purpose of this project, the anchor will not be modelled in SIMA; only a fixed node will be used.

2.4 Park Design and Arrangements

In addition to constraining movement to protect the cables and umbilicals and limiting movement of the wind turbine, it is also necessary to maintain the park arrangement so that there is limited effect of wind turbine wake. In research by N.O. Jensen [22], it is assumed that the wake interaction of wind turbines can be modelled linearly. Thus, it is important to arrange the turbines in such a manner to avoid wind shadows and excessive wake turbulence and effects, as it would decrease the efficiency of the park.

It has been shown that for turbines spaced 8-10 rotor diameters apart in the down wind direction and at least 5D apart in the crosswind direction that losses due to wake interference are <10% [30]. Therefore, the mooring is crucial in ensuring that the turbines maintain a position that allows “clean air”, i.e. no wind shadows. The mooring should be designed such that the maximum allowable offset in drift does not have a large influence on the wake effects.

CHAPTER 3

BASIS OF DESIGN

This section outlines the design of the FOWT, including the RNA, the substructure, and the environmental conditions used for analysis.

3.1 Location

The wind turbine will be located at a depth of 600 m in the Norwegian North Sea. The park simulations will assume a consistent water depth of 600 m. In reality, the seabed would vary throughout the farm.

3.2 Coordinate System

All floating and submerged bodies offshore are subjected to a variety of external environmental loads [15]. In seakeeping applications, the translational and rotational motions are defined as shown in Figure 3.1 and Table 3.1.

Table 3.1: Degree of freedom definitions

Degree of Freedom	i	**Description**
Surge	1	Translation in $x-$direction
Sway	2	Translation in $y-$direction
Heave	3	Translation in $z-$direction
Roll	4	Rotation around $x-$axis
Pitch	5	Rotation around $y-$axis
Yaw	6	Rotation around $z-$axis

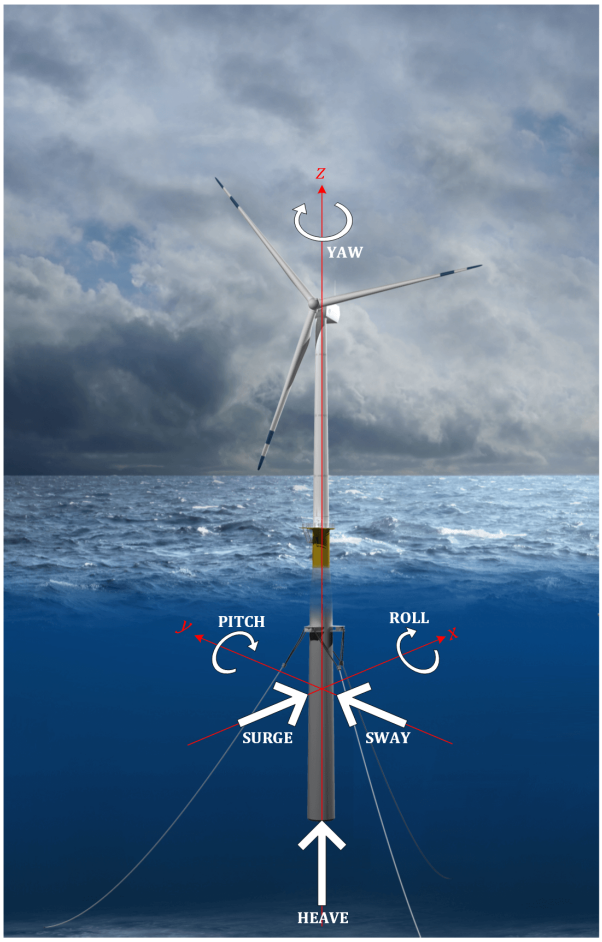

Figure 3.1: Visualisation of DoF system and rigid body motions [23] (modified in Visio).

3.3 The DTU 10 MW Reference Wind Turbine

The DTU 10 MW reference wind turbine is used for simulations in this project. The current Hywind Scotland Pilot Park uses the Siemens 6 MW wind turbine model [1]. However, one of the reasons for moving a wind farm further offshore in deeper water is the freedom to use larger turbines (due to more lenient noise restrictions) with a higher energy yield, which reduces the levelised cost of energy (LCOE).

The DTU 10 MW RWT was developed by the Wind Energy department at DTU. This turbine was developed as an upscaled version of the NREL 5MW wind turbine for use as a reference wind turbine in developmental projects. The NREL 5MW wind turbine has been used as a reference wind turbine in older projects.

3.3.1 Properties of the DTU 10MW RWT

The basic properties of the wind turbine are provided in Table 3.2. For further information refer to the DTU Wind Energy report "*Description of the DTU 10 MW Reference Wind Turbine*" [2].

Table 3.2: Key parameters of the DTU 10 RWT [2]

Wind Regime	IEC Class 1A	[-]
Rotor Orientation	Clockwise rotation - Upwind	[-]
Control	Variable Speed, Collective Pitch	[-]
Cut-in Wind Speed	4	[m/s]
Cut-out Wind Speed	25	[m/s]
Rated Wind Speed	11.4	[m/s]
Rated Power	10	[MW]
Number of Blades	3	[-]
Rotor Diameter	178.3	[m]
Hub Diameter	5.6	[m]
Hub Height	119	[m]
Drive Train	Medium Speed, Multiple-Stage Gearbox	[m]
Rotor Speed Range	6.0-9.6	[rpm]
Maximum Tip Speed	90	[m/s]
Rotor Mass	227 962	[kg]
Nacelle Mass	446 036	[kg]
Tower Mass	628 442	[kg]
1P Frequency	0.10 – 0.16	[Hz]
3P Frequency	0.30 – 0.48	[Hz]

3.3.2 Aerodynamic Design and Performance

The design of the DTU 10MW RWT is optimised based on the BEM theory and CFD. This means that the blades are pitched and twisted in order to achieve maximum performance for the wind speed. It also means that the blade is partitioned into several airfoils along the length; the shape of the individual airfoils are optimised for the relative position along the blade. The rotor control is such that the turbine operates at low or zero pitch and a design TSR= 7.5 up until 9.6 rpm (close to rated power). The blades are then pitched to achieve rated power. A TSR of 7.5 was chosen for design; this corresponds to the maximum power coefficient

The power and thrust curves based on this research are presented in Figures 3.2 and 3.3 respectively, as are the plots for the corresponding power (Figure 3.4) and thrust (Figure 3.5) coefficients. These plots were generated from the HAWTOPT tool that uses the BEM theory to analyse the performance of wind turbines [2]. As expected, the thrust decreases after the rated wind speed due to the feathering of the blades to maintain rated power. This is shown in the corresponding plot for the power curve (Figure 3.2) where the theoretical mechanical power output increases until rated wind speed, after which the rated power is maintained until cut-out.

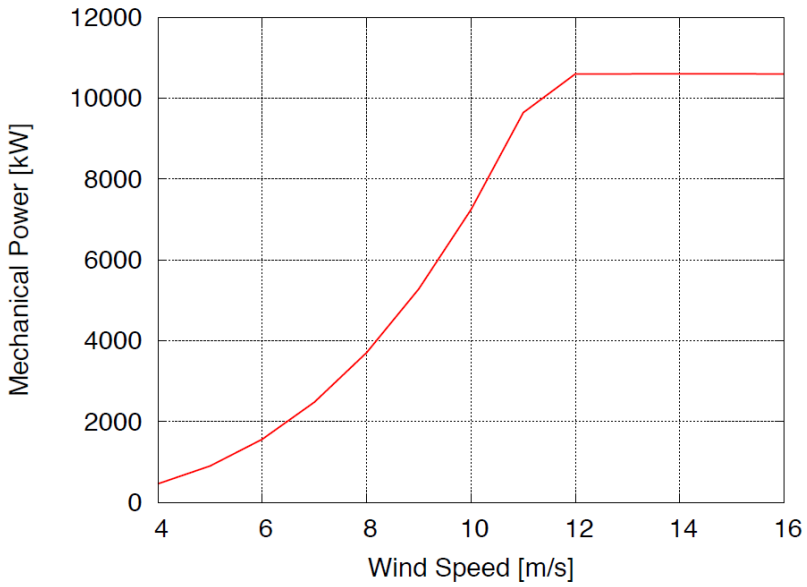

Figure 3.2: Power Curve for DTU 10MW RWT based on the HAWTOPT tool[2]

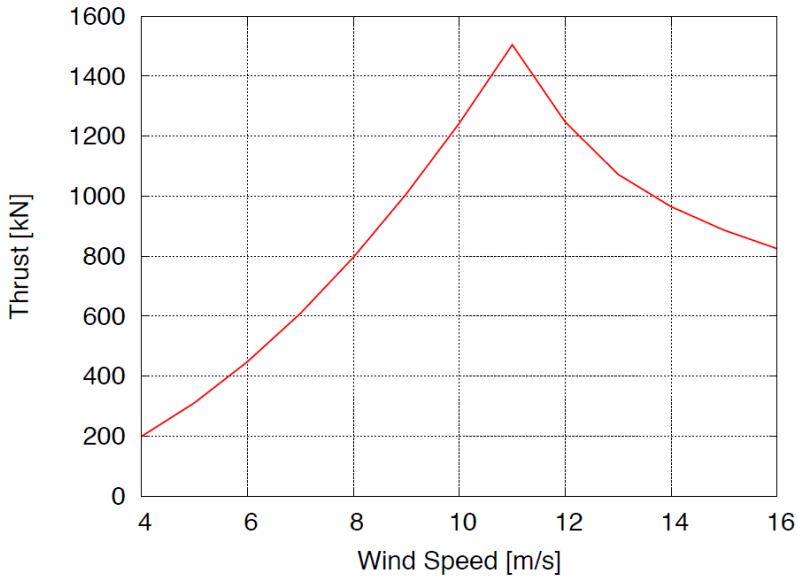

Figure 3.3: Thrust Curve for DTU 10MW RWT based on the HAWTOPT tool [2]

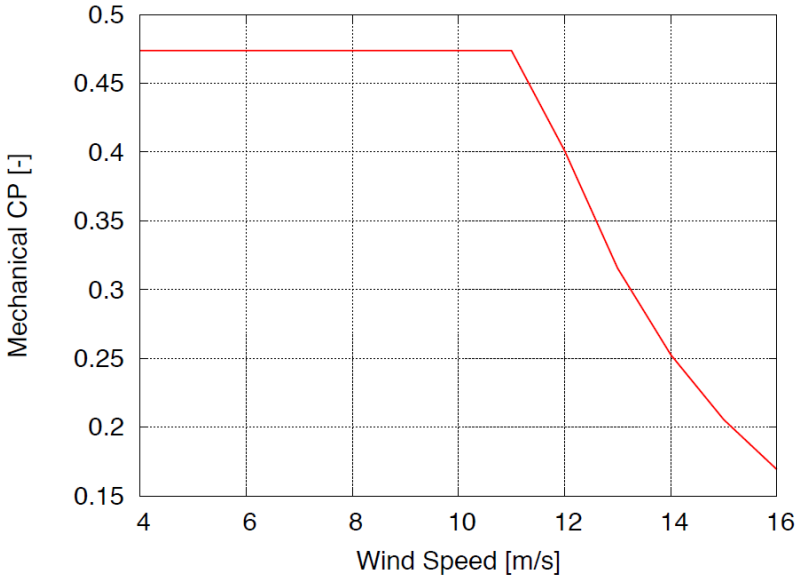

Figure 3.4: Power Coefficient for DTU 10MW RWT based on the HAWTOPT tool[2]

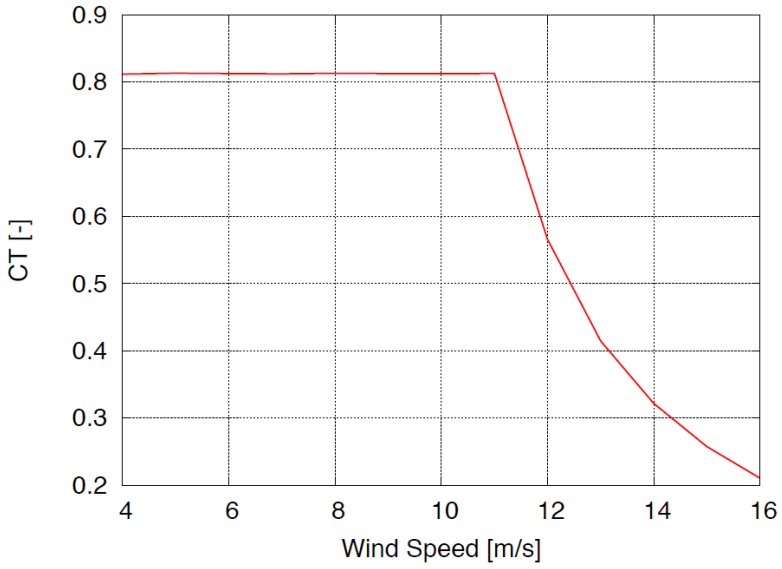

Figure 3.5: Power Coefficient for DTU 10MW RWT based on the HAWTOPT tool [2]

It should be noted that values obtained for the power and thrust using this BEM-based tool are purely theoretical and that the actual measured values will differ.

3.3.3 Structural properties of the DTU 10MW RWT tower

The properties of the tower for the DTU 10MW RWT are provided in the aforementioned report by DTU Wind Energy. As modification of the tower is out of the scope of this project, only the basic parameters of the tower are discussed here.

The tower is made of S355 steel as dictated by the DIN EN 10025-2 European standard. The tower is cone-shaped and the outer diameter varies from $D = 8.3$ m at the bottom to $D = 5.5$ m at the top. The tower is divided into sections where the thickness is constant for each section. The thickness varies from 38 mm at the bottom (where more stiffness and corrosion allowance is needed) to 20 mm at the top. The overall dimensions and structural properties are summarised in the DTU Wind Energy report [2] and are not presented here. The effective density is taken as an 8% increase of the mass density of the tower in order to compensate for the mass of the appendages and secondary structures attached to the tower. The exact section properties can be found in the published report by DTU Wind Energy [2].

3.4 The Statoil Hywind Scotland Pilot Park

This project draws from the the experience of the Equinor (formerly *Statoil*) Hywind Pilot Park project and can serve as research for future extensions of Hywind. The idea for a floating wind turbine project was initiated in 2001; after many years of research, the first demo was installed in offshore Karmøy, Norway in 2009. The test unit consisted of a 2.3 MW wind turbine and with a rotor diameter of 85 m. This demo concept has been tested and validated for 8 years. It has experienced a wave height of $H_{max} = 18$ m and wind speeds of up to $V_{max} = 40$ m/s [36].

In October 2017, the Hywind Scotland Pilot Park was commissioned and started production. It is the first floating commercial wind park and is located in Buchan Deep over an area of 15 km^2, off the coast of Scotland (Figure 3.6). The park consists of five 6 MW wind turbines for a total capacity of 30 MW which can provide clean energy to over 12 000 UK homes. An overview of characteristics of the park turbine is presented in Figure 3.7 and Table 3.3.

Figure 3.6: Map showing overall location of the Hywind Scotland Pilot Park. [36]

Table 3.3: Characteristics of the Hywind Scotland Pilot Park [1], [36]

Blade length	75	[m]
Rotor diameter	154	[m]
Turbine capacity	6	[MW]
Tower height	83	[m]
Tower diameter (max)	7.5	[m]
Hub height	98	[m]
Spar (substructure) Length	91	[m]
Spar draught	78	[m]
Spar diameter (max)	14.5	[m]
Total turbine height	178	[m]
Mooring type	Chain	[-]
Line length	691-875	[m]
Mooring system radius	600-1200	[m]
Anchor type	Suction Bucket	[-]
Depth range	95-129	[m]
Distance from shore	25	[km]
Average wind speed	10.1	[m/s]
Design life	20	[years]

3.4.1 Hywind Scotland Mooring System.

Each turbine in the Scotland Hywind uses approximately 2400 m of chain [36] total. The mooring design uses a bridle system in order to provide the yaw stiffness of the spar under environmental loading. Figure 3.8 shows the bridle system for the mooring design. This bridle configuration

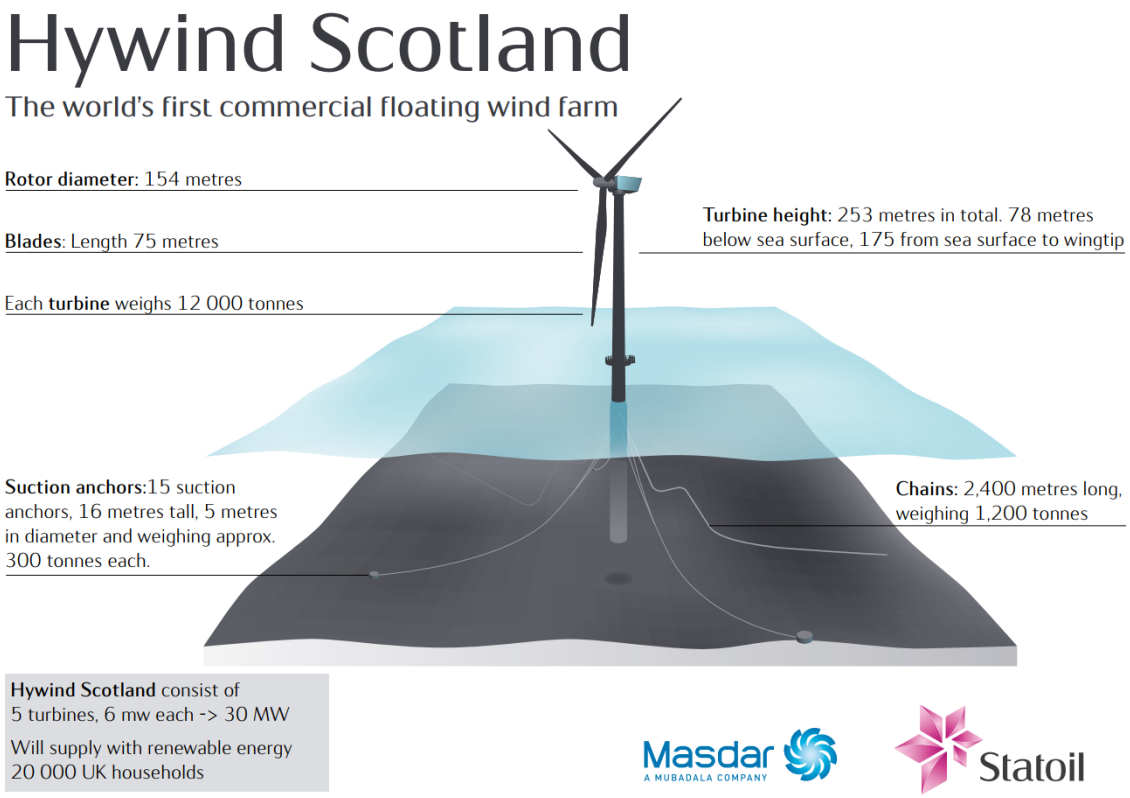

Figure 3.7: Map showing overall location of the Hywind Scotland Pilot Park. [36]

segues into a conventional 3-line mooring arrangement. Each line is attached to a single suction anchor (15 anchors total, 3 for each turbine) measuring 16 m in height and 5 m in diameter. Two bridle ends from 2 different mooring lines are attached to separate padeyes on a single fairlead for attachment to the spar keel. The bridle ends for each mooring line are then attached further down to a chain plate which connects it to a single chain. This single chain is then connected to the anchor point.

3.5 Codes and Standards

The following codes and standards were used as guidance for this project.

- DNV-OS-E301 Position Mooring [7]
- DNV-OS-J101 Design of Offshore Wind Turbine Structures [9]
- DNV-OS-J103 Design of Floating Wind Turbine Structures [10]
- DNV-RP-C205 Environmental Conditions and Environmental Loads [8]

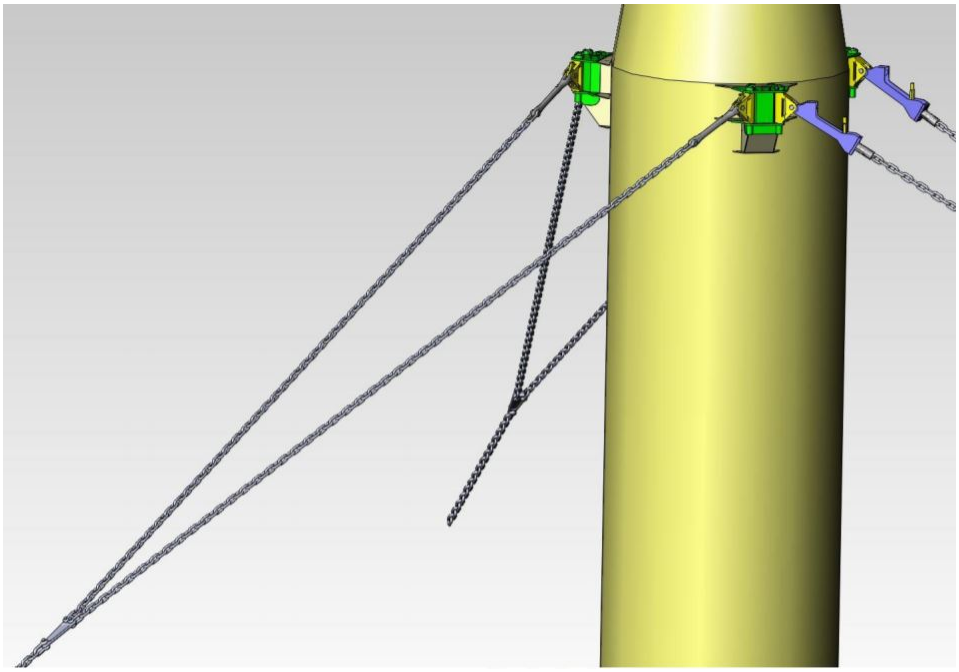

Figure 3.8: Bridle system for mooring restraint. [36]

- IEC 61400-3:2009 Wind turbines - Part 3: Design requirements for offshore wind turbines [21]

3.6 Basic Information for a Single Turbine

The model used in this analysis was provided from NTNU's Department of Marine Technology, Group of Marine Structures as a complete SIMA model at a water depth of 320 m. This model is an amalgamation of the DTU 10MW RWT and the spar substructure designed by Xue [41]. The basic properties of the model are presented in Table 3.4. A visualisation of the provided SIMA model is shown in Figure 3.9 showing the mooring line labels and the orientation. The origin (0,0,0) of the model is set at the waterline in the middle ($xy-$plane) of the spar. The centre of gravity of the system was extracted from the report "*Design, numerical modelling and analysis of a spar floater supporting the DTU10MW wind turbine*" [41].

Table 3.4: Basic parameters in SIMA for provided wind turbine model including mooring

Hub Height (z)	119.00	[m]
Rotor Diameter	178.00	[m]
Spar Diameter (top)	8.30	[m]
Spar Diameter (bottom)	12.00	[m]
Spar Draught	120.00	[m]
Water Depth (z)	-320.00	[m]
Fairlead Position (z)	-70.00	[m]
Mooring Line Length	902.20	[m]
Mass per Length	155.41	[kg/m]
Total mass of 1 Line	140.21	[tonne]
Anchor Radius	855.17	[m]
Mass of Wind Turbine (excluding mooring)	12378.56	[tonne]
CoG of System (z)	-74.6	[m]

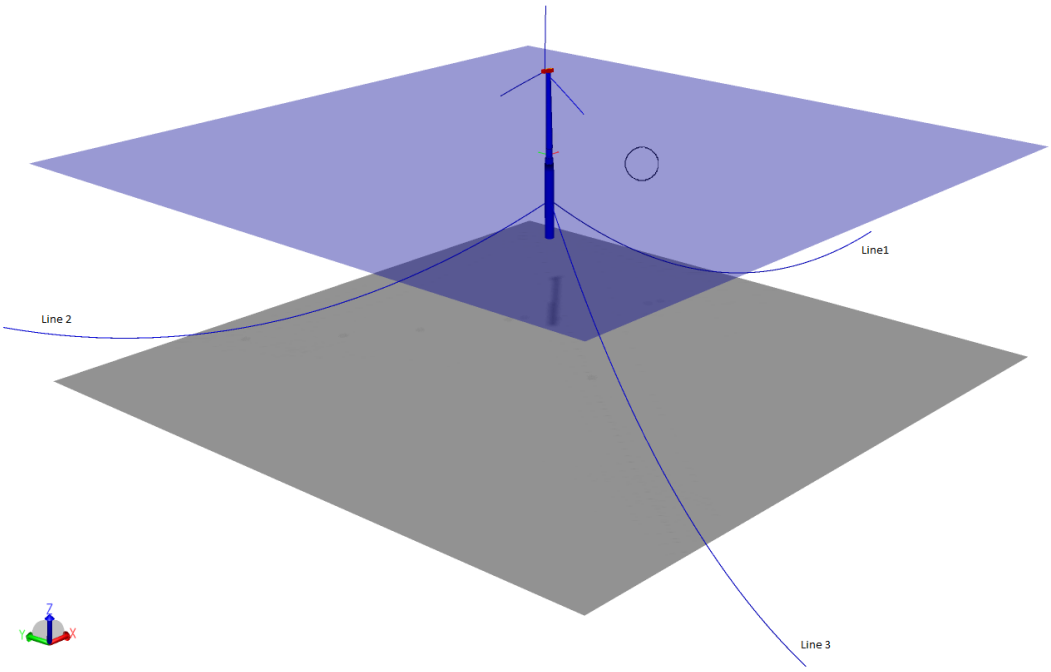

Figure 3.9: Visualisation of SIMA Model.

3.6.1 The Spar Substructure

A spar is a long cylindrical substructure that has been favoured in O&G applications for its low waterplane area, making it less susceptible to heave motion under wave loading. There are three types of spars in O&G applications however the type used here and in Hywind Scotland is the "classic" spar shape. The stability is controlled by ballasting the lower section of the cylinder so

that the centre of gravity is located well below the waterline. This is preferred for wind turbines as it greatly reduces capsize risk (virtually impossible) in adverse weather conditions and maintains the pitch of the floater in operation.

3.7 Software

SIMA is the main tool used in this project for simulations and is described as a "*complete solution for simulation and analysis of marine operations and floating systems*" [31]. It is a workbench developed by *SINTEF Ocean* (formerly *MARINTEK*) which allows the user to create and analyse in the marine technology field. SIMA provides visualisation of results and graphical representations of the model. It consists of a graphical user interface and supports the text-based input physics engines SIMO and RIFLEX. SIMO and RIFLEX can be used separately or coupled (as in this project). SIMO is used for the modelling of marine operations, such as the wind turbine and spar, and RIFLEX is used for the analysis of risers and other slender structures such as the mooring lines.

MATLAB and Microsoft Excel are used for post processing the results from SIMA. Visio is used for drawing and modifying representative diagrams.

CHAPTER 4

LOAD CASES AND ENVIRONMENTAL DATA

In this chapter, the environmental data and load cases used in the simulations are presented. Unlike the Gulf of Mexico, the North Sea does not have an expansive collection of freely available metocean data. Thus, models based on hindcast data were used for analysis. DNV-RP-C205 and IEC 61400-1 are used as guidance for selectinging and applying the environmental data.

4.1 Site selection

The papers by Johannessen et al. [24] and Li et al. [28] are used for metocean data for this project. Site 14 was selected from the report by Li et al. [28] since this site had the most severe data of the North Sea. This data set was then cross-checked with two other reports by Fugro (*Wind and wave frequency distributions for sites around the British Isles* [13]) and Deltares (*Extreme offshore wave statistics in the North Sea* [34]). Table 4.1 presents the data used from Site 14.

4.2 Load Cases

The load cases are selected as those which are thought to have the greatest contribution to the loads on the wind turbine structure (including the tower and spar). These three load cases are summarised in Table 4.2.

Four load cases with steady wind, waves and current are used for the initial analysis of the wind turbine. Load case four was selected as a subset of load case three. The loads are considered for the following four cases:

Table 4.1: Metocean data extracted from [28]

Site number	14
Area	North Sea
Name	Norway 5
50-year mean wind speed at 10 m height U_{10}	33.5 [m/s]
50-year significant wave height H_s	11.0 [m]
Mean value of T_p	11.1 [s]
Conditions with maximum H_s **on the 50-year contour**	
Mean wind speed at 10 m height U_{10}	31.2 [m/s]
Significant wave height H_s	15.6 [m]
Mean value of T_p	14.5 [s]

1. ***Rated wind speed***: Thrust on the wind turbine is at a maximum but waves are relatively low. Operating case.

2. ***Cut-out wind speed***: High winds, but lower thrust on the wind turbine than at rated and moderately high seas. Operating case.

3. ***50-year conditions***: Used for ULS analysis. This provides the maximum 50 year wind on the wind turbine and the corresponding wave and current. Low thrust on turbine, but high winds and waves. Non-operating case.

4. ***Maximum wave height in 50 years***: Similarly to load case 3, this provides the maximum wave height in 50 years with the corresponding wind speed. This wave was significantly higher than the 50-year condition. Upon further discussion with Prof. Kjell Larsen and consultation of data from Fugro [13] and a technical report from Deltares [34] it was concluded that this last case will be discarded from analysis, as the conditions are far more severe than expected. Since the wind turbine spars are not manned, it is unnecessary to use such severe values for analysis as it will lead to an over-design of the mooring system. Since Fugro is often contracted for metocean surveys for multinational O&G companies, it was deemed as a reputable source for data. Additionally, in the preliminary analysis in Chapter 5, the line tensions for load case 3 and 4, as well as the surge, and pitch offsets are within ±4% of each other. Therefore load cases 1 to 3 are sufficient for analysis in this project.

The wind, wave, and current are applied in the same direction at a heading of 0° for all cases unless explicitly stated otherwise. The load case matrix used for initial environmental analysis is shown in Table 4.3. The cells highlighted in grey are the calculated values using the methods described below.

Table 4.2: Summary of load cases

Load Case Number	**Description**	**Status**	**Thrust loads on wind turbine**	**Wind loads on tower**	**Wave loads on spar**
1	Rated wind speed	Operating	High	Low	Low
2	Cut out wind speed	Operating	Moderate	Moderate	Moderate
3	50-year storm conditions	Non-operating	Low	High	High

Table 4.3: Load case matrix for initial environmental analysis

Load Case	**Wind Speed at:**		**Significant Wave Height**	**Peak Period**	**Current Velocity**
	z =Hub Height	z =10 m			
	U_z [m/s]	U_{10} [m/s]	H_s [m]	T_p [s]	V_c [m/s]
1	11.40	8.90	3.71	7.21	0.27
2	25.00	19.52	9.38	11.47	0.59
3	42.90	33.49	10.96	11.06	1.00
4[1]	39.97	31.20	15.60	14.80	0.94

4.3 Wind and Wind Models

The wind conditions for load cases 1 and 2 are dictated by the rated and cut out wind speeds for the wind turbine. However, these wind speeds U_z are taken at the hub height z. In order to translate this to the wind speed at the standard 10 m height U_{10}, the inverse of the log law [28] is used. This relationship is given in Equation 4.1. These winds were then applied to 2-parameter Weibull distribution (Equation 4.2) in order to find the corresponding probability of occurrence. In Equation 4.2, $P(U_{10})$ is the probability of occurrence for a particular wind speed at 10 m reference height and U_{10} is the wind speed at 10 m reference height.

$$U_z = U_{10}\left(\frac{z}{10}\right)^{0.1} \tag{4.1}$$

$$P(U_{10}) = 1 - \exp\left[-\left(\frac{U_{10}}{\beta}\right)^{\alpha}\right] \tag{4.2}$$

Where $\alpha = 1.708$ and $\beta = 8.426$ are dimensionless coefficients for typical North Sea cases.

4.3.1 Steady Wind

For the initial environmental analysis of the supplied model at 320 m water depth, a steady wind was applied to the wind turbine. This means the wind speed varied according to the logarithmic

[1]This load case is eliminated from analysis for the deep water models.

profile but did not vary in time or in the $xy-$plane. This does not mimic the turbulence or randomness that the wind turbine would experience in real life.

4.3.2 TurbSim

TurbSim [27] is a tool from NREL for use in wind turbine simulations. It is a stochastic, coherent, turbulence code developed based on several spectral models including the IEC Kaimal and Von Karman Models. To produce the wind files needed in these simulations, the Kaimal spectrum was used as input. The wind files are also based on the wind speed expected at hub height. The wind files produced by TurbSim varies spatially in three dimensions as well as over time. It is therefore imperative to define a reasonable mesh (i.e. the amount of data points over an area) and to ensure that the area completely encapsulates the swept area of the wind turbine's blades. TurbSim wind files are used in the secondary analysis of the model at 320 m and in the complete model at 600 m.

4.3.2.1 Errors and Assumptions

The TurbSim code was validated for a multi-row wind farm at the San Gorgonio Pass in California, USA [27]. However, it was only validated up to a height of 50 m above ground level. Therefore, since these simulations are offshore, at a hub height of 119 m, it is possible that the margin of error is larger.

4.3.2.2 Kaimal Wind Spectrum

The Kaimal wind spectrum describes the turbulent wind climate at the location of a turbine in terms of a power density spectrum. Equation 4.3 shows the Kaimal spectrum used as it relates to the frequency f, the integral length scale L_U, and the 10-minute average of the observed wind velocity V_{10min} [8]. The variance in wind speed is represented by σ_U.

$$S_u(f) = {\sigma_U}^2 \frac{6.868 \frac{L_U}{V_{10\,\mathrm{min}}}}{\left(1 + 10.32 \frac{f L_U}{V_{10\,\mathrm{min}}}\right)^{\frac{5}{3}}} \tag{4.3}$$

L_U may be calculated using Equation 4.4 according to the specifications in Eurocode 1 [8], where z_0 is terrain roughness, or Equation 4.5 according to [21], which is independent of terrain roughness.

$$L_U = 300 \left(\frac{z}{300}\right)^{0.46 + 0.074\ \ln z_0} \tag{4.4}$$

$$L_U = \begin{cases} 3.33z & \text{for } z < 60 \text{ m} \\ 200 \text{ m} & \text{for } z < 60 \text{ m} \end{cases} \tag{4.5}$$

The spectrum can then be used to generate time series of the wind field for simulations using Equations 4.6 and 4.7 [4].

$$V(t) = \overline{V} + \sum_{p=1}^{M} b_p \cos\left(\omega_p t - \epsilon_p\right) \tag{4.6}$$

where

$$b_p = \sqrt{2S_W\left(f_p\right)\Delta f} \tag{4.7}$$

4.3.3 NPD Wind

NPD wind is used as input for the simulations which use the simplified model as SIMA cannot process the TurbSim wind without an actual wind turbine present. Since TurbSim also produces wind speeds at a point in space, over the swept area of the wind turbine blades, the average of these points would need to be used for the simplified model as there is only a representative point mass in place of the RNA. NPD wind varies randomly over time, where the spectrum is defined by U_{10} (the 1- hour mean speed at an elevation of 10-m above MWL) and is considered a suitable substitute for taking the average of all the points of the TurbSim wind files. The NPD wind model is more complex than the steady wind, but less realistic than using a TurbSim wind file. The one hour mean NPD wind speed is given in Equation 4.8.

$$\overline{U}(z) = \overline{U}_{10}\left[1 + 0.0573\sqrt{1 + 0.15\overline{U}_{10}}\ln\frac{z}{z_{10}}\right] \tag{4.8}$$

4.4 Waves

The 50-year metocean conditions for U_{10}, H_s, and T_p are supplied in the paper by Li et al [28]. To calculate the wave heights for load cases 1 and 2, the probability of occurrence from the known wind speed $P(U_{10})$ was then used to back calculate the wave height using the Weibull distribution (Equation 4.9). The values for α (Equation 4.10) and β (Equation 4.11) were calculated from the equations for the conditional distribution of H_s for a given wind speed from the paper by Johannessan et al. [24].

$$H_s = \exp\left[\frac{\ln[-\ln[1 - P(U_{10})]]}{\alpha} + \ln\beta\right] \tag{4.9}$$

where:

$$\alpha = 2.0 + 0.135 \cdot U_{10} \tag{4.10}$$

$$\beta = 1.8 + 0.100 \cdot U_{10}^{1.322} \tag{4.11}$$

The peak period was modelled from the calculated H_s values using the relationship shown in Equation 4.12 [8].The α value used here is calculated from T_p and H_s values in load case 4 since this gave the most reasonable values for T_p when compared to other statistical data of the same H_s in the Norwegian North Sea.

$$T_p = \alpha\sqrt{H_s} \tag{4.12}$$

The wave environment is then applied in SIMA as a 3-parameter JONSWAP spectrum [8]. The description for the JONSWAP spectrum is given in Equation 4.13

$$S_\eta(f) = (1 - 0.287 \cdot \ln\gamma)0.3125 \cdot H_s \cdot f_p^4 \cdot f^{-5} exp\left(-\frac{5}{4}\left(\frac{f}{f_0}\right)^{-4}\right)\gamma^{\exp\left(-\frac{(f-f_p)^2}{2\sigma^2 f_p^2}\right)} \tag{4.13}$$

Where γ is the peak-shape parameter and:

$$\sigma = \begin{cases} 0.07 & \text{for } f \leq f_p \\ 0.09 & \text{for } f > f_p \end{cases}$$

4.5 Current

There is little to no current data freely available for the North Sea; therefore section 4.1.4.4 of DNV RP C205 [8] was used as a basis for the current calculation as it is considered to be a conservative estimate. This section describes the relationship of the wind generated current velocities and is advised to be used in the case of missing reliable data. The current was applied as an associate current, i.e. constant from the waterline to seabed. Equation 4.14 describes how the current was calculated. Since the current is calculated based on the wind speed,it is assumed co-directional with the wind speed for this project . In reality, the current would vary with respect to water depth and cardinal direction.

$$V_c = 0.03 \cdot U_{10} \tag{4.14}$$

CHAPTER 5

PRELIMINARY ANALYSIS AND RESULTS FOR 320 M MODEL

This section describes the analysis and results done in SIMA for the supplied model of the wind turbine and mooring system at 320 m water depth.

5.1 Decay test

Decay tests were performed to determine the natural frequency of system in surge, heave, pitch, and yaw (DoFs 1, 3, 5, and 6). Checking the natural frequency indicates whether or not the floating body and mooring responds as expected. It is also used for comparison when the mooring system is changed. For each of these decay tests, a force (or moment) was applied to the system whilst under no environment forcing. The results were then post processed using the supplied read_Decay.m MATLAB code. The load case matrix and the natural frequency results are shown in Table 5.1. For a consistency check, a decay test in heave was performed three times to ensure that the results were consistent.

Table 5.1: Applied forces for decay tests and resulting natural frequencies

Motion	**Surge Force** [N]	**Heave Force** [N]	**Thrust Force** [N]	**Yaw Moment** [N·m]	**Location**	**Natural Frequency** [Hz]	**Natural Period** [s]
Surge	1.555×10^6	[−]	[−]	[−]	CoG $+x$	0.007	138.7
Heave	[−]	1.632×10^6	[−]	[−]	Bottom of spar in $+z-$direction	0.032	31.6
	[−]	2.176×10^6	[−]	[−]		0.032	31.6
	[−]	2.720×10^6	[−]	[−]		0.032	31.6
Pitch	[−]	[−]	1.55×10^6	[−]	Hub $+x$	0.027	37.6
Yaw	[−]	[−]	[−]	5.00×10^6	About $z-$axis	0.130	7.7

It is important for the spar floater natural frequencies to avoid the 1P and 3P natural frequencies of the wind turbine. The 1P frequency is the rotational frequency of the rotor and the 3P frequency is the frequency at which the blade passes the tower. Here, the yaw natural frequency falls within the 1P frequency. Though excitation was not observed during any of the simulations under environmental loading, this will be addressed in the bridle design for the deep water mooring system.

Figure 5.1 shows an example of the output from MATLAB for the decay tests. The applied force was calculated to displace the spar by ~4 m. A steadily increasing force was applied to the spar until the calculated force was reached after 500 s, then held steady for the next 1500 as seen in the plot. After, the force is removed and the body is allowed to vibrate at its natural frequency. This process was repeated for all 6 load cases in Table 5.1 above to determine the natural period and damping.

This test was also used a sanity check; rough hand calculations were done to determine the force F_3 needed to displace the spar by a certain amount as shown in Equation 5.1. This equation relates the waterplane area of the spar A_w to the heave displacement η_3. It was then checked that the floater was displaced by this amount once the force was applied in SIMA.

$$F_3 = \rho \cdot g \cdot A_w \cdot \Delta\eta_3 \tag{5.1}$$

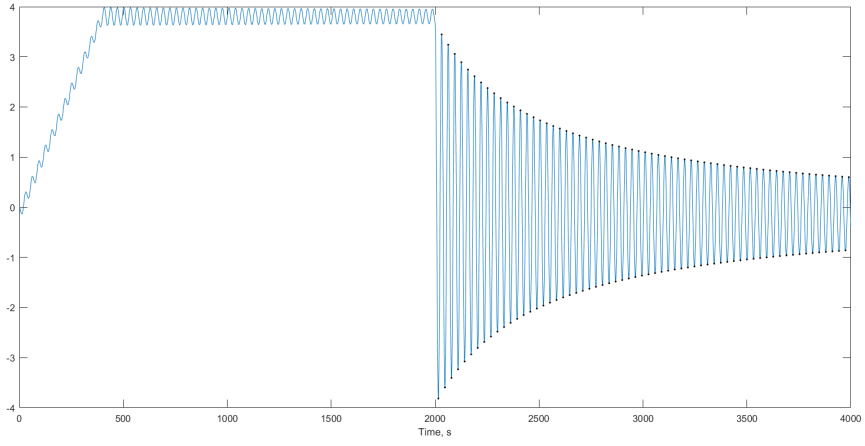

Figure 5.1: Heave decay plot

5.2 Environmental Loads

The load cases previously presented in Section 4.2, Table 4.3 were applied to the SIMA model at 320 m water depth. For the wind conditions, TurbSim [27] was used to generate a fluctuating

3-component wind file. The results from those load cases are presented and discussed in this section.

Table 5.2 shows the maximum and average surge, pitch, and yaw displacements of the spar under the four environment conditions. The maximum yaw is presented since the bridle for the deep water needs to be modelled. The surge offsets are presented since it is the main consideration for the design of the mooring. The surge offsets are over 10% of the water depth for all cases except at cut-out wind speed. A rule of thumb used in industry is to limit the offset to 10% of the water depth, and this will be followed in the deep water design. In reality, the allowable surge offset is dictated by the minimum bending radius (MBR) of the electrical cables; if the surge or sway offset is too large, this can cause a severe bend in the cable beyond its MBR that will damage the cable. The pitch rotation remains under 12° for all cases, however it should ideally be limited to 10° since the wind turbine is designed to operate perpendicular to incoming wind flow and a large pitch rotation can cause inefficient operation. Load cases 1, 3, and 4 cause the highest displacements due to the high thrust force at the hub for load case 1 and high wave forces on the spar and wind forces on the tower for load case 3 and 4. The yaw under the 50-year conditions is above 25° and while the wind turbine controller can correct the yaw of the RNA, it is desirable to reduce the spar yaw in the bridle design. As expected, the average yaw in operation is approximately 0°. In load cases 3 and 4, the average is approximately 3°; since the turbine is not in operation here, the slight yaw is not of concern.

Table 5.2: Surge, pitch, and yaw offsets for model at 320 m WD under turbulent wind

Load Case	**Surge**				**Pitch**		**Yaw**	
	Maximum		**Average**		**Maximum**	**Average**	**Maximum**	**Average**
	[m]	[%]	[m]	[%]	[°]		[°]	
LC1	49.3	15.4%	32.8	10.2%	11.94	7.10	7.67	0.33
LC2	25.5	8.0%	18.2	5.7%	7.35	3.33	13.34	-0.27
LC3	42.8	13.4%	29.7	9.3%	10.01	4.51	26.53	3.20
LC4	42.5	13.3%	29.2	9.1%	9.96	4.39	24.99	3.15

Figures 5.2 through 5.5 show the line tensions for each of the lines under the different loading conditions. These plots show the full time series including the transients so that the start up of the system can be seen. Lines 2 and 3 are the windward lines in this case and will therefore experience the most tension. Load cases 3 and 4 cause the highest tensions. For the time series plots, the first 200 seconds are taken as transient when calculating the maxima, minima, and averages of the line tensions and offsets. This is due to the start up of the control system and turbine which, when applied with the metocean loading, feathers and adjusts the pitch of the turbine, causing irregularities in the time series.

The time series plot for Load Case 1 is shown in Figure 5.2. The influence of the low frequency (LF) motion is very distinct in this plot and averages a period of 140 s. The wave frequency (WF)

influence is seen in the smaller peaks of this plot and the period matches that of the wave period of Load Case 1 (~ 7 s). The LF motion has greater influence on this plot since the wind loads dominate the motion due to the high thrust force. For load cases 2-4 the influence of the WF motion is more obvious here since the there is less influence of the wind loading on the structure. Regardless, the periods of the WF motion correspond with the wave period input for all load cases.

Table 5.3: Line tensions of the supplied model at 320 m WD under environmental loading

Load Case	**Line**	**Tension** [kN]		
		Minimum	**Maximum**	**Average**
LC1	Line 1	1297.1	1715.9	1448.6
	Line 2	2052.3	3387.7	2588.9
	Line 3	2035.6	3552.7	2591.4
LC2	Line 1	1386.6	1805.2	1577.6
	Line 2	2006.7	2673.3	2282.3
	Line 3	1886.0	2482.7	2170.5
LC3	Line 1	838.9	2044.1	1429.4
	Line 2	1190.7	3613.8	2525.7
	Line 3	1513.0	5605.2	2703.9
LC4	Line 1	834.1	2074.1	1433.6
	Line 2	1177.1	3563.5	2509.0
	Line 3	1498.3	5405.6	2687.3

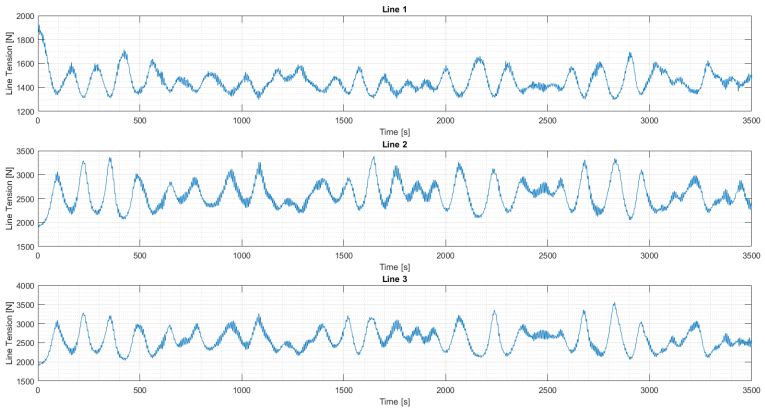

Figure 5.2: Line tensions for Load Case 1: rated wind speed

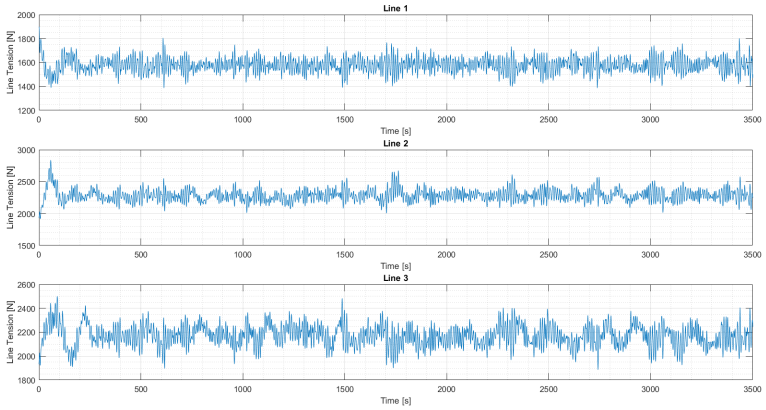

Figure 5.3: Line tensions for Load Case 2: cut-out wind speed

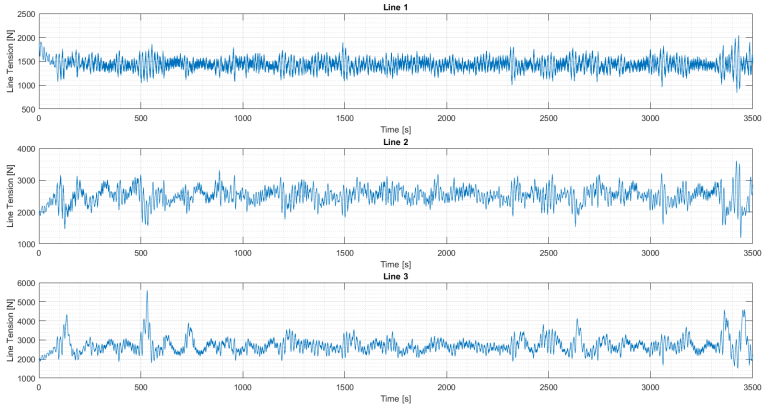

Figure 5.4: Line tensions for Load Case 3: 50 year conditions with maximum U_w

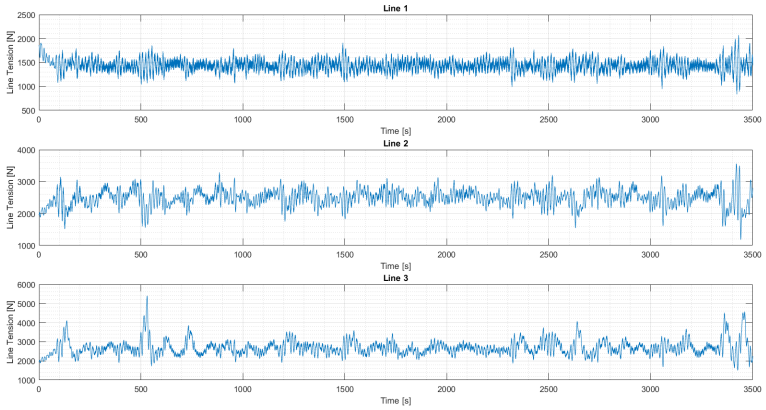

Figure 5.5: Line tensions for Load Case 4: 50 year conditions with maximum H_s

CHAPTER 6

THE DEEP WATER MODEL

This chapter presents the design and modelling process of the mooring lines for the DTU 10MW wind turbine in 600 m water depth. For brevity and clarity, the mooring line at 600 m will henceforth be referred to as the 600m-model. Similarly, the mooring line at 320 m water depth will be referred to as the 320m-model. Please note that the wind turbine (DTU 10MW RWT) and spar (design by Xue [41]) remain the same for both models; only the mooring line configuration and water depth change. The environmental conditions applied also remain the same with the exception that the current is extended to 600 metres below water level and 3 more seeds per load case are used in the simulations in order to verify the 600m-model. From this point on only load cases 1-3 are used for simulations.

6.1 Mooring Design Process

- First, a catenary mooring was selected since it is the most commonly used in industry, as well as used in the Hywind Scotland Pilot Park which also uses a spar substructure.
- Using the catenary equation described in Section 6.2, as well as guidance from the Hywind Scotland mooring system and the original mooring system of the 320m-model, an initial mooring configuration was determined.
- A 3-line mooring configuration was used as it is a proven method in industry. Redundant lines are not used since the wind turbines are unmanned and have lower environmental risk in case of failure (than O&G platforms).

- The yaw stiffness matrix that was present in the 320m-model was removed and the bridle was modelled. The midline length of the bridle was increased until the yaw natural frequency was out of range of the 1P and 3P frequencies and the displacement did not cause a failure (within SIMA) of the mooring line.
- The same decay tests from the previous section were also performed. The surge, heave, and pitch frequencies were checked to ensure that they remained within 5% of values found in the 320m-model.
- The environmental load cases previously described were applied. Several iterations of pretension and line properties were then tested until the surge displacement was within 10% water depth (<60 m) for all load cases. The floater (with no environment present) was checked at each iteration to ensure that the spar remained at the origin in the static position. The weight of the whole system changed every time the line configuration changed. As a result, the buoyancy of the spar was correspondingly adjusted each time so that the waterline remained at the design level.
- The mooring system and model were then verified using 3 more wind and wave seeds. The wind seeds are adjusted in TurbSim wind file generator and the wave seed is changed directly in SIMA.
- The ULS checks were then performed.

The greatest challenge in designing the mooring was the dimensioning of the line. It is necessary to have a high enough tension to maintain the wind turbine within a particular surge radius and avoid slack lines, but low enough so that the breaking strength is not exceeded in extreme conditions. Additionally, it is important to have a short enough line for economic reasons; that is, the cost of the line and that the mooring footprint does not occupy an unreasonably large area.

6.2 The Catenary Equation

Basic static analysis of a catenary is used for initial design and configuration. This will give a general idea of the characteristics the selected mooring will need to have in order to maintain equilibrium. Figure 6.1 shows the set up of the problem. The line tension can be broken down into its vertical (T_z) and horizontal (T_H) components.

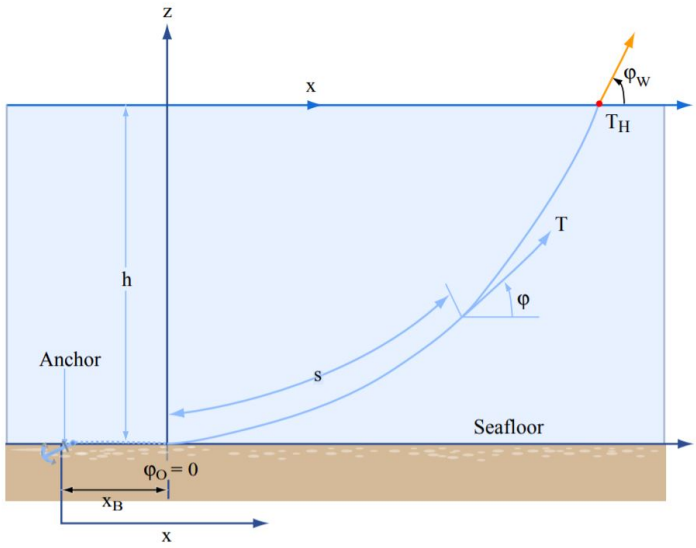

Figure 6.1: Diagram of catenary forces [29]

The line configuration is given by Equations 6.1 and 6.2. The tension along the line is shown by Equations 6.3 and 6.4. Here, w is the weight of the line.

$$s = \frac{T_H}{w}\sinh\left(\frac{w}{T_H}x\right) \tag{6.1}$$

$$z + h = \frac{T_H}{w}\left[\cosh\left(\frac{T_H}{w}x\right) - 1\right] \tag{6.2}$$

$$T = T_H + wh + \left(w + \rho g A\right)z \tag{6.3}$$

$$T_z = ws \tag{6.4}$$

Equation 6.5 gives the minimum length for a suspended length of mooring line when provided with the maximum line tension. For the initial calculations, this is set as the desired pretension of the line.

$$l_{min} = h\left(\frac{2T_{max}}{wh} - 1\right)^{\frac{1}{2}} \tag{6.5}$$

The horizontal force for that tension is then Equation 6.6.

$$T_H = T - wh \tag{6.6}$$

However, the length on the seabed must also be taken into account. This so called “horizontal line scope" is calculated using Equation 6.7.

$$x = \frac{T_H}{w}\sinh^{-1}\left(\frac{wl_{min}}{T_H}\right) \tag{6.7}$$

The vertical force at the fairlead is then shown by Equation 6.8.

$$T_z = wl_{min} \tag{6.8}$$

Equations 6.1 through 6.8 are only for an initial static analysis for a uniform inelastic line. These are used to determine an initial line configuration, then optimisation is done in SIMA to refine the properties and layout.

6.3 Mooring Line Selection and Dimensioning

The mooring line was designed based on the basic catenary theory presented in Section 6.2. The horizontal tension T_H was set as the desired pretension and from this, the minimum suspended length is found based on the MBS of mooring line selected. Consultation from Prof. Kjell Larsen indicated that it is common industry practice to seek a pretension of 10-25% of the MBS in the initial line selection. An excess of 100 m was also added to allow for the on-bed section; there should be no vertical tension component near the anchor point. After analysing several combinations of mooring line, including a purely polyester line with point masses, a chain-polyester-chain mooring line was selected. This combination was selected for the high durability of polyester line, combined with the weight of the chain. For the polyester section, Bridon Superline Polyester for permanent mooring was selected and for the chain section, Ramnäs Bruk Studless chain was selected; the properties of these two lines are shown in Table 6.2. The dimensions for the selected mooring line are shown in Table 6.3 and Figure 6.2.

The choice of using a chain-poly-chain configuration is twofold: the chain is added to the hang off region to increase the weight of the line without using point masses and chain is used on the seabed section to provide adequate weight for the restoring force when it is lifted off. Using chain near the seabed also prevents abrasion of the polyester lines or the infiltration of sand particles into the fibres which will negatively affect the fatigue life [35]. A purely chain line is too heavy for the spar at this depth. The chain and polyester must be carefully selected so that the MBSs are nearly the same for consistency throughout the line. For this project, the polyester selected has only 0.10% greater MBS than the chain.

Table 6.1: Comparison results of mooring configurations

	First Iteration	**Final Iteration**
Pretension [kN]	746	2904
Surge Displacement for LC3 [m]	187.4	48.5
Line Length [m]	3279	2829
MBS [kN]	22563	14715
Fairlead Radius [m]	6.5	8.0
Bridle Midline Length [m]	70	80

Table 6.2: Properties of selected mooring lines

	Bridon Superline Polyester Line	**Ramnäs Bruk Studless Chain**
Unit Mass in Air [kg/m]	33.6	432.0
Axial Stiffness [MN]	296.1	6309.3
Diameter [m]	0.229	0.265
Tension Capacity (MBS) [MN]	14.715	14.700

Table 6.3: Dimensions of selected mooring lines

Segment 1 (including Bridle Mid-length) - Chain [m]	450
Segment 2 - Polyester [m]	2129
Segment 3 - Chain [m]	350
Total Length [m]	2929
Footprint [m]	2862

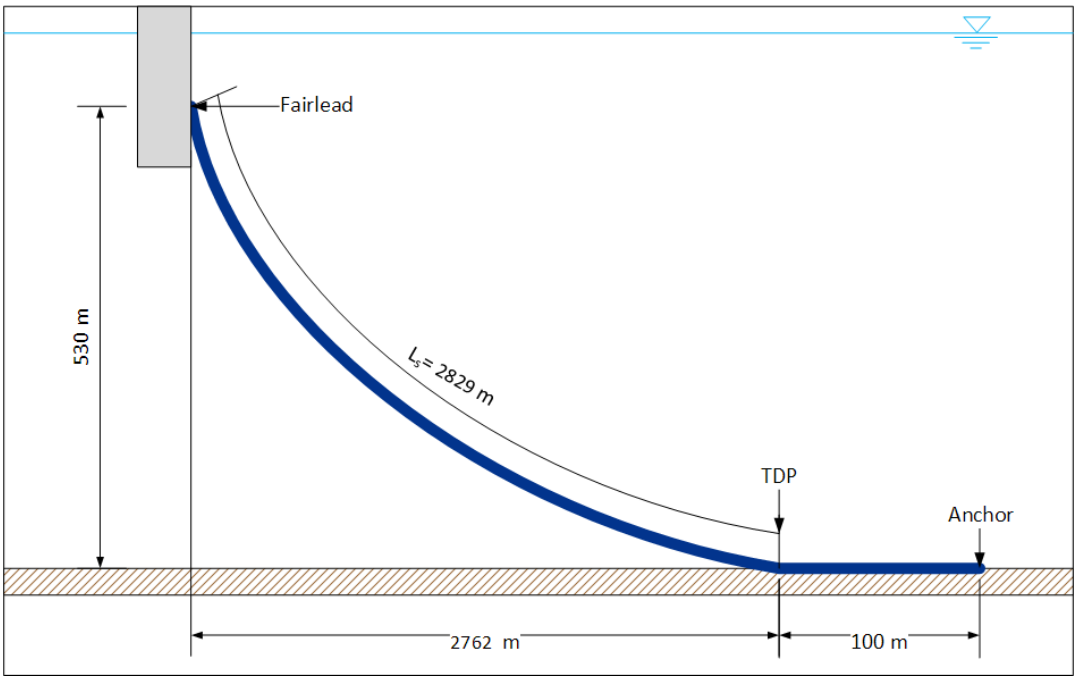

Figure 6.2: Visual representation of catenary dimensioning [Visio]

6.3.1 Design of the Bridle

A bridle (sometimes called a “crow’s foot") is often used in mooring of floating bodies to control the motion in yaw (rotation about the $z-$axis). For the 320m-model, a bridle was not modelled, instead a corresponding stiffness matrix was applied under the assumption that this would limit

the yaw of the spar similarly to a bridle. For the 600m-model, a bridle was designed. The fairleads were shifted 60° such that one bridle end from two mooring lines can be attached to a single fairlead and the anchor points will remain in the same general direction as the 320m-model. A schematic of the mooring lines in the xy-plane is shown in Figure 6.3 where the red dots indicate the anchor point, the black dots are where the bridle connects to the main mooring line, and the yellow dots are the fairlead placement. This diagram is not to scale.

Figure 6.4 shows the dimension of the bridle length. For the initial static configuration, the mid-line length (80 m) is used in calculations. This length was adjusted in order to control the yaw of the turbine under environmental loading. It was noticed there was approximately 15° of yaw movement in the most extreme cases. To limit this, the midline length was increased. However, lengthening by 20 m only reduced the yaw displacement a fraction of a degree, and as such, the fairleads were moved further out at a greater radius from the centre to restrict the motion more efficiently as shown in Table 6.4. With the current model, there is a maximum yaw displacement of ~ 7.5°, which significantly improves on the 320m-model which had a maximum yaw displacement of ~ 26°.

Table 6.4: Yaw Displacement with respect to fairlead position from centre

Distance from (0,0) [m]	**Maximum Yaw Displacement [°]**
6.5	26.5
8.0	6.91

6.3.2 Snap loads

Snap loads are defined as a sudden increase in tension after a period of slack (zero tension) [20]. This can cause high loads and failure within a mooring line, so care must be taken to ensure that there is always some pretension in the mooring line. In an effort to avoid slack lines (the results of the iteration process indicated slack events in the time series), the pretension was increased to 2904 kN or 20% of the MBS of the mooring line. Weller et al. [37] indicated that infrequent snap loads may be allowed and should not cause damage so long as the loading does not exceed the load capacity of the line.

6.3.3 Errors and Assumptions

It was assumed that the axial stiffness (EA [N]) of the line remains constant and was calculated using Equation 6.9 (provided by Prof. Kjell Larsen) where MBS is the minimum breaking strength and T_m is the mean tension. As a simplification, the desired pretension was used as T_m. However it is known that polyester lines can behave elastically to a certain extent and that the stiffness changes in accordance with the loads on the mooring lines (i.e. the stiffness EA is a function of the mean tension on the line). Using a constant stiffness may induce an error in the capacity of

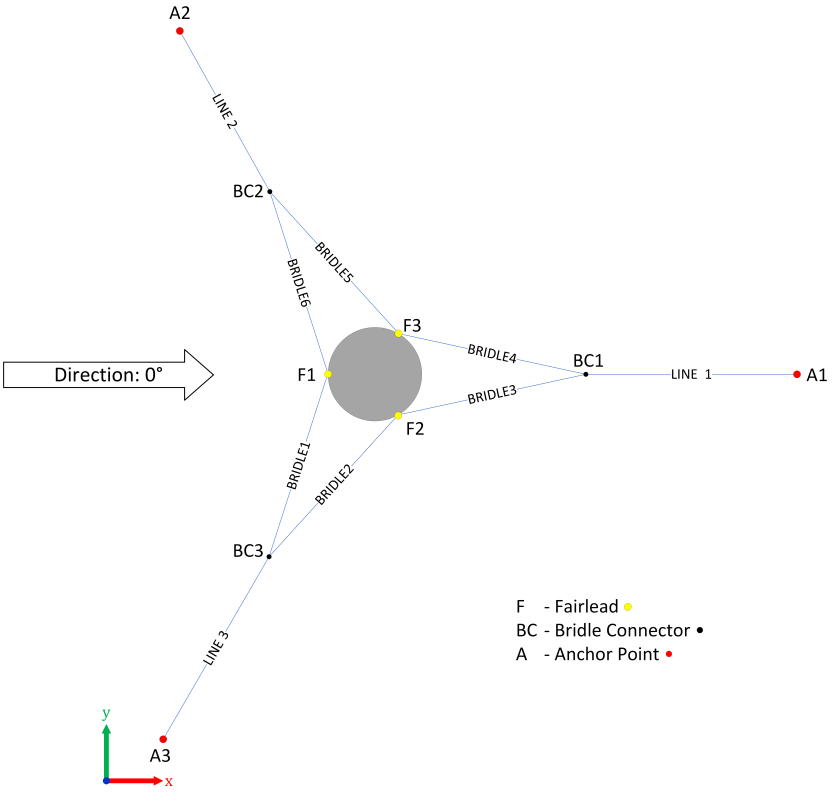

Figure 6.3: Orientation and new mooring configuration (with bridle) [Visio]

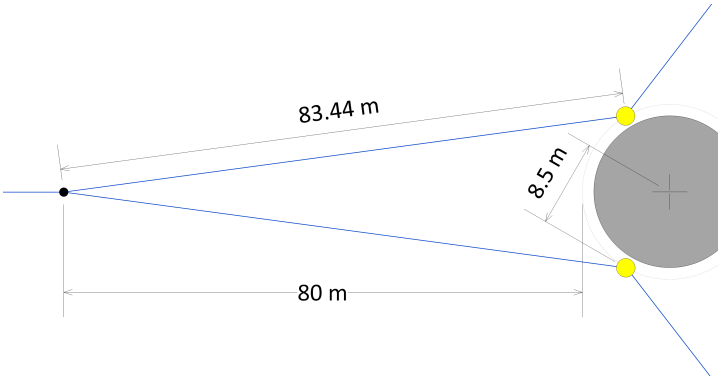

Figure 6.4: Bridle dimensioning [Visio]

the lines so this should be treated with care. However for this thesis, a constant stiffness is used.

$$EA = \text{MBS}\left(20 + 25.5\left(\frac{T_m}{\text{MBS}}\right)\right) \tag{6.9}$$

Marine growth is not accounted for. It is assumed that the polyester line will not suffer from UV degradation since the fairleads are located 70 m below MWL and damaging UV rays will not penetrate to that depth. Direct wave and current loads on the line are not considered as these

are negligible in comparison to the effect of the motions of the spar floater. The added mass and drag forces from the motion of the floater is accounted for in SIMA using added mass and drag coefficients as modelled by Xue [41]. The connection hardware at the fairleads, seabed, and the polyester-chain transitions are not modelled.

6.4 Environmental Analysis and Results

The same environmental conditions as presented in Section 4.2 Table 4.3 are applied to the 600m-model with the exception that the current extends to 600 m water depth instead of 320 m and load case 4 is discarded. The same TurbSim wind files are also used for both models.

Table 6.5 shows the results of the initial seed run. In these results, no slack lines are observed, mitigating the risk of snap loads. The maximum tensions observed also occur in the main line and not in the bridle, and the minimum tensions occur in the bridle as expected. Figures 6.5 through 6.7 are the time series of the line tensions of the 600m-model. The LF and WF induced tensions can also be be observed here, with the LF motion being most dominant in Load Case 1. The model is behaving as expected and will be verified using 3 more wind and wave seeds.

Table 6.5: Line tension extrema for 600m-model under environmental loading

		Tensions [kN]		
		LC1	**LC2**	**LC3**
Line 1	**Min**	2050.0	2060.0	1850.0
	Max	2590.0	2650.0	2610.0
Line 2	**Min**	3100.0	3160.0	3220.0
	Max	3870.0	3540.0	3690.0
Line 3	**Min**	3100.0	3020.0	3240.0
	Max	3910.0	3430.0	3750.0
Bridle 1	**Min**	1390.0	1800.0	2010.0
	Max	3420.0	3180.0	3140.0
Bridle 2	**Min**	575.5	544.3	816.6
	Max	2530.0	1870.0	1840.0
Bridle 3	**Min**	966.3	769.8	1100.0
	Max	1710.0	2030.0	1640.0
Bridle 4	**Min**	1100.0	862.0	1060.0
	Max	1810.0	2160.0	1610.0
Bridle 5	**Min**	605.1	660.1	742.5
	Max	2290.0	2130.0	1770.0
Bridle 6	**Min**	1450.0	1590.0	2090.0
	Max	3450.0	3140.0	3130.0

Table 6.6: Extreme tension locations

	LC1	LC2	LC3
Max Tension [kN]	3910.0	3540.0	3750.0
Location	Line 3	Line 2	Line 3
Min Tension [kN]	575.5	544.3	742.5
Location	Bridle 2	Bridle 2	Bridle 5

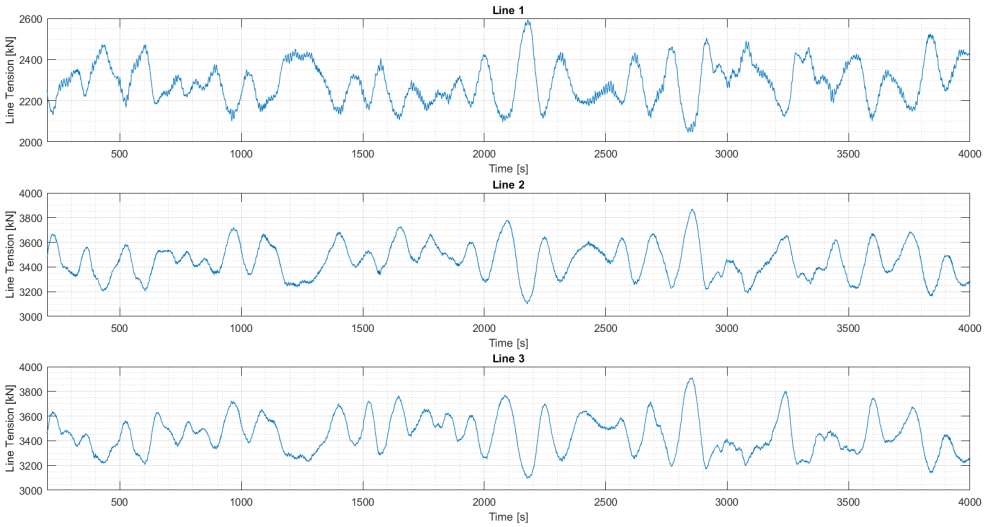

Figure 6.5: Time series of line tensions for deepwater model - Load Case 1

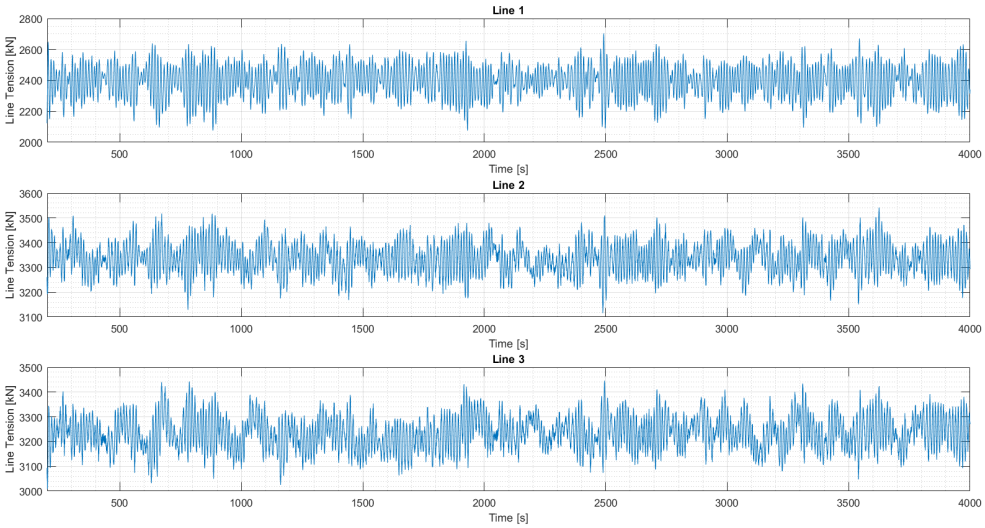

Figure 6.6: Time series of line tensions for deepwater model - Load Case 2

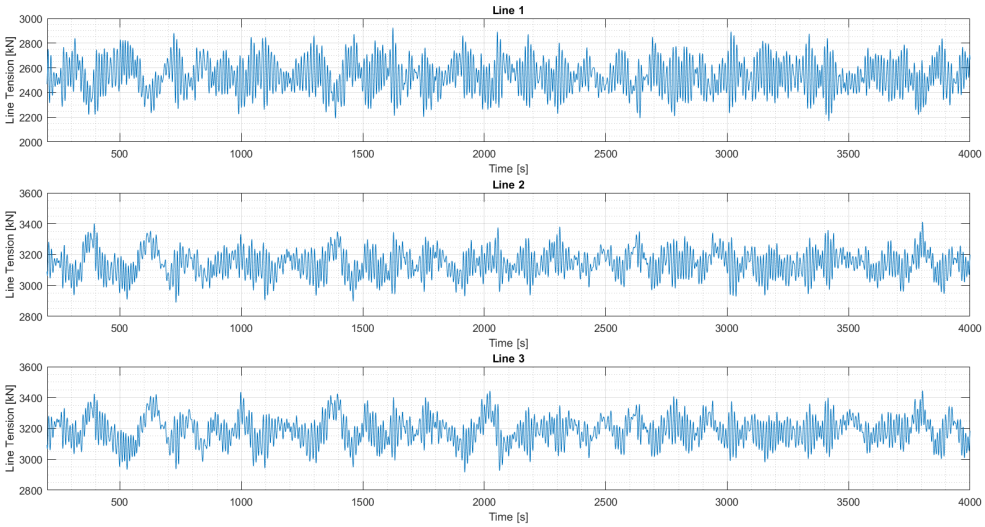

Figure 6.7: Time series of line tensions for deepwater model - Load Case 3

6.5 Comparison with the 320 m model

This section compares the performance of the two mooring line models. It should be again noted that the 320m- model uses purely chain mooring whereas the 600m-mooring uses a combination of chain and polyester line.

6.5.1 Natural Periods

Table 6.7 shows the comparisons of the natural periods of both water depth models. The heave and the pitch do not change much as these natural periods are mainly dictated by spar properties. The differences can be accounted for in the weight of the lines and subsequent change in buoyancy/ballast of the spar. The yaw, as previously mentioned, was controlled using an applied stiffness matrix which was removed once the bridle was modelled. Even though the natural period is now more than double that of the original natural period, this translates into a lower natural frequency which is now out of 1P frequency range. The bridle design is therefore an improvement over the original model.

The surge natural period is affected by the mooring lines and remains within an acceptable range (over 100 s).

Table 6.7: Natural period comparison between 320m-model and 600m-model

Degree of Freedom	**320m-model**		**600m-model**		**Difference**
	f_n [Hz]	T_n [s]	f_n [Hz]	T_n [s]	
Surge	0.007	138.7	0.007	137.1	1.09%
Heave	0.032	31.6	0.030	32.8	3.82%
Pitch	0.027	37.6	0.028	36.0	4.29%
Yaw	0.130	7.7	0.056	17.8	131%

6.5.2 Spar Offset

Table 6.8 presents the surge pitch and yaw offsets for 3 load cases under the original wind and wave seed. This mooring system improves the yaw offsets to <7° for all load cases. The surge offsets all remain under 10% of the water depth and are therefore acceptable for this project.

Table 6.8: Maximum surge offsets for 320m-model and 600m-model

	320m-model					**600m-model**				
	Surge [m]		**Pitch** [°]		**Yaw** [°]	**Surge** [m]		**Pitch** [°]		**Yaw** [°]
	Max	**Avg**	**Max**	**Avg**	**Max**	**Max**	**Avg**	**Max**	**Avg**	**Max**
LC1	49.3	32.8	11.9	7.10	7.67	56.5	36.3	11.5	6.86	4.50
LC2	25.5	18.2	7.35	3.33	13.3	30.0	24.5	7.45	3.84	6.91
LC3	42.8	29.7	10.0	4.51	26.5	40.1	30.2	6.24	2.75	0.81

6.6 Verification of model

The model was then verified by running simulations for 3 more random wind and wave seeds. The seed numbers were generated using the “RAND” function in Microsoft Excel. The wind seed number was changed directly in the TurbSim generator and the wave seed number was adjusted accordingly in SIMA. The seed variation is done to ensure that the model acts as expected and that no extreme outliers occur. It was found that line (excluding the bridle) seed deviation percentage was no more than 2.5% for the line tension extrema and averages. The percentage deviations for both the average and maximum offsets also remain within 6.3% of each other. Table 6.9 shows the averages of the line tension averages for all the seeds. The averages of the tension extremes are presented in Table 6.10. The offsets averages and extremes for all load cases are presented in Table 6.11. When finding the averages, maxima, and minima, the first 200 seconds were not accounted for as the data in this was considered transient and would give an inaccurate representation of the real values. No occurrences of slack lines, or line uplift at the seabed near the anchor point were observed in any of the seeds at any point during the time series.

Table 6.9: Average of line tension averages of all seeds

	Tensions [kN]		
	LC1	**LC2**	**LC3**
Line 1	2290.0	2393.9	2258.5
Line 2	3447.7	3339.2	3454.6
Line 3	3447.1	3235.1	3500.6
Bridle 1	2802.4	2582.2	2725.5
Bridle 2	1018.0	1042.4	1147.7
Bridle 3	1307.2	1340.6	1369.8
Bridle 4	1454.9	1511.4	1359.0
Bridle 5	998.5	1250.2	1112.2
Bridle 6	2825.3	2471.0	2720.1

Table 6.10: Average of line tension extrema of all seeds

		Tensions [kN]		
		LC1	**LC2**	**LC3**
Line 1	**Min**	2037.7	2057.1	1826.1
	Max	2554.1	2678.6	2583.5
Line 2	**Min**	3127.0	3137.5	3219.3
	Max	3889.8	3550.5	3696.3
Line 3	**Min**	3120.6	2989.6	3261.0
	Max	3926.1	3460.2	3771.5
Bridle 1	**Min**	1500.2	1670.1	2116.0
	Max	3433.6	3148.8	3210.5
Bridle 2	**Min**	593.5	568.0	749.4
	Max	2462.5	2009.9	1743.8
Bridle 3	**Min**	939.5	747.2	1091.8
	Max	1728.0	2103.1	1652.5
Bridle 4	**Min**	1042.1	823.5	1043.0
	Max	1838.6	2166.0	1631.2
Bridle 5	**Min**	599.1	665.5	711.0
	Max	2346.4	2292.2	1727.7
Bridle 6	**Min**	1562.3	1471.4	2114.4
	Max	3480.7	3137.7	3188.6

Table 6.11: Averages of offset maxima and averages for all seeds

	Surge				**Pitch**		**Yaw**
	Maximum		**Average**		**Maximum**	**Average**	**Maximum**
	[m]	% Offset	[m]	% Offset	[°]	[°]	[°]
LC1	56.3	9%	36.0	6%	11.2	6.8	4.4
LC2	30.7	5%	24.6	4%	7.4	3.8	7.4
LC3	40.3	7%	30.3	5%	7.3	2.8	0.8

6.6.1 ULS Checks

Even though the line loads observed in simulations do not exceed the breaking strength of the polyester or chain line selected, ULS checks must be done to ensure that the mooring system is in compliance with governing standards. This is done to ensure the safety of the mooring system, prevent tragic accidents, and as a precaution in the case of freak events.

The ULS checks for this project are done in accordance with DNV-OS-J103 [10]. The checks are performed by ensuring that the design tension T_d is less than the characteristic capacity S_C of the selected mooring line (Equation 6.10). The characteristic capacity of the mooring line is calculated using Equation 6.12. In this project the MBS of the chain is used since it is lower than the breaking strength of the polyester line. The load factors are then applied and T_d is calculated using Equation 6.11. DNV defines the characteristic mean tension $T_{c,\,mean}$ as the average of the line tension under 50-year environmental loading and the characteristic dynamic tension $T_{c,\,dyn}$ as the maximum value the line experiences under the same loading. Out of interest, the checks were done for all load cases. The load factors for both the high and normal safety classes are shown in Table 6.12.

$$S_C > T_d \tag{6.10}$$

$$T_d = \gamma_{mean} \cdot T_{c,\,mean} + \gamma_{dyn} \cdot T_{c,\,dyn} \tag{6.11}$$

$$S_C = 0.95 \cdot S_{MBS} \tag{6.12}$$

Table 6.12: ULS load factor requirements for design of mooring lines from DNV-OS-J103 [10]

Load Factor	**Normal Safety Class**	**High Safety Class**
γ_{mean}	1.3	1.5
γ_{dyn}	1.75	2.2

The ULS checks for both the high and normal safety class are presented in Table 6.13. The checks indicate that this configuration passes for all lines and all load cases.

Table 6.13: High and normal safety class ULS Checks for all load cases

		Characteristic Tensions		**High Safety Class**		**Normal Safety Class**	
		$T_{c,\ mean}$ [kN]	$T_{c,\ dyn}$ [kN]	T_d [kN]	$S_C > T_d$	T_d [kN]	$S_C > T_d$
LC1	**Line 1**	2876	2554	9933	PASS	8208	PASS
	Line 2	2921	2679	10274	PASS	8485	PASS
	Line 3	2921	2670	10256	PASS	8470	PASS
LC2	**Line 1**	2793	3890	12747	PASS	10438	PASS
	Line 2	2974	3551	12272	PASS	10080	PASS
	Line 3	2974	3626	12439	PASS	10212	PASS
LC3	**Line 1**	2648	3926	12609	PASS	10313	PASS
	Line 2	3094	3460	12253	PASS	10078	PASS
	Line 3	3094	3690	12759	PASS	10480	PASS
S_C = 13965 [kN]							

CHAPTER 7

THE SIMPLIFIED MODEL

This chapter discusses the simplified model of the 600m-model for use in a park arrangement. The SIMA programme cannot process multiple rotating turbines, and so the model must be simplified in order to assess the park arrangement of the mooring lines in SIMA. From this section forward, the complete model with a rotating turbine at 600 m water depth will be referred to as the "full model", and the model that is simplified model will be referred to as the "simplified model".

7.1 Simplifying the Wind Turbine

7.1.1 Background Information

This model is based on a master thesis project *Design of Mooring Systems for Large Floating Wind Turbines in Shallow Water* [19] by Kjetil Hole, who uses the same DTU 10MW RWT atop a semi-submersible floater. This project derived quadratic wind coefficients using the thrust curves of the wind turbine based on the selected wind speed (of the load case). As such, 3 sets of quadratic wind coefficients were derived, as well as one quadratic damping coefficient for each load case which represents the aerodynamic damping of the wind turbine. The turbine was simplified to a point mass and then the quadratic wind coefficients were applied. The decay and environmental tests were then compared to full model.

7.1.2 Simplification procedure

This section explains the procedure in developing the simplified model. The turbine is first reduced to a point mass and then the quadratic wind coefficients are found. The quadratic

damping coefficient is taken from the aforementioned master thesis by K.B. Hole [19].

7.1.2.1 Reducing RNA to point Mass

The following procedure was followed to find the representative lump mass.

1. Table 4.10 in the DTU Wind Energy Report [2] presents the blade cross section mass properties and centres. Since the table gives the blade properties at 51 intervals, the blade is divided into 50 sections. The mass of a single blade is found by multiplying the mass per length given in the table by the length of each section. The centre of mass of each section is assumed to be at the centre of the section along the blade, i.e. at the midpoint of the radius between two intervals. The parallel axis theorem (Equation 7.1) was used to find the moment of inertia around the shaft of the blades, the midpoint radii and the mass of the section. Summing these moments of inertia gives the moment of inertia I_{xx} of the blades about the main bearing around the $x-$axis.

2. Using the given masses and moments of inertia (Table 7.1), the parallel axis theorem was used to reduce the blades, hub mass, and nacelle to a representative point mass as shown in Figure 7.1. For this, the $x-$ and $y-$ moments of inertia are now taken at the yaw bearing, where the CoG of the representative point mass is assumed to act.

3. In SIMA, the blades, nacelle, and hub mass components were removed. These masses were then replaced with the representative point mass and the calculated moments of inertia. Table 7.2 shows the masses and moments of inertia calculated for the blades, nacelle, and hub mass, along with the sum total. These values are input into the SIMA model.

4. A decay test was performed on the new model with no environment. The simplified model with the representative point mass but without the quadratic wind coefficients was subjected to the same decay tests as for the full model in Chapter 6. The mooring system and other structural properties remain the same in the model. Only the blades, nacelle, and hub are removed and replaced with the point mass. The natural frequencies of the simplified model were then compared to the natural frequencies of the full model.

$$I_o = I_c + md^2 \tag{7.1}$$

I_o – moment of inertia of object about point O

I_c – moment of inertia of object about centroid

m – mass of object

d – distance between O and centroid

Table 7.1: Nacelle and Hub Properties [2]

Elevation of Yaw Bearing above Ground	119	[m]
Vertical Distance along Yaw Axis from Yaw Bearing to Shaft	2.75	[m]
Distance along Shaft from Hub Center to Yaw Axis	7.07	[m]
Distance along Shaft from Hub Center to Main Bearing	2.7	[m]
Hub Mass	105 520	[kg]
Hub Inertia about Low-Speed Shaft	325 671	[kg·m^2]
Nacelle Mass	446 036	[kg]
Nacelle Inertia about Yaw Axis	7 326 346	[kg·m^2]
Nacelle CM Location Downwind of Yaw Axis	2.687	[m]
Nacelle CM Location above Yaw Bearing	2.45	[m]

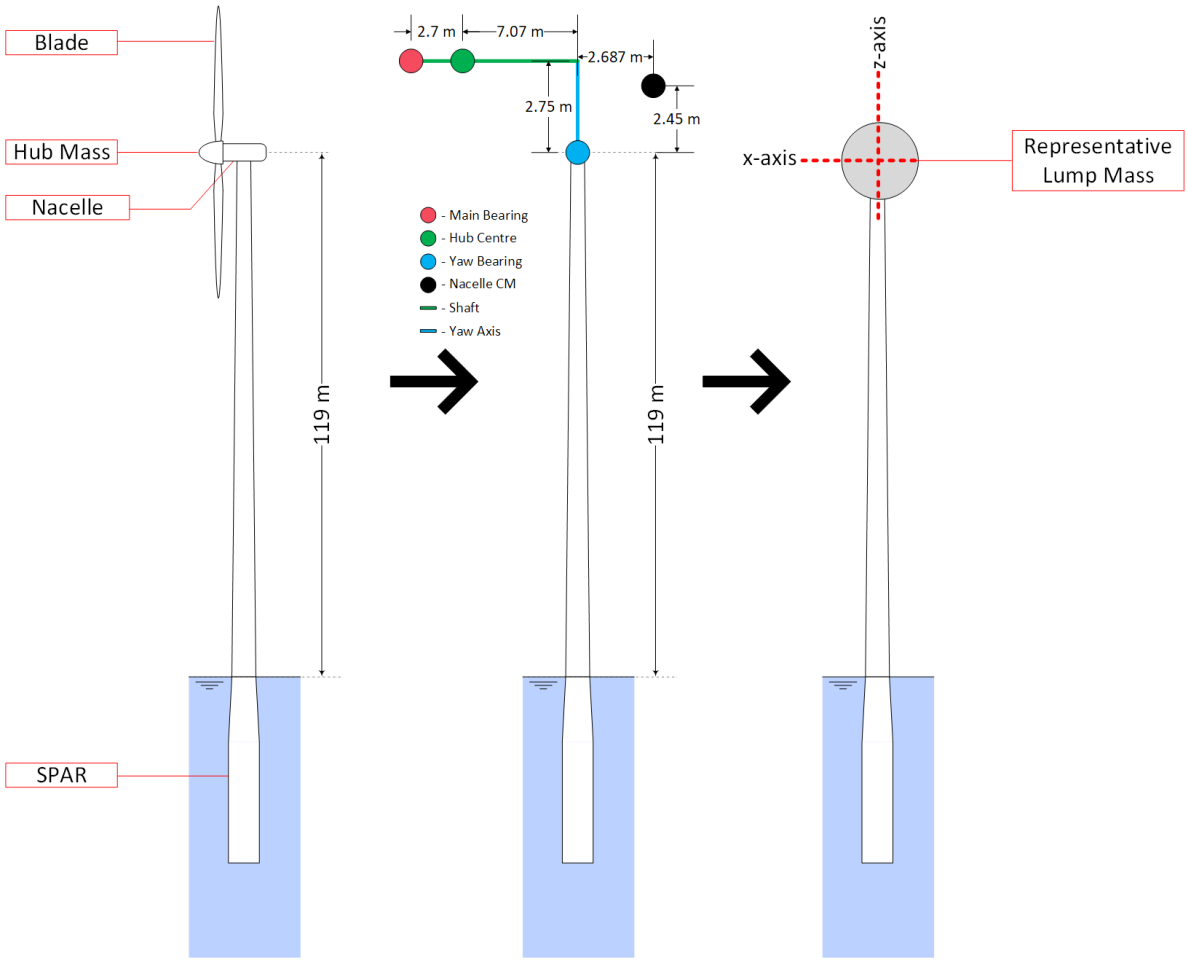

Figure 7.1: Graphic representation of simplified model [Visio]

As shown in Table 7.3, the surge, heave, and pitch natural frequencies of the simplified model are all within ±1% of the natural frequencies from the full model. The yaw natural frequency is

Table 7.2: Moments of inertia for representative point mass

	Mass [kg]	I_{xx} [kg·m^2]	I_{yy} [kg·m^2]	I_{zz} [kg·m^2]
Blades	1.22E+05	4.43E+06	1.52E+09	1.17E+07
Hub Mass	1.06E+05	1.12E+06	1.32E+09	5.27E+06
Nacelle	4.46E+05	2.68E+06	5.54E+09	7.33E+06
Total	6.74E+05	8.23E+06	8.38E+09	2.43E+07

slightly lower. This may be accounted for from errors in calculating local inertia (and centre of gravity) of the blades and therefore the application of the parallel axis theorem. The flexibility of the blades (movement of relative CoG) may have also contributed to the change in the system dynamics as a whole. The yaw frequency is of less concern than the surge, heave, and pitch frequencies in this project as it does not contribute as much to the line tensions or surge offset. It should also be noted that the yaw contribution of the blades will have a more significant impact on the yaw natural period of a spar than that of a semi-submersible (as used in [19]). Therefore the < 10% difference in yaw natural frequency is considered acceptable for this project. Figure 7.2 compares the natural frequency of the two models graphically.

Table 7.3: Comparison of natural periods between full and simplified model

	Full Model		**Simplified Model**		**Percent**
DOF	f_n [Hz]	T_n [s]	f_n [Hz]	T_n [s]	**Difference**
1 - Surge	0.007	137.1	0.007	137.2	0.05%
3 - Heave	0.030	32.8	0.030	32.8	0.02%
5 - Pitch	0.028	36.0	0.028	35.8	-0.62%
6 - Yaw	0.056	17.8	0.060	16.7	-6.48%

7.1.2.2 Application of the quadratic wind coefficients

The quadratic wind coefficients were applied for the 3 sets of load cases to the simplified model, and then 4 sets of seeds were run to compare the results for the full model. Since SIMA cannot process TurbSim files without a rotating turbine, the NPD wind model was used for this section. It was found that the coefficients used from the aforementioned master thesis [19] resulted in dissimilar (when compared to the full model) line tensions for the rated and 50-year load cases. Additionally, these coefficients consider the wind loads on the tower, which were originally neglected when checking the environmental loads on the full model. The tower loads are more significant for the 50-year case since the force of the wind on the tower is more dominant than the force on the wind turbine when the blades are pitched. For operating cases, the aerodynamic load on the rotor is the dominant load.

Another error was also found in the wind turbine controller file where the blades were not being pitched (feathered) correctly after cut out wind speed such that higher-than-expected loads were being applied to the wind turbine, causing large differences between the results of the full and

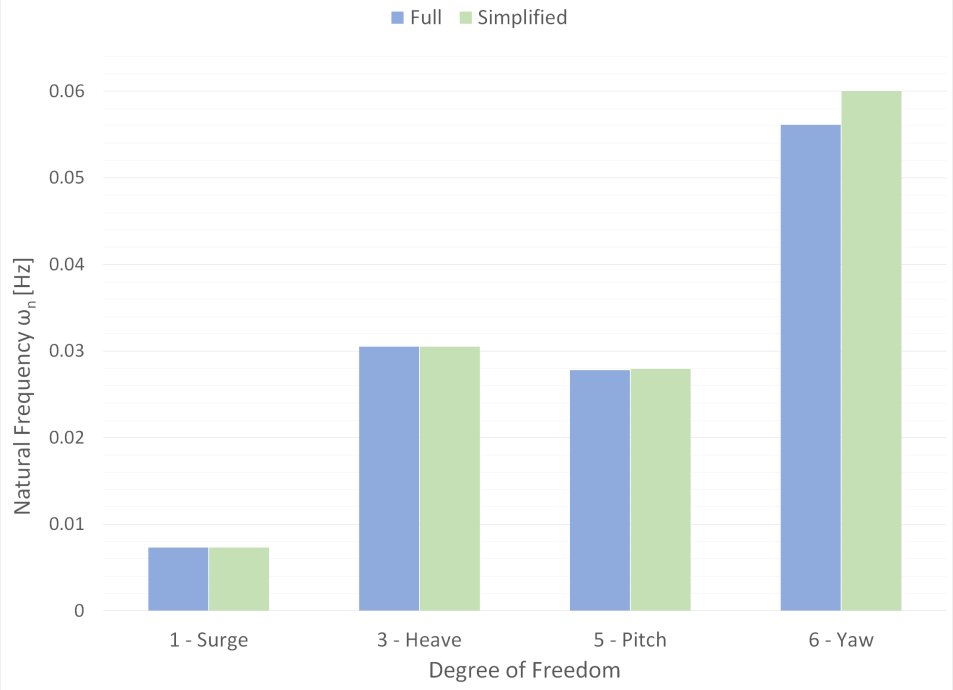

Figure 7.2: Graphical representation of decay comparison [Visio]

simplified models, as well as snap loads and large offsets in the 50-year conditions. Due to these inconsistencies, new coefficients needed to be derived, and the original environmental analysis had to be redone (the results presented in Chapter 6 are the corrected results).

To find the new quadratic wind coefficients, the following steps are implemented:

1. The spar was kept at a fixed position in SIMA and then the environmental load cases with a stationary uniform wind were applied in line with the wind turbine. The U_{10} average of the wind for each load case with a logarithmic profile is used. A stationary uniform wind is used here since any temporal or spacial variations may cause an inaccuracy in the calculated coefficients and the controller dynamics cannot be modelled in the simplified model. The current and wave conditions remain the same as for the full model simulation. It was ensured that the wind force acted on both the turbine and the tower superstructure.

2. Once the simulations for each load case was run, the shear and moment at the base of the tower was extracted from the RIFLEX output.

3. Using the base shear and moment for each load case, the coefficients were found using Equations 7.2 and 7.3 below where v is the wind speed at a 10 m height, C_F is coefficient corresponding to Surge motion and C_M is the coefficient corresponding to Pitch motion. F

and M are the base shear and moment respectively. The calculated C_F and C_M coefficients are therefore C1 and C5 respectively for the quadratic wind coefficients at direction 0°.

4. These wind coefficients were applied to the representative point mass in SIMA. This model was then verified using 4 seeds for each load case. These simulations used an NPD wind, and the same current and wave data as for the full model. This means that there is a single SIMA model for each load case. The time step for the dynamic analysis was also increased to 0.1 s compared to the time step of 0.005 s used in the full model simulations. The quadratic wind coefficients applied for the three load cases are presented in Appendix B.

5. The average line tensions and surge, pitch, and yaw offsets for the simplified model were then compared to the full model.

$$F = C_F v^2 \tag{7.2}$$

$$M = C_M v^2 \tag{7.3}$$

7.2 Results and Discussion

Table 7.4 shows the average tensions of all four seeds for each load case, for both the full and simplified model. Tables 7.5 and 7.6 show the extreme offsets for surge and pitch for the full and simplified model. The yaw is disregarded here as it is not considered a governing offset for this particular section of this project, and the yaw coefficients were not calculated. These values are an average of the 4 seeds and the complete individual results can be found in Appendix C. It was also found that the standard deviation between seeds for the simplified model was significantly less for both the offsets and the line tensions when compared to the standard deviation from the full model results. The average tensions varied by less than 0.5% (percentage deviation) and the average surge and pitch offsets varied by less than 1.1% (percentage deviation) (Table 7.7). The lack of variation in the seeds can be accounted for in the absence of turbulence in the wind model. The NPD wind will inherently have less variation than the TurbSim wind, resulting in less varied results.

As seen from Table 7.4, the simplified model is within ±5% of the line tensions of the full model. The operating cases have < 5% surge difference, but Load Case 3 is approximately 11% higher offset. Since this offset contributes only around 5 m difference, and this difference is on the more conservative side, the decision was made that this simplified model with the coefficients is acceptable for the purpose of array analysis. Some of the differences can also be accounted for in the fact that an NPD wind (with no turbulence) was used for the simplified model rather than the TurbSim wind file as in the full model.

Table 7.6 shows the average pitch comparisons for each load case. Even though the difference in pitch is greater than 10% for Load Case 3, the difference is only 0.3°. Additionally, this difference is a more conservative value as in the offsets and therefore this difference is accepted.

Figures 7.4, 7.5 and 7.6 show the power spectral density of the three line tensions for both the full and simplified models for load cases 1, 2, and 3 respectively. The transients are neglected in these spectra. In all three load cases the low frequency values look quite different. This may be attributed to the turbulence present in the wind for the full model; the simplified model uses the NPD wind model that varies only in time and not in space. In load case 1, there is greater power in the full model, but in load cases 2 and 3, the simplified model is higher. As expected signals of the higher frequencies associated with the waves are almost exactly the same since this was not changed between the two models. The time series comparisons for the surge offset are located in Appendix C.

Table 7.4: Line Tension [kN]) comparison between full and simplified models

		Full Model			**Simplified Model**			**% Difference**		
		LC1	**LC2**	**LC3**	**LC1**	**LC2**	**LC3**	**LC1**	**LC2**	**LC3**
Line1	**Min**	2037.7	2057.1	1827.8	2111.1	1980.7	1812.7	-4%	4%	1%
	Avg	2290.0	2393.9	2258.5	2268.4	2365.8	2210.2	1%	1%	2%
	Max	2554.1	2678.6	2584.9	2451.8	2698.6	2545.3	4%	-1%	2%
Line2	**Min**	3127.0	3137.5	3220.3	3236.5	3071.3	3278.8	-4%	2%	-2%
	Avg	3447.7	3339.2	3454.6	3471.6	3317.5	3540.8	-1%	1%	-2%
	Max	3889.8	3550.5	3697.6	3737.1	3568.7	3833.4	4%	-1%	-4%
Line3	**Min**	3120.6	2989.6	3260.3	3239.5	3057.6	3278.1	-4%	-2%	-1%
	Avg	3447.1	3235.1	3500.6	3472.6	3317.0	3540.8	-1%	-3%	-1%
	Max	3926.1	3460.2	3771.8	3735.6	3569.0	3820.2	5%	-3%	-1%

Table 7.5: Comparison of average surge offsets

	Full Model		**Simplified Model**		**Percent**
	Surge [m]	**% Offset**	**Surge [m]**	**% Offset**	**Difference**
LC1	36.0	6.00%	37.0	6.17%	3%
LC2	24.6	4.10%	25.8	4.31%	5%
LC3	30.3	5.05%	33.8	5.63%	11%

Table 7.6: Comparison of average pitch offsets

	Full Model	**Simplified Model**	**Percent**
	[°]	[°]	**Difference**
LC1	6.8	6.7	-1.7%
LC2	3.8	3.6	-6.6%
LC3	2.8	3.1	11.2%

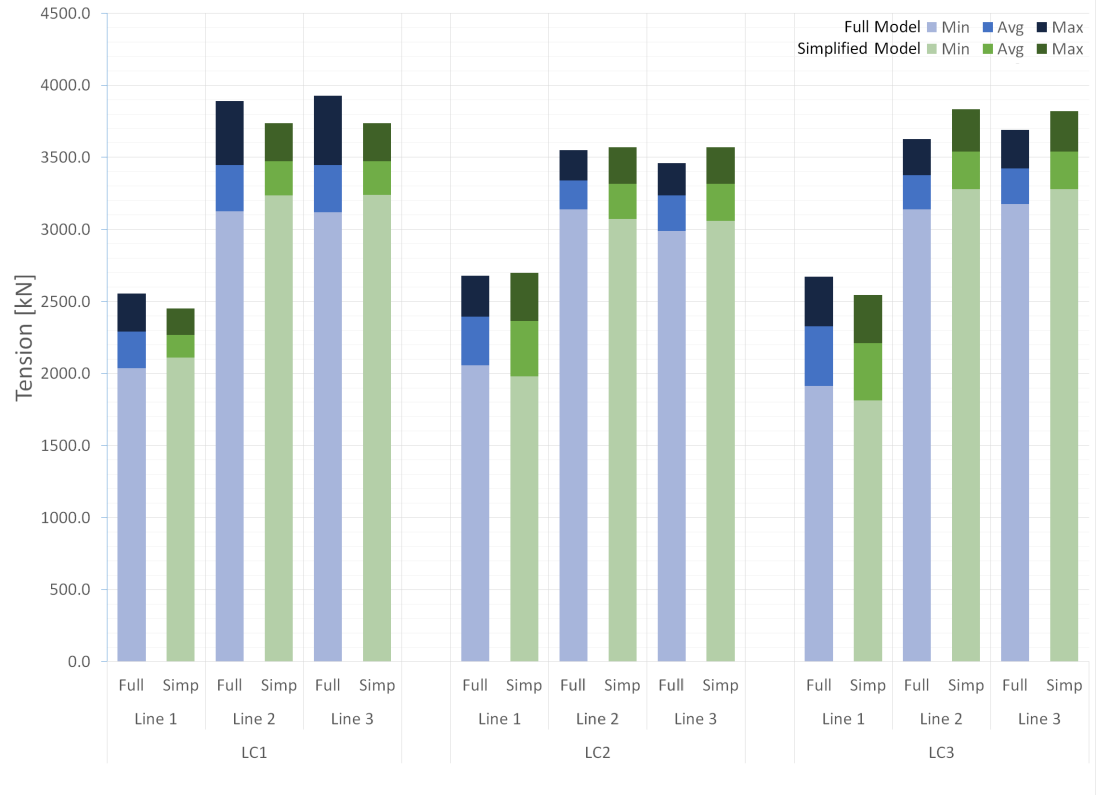

Figure 7.3: Graphical representation of tension comparison

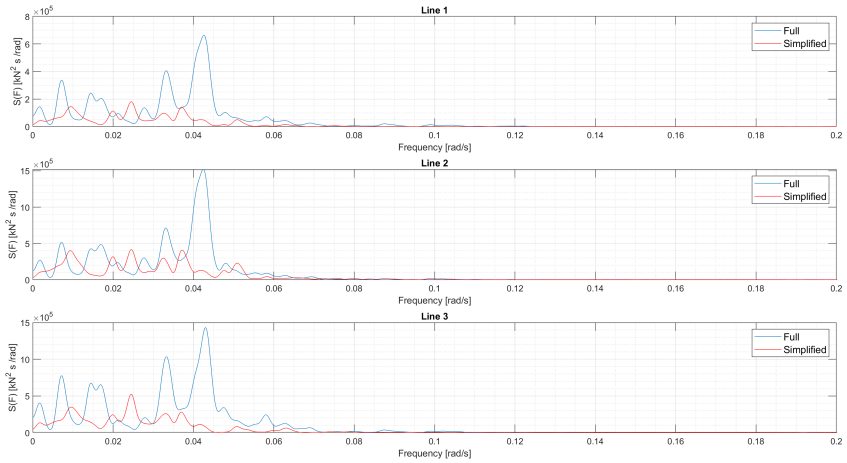

Figure 7.4: PSD of line tensions comparing the deepwater and simplified model - Load Case 1

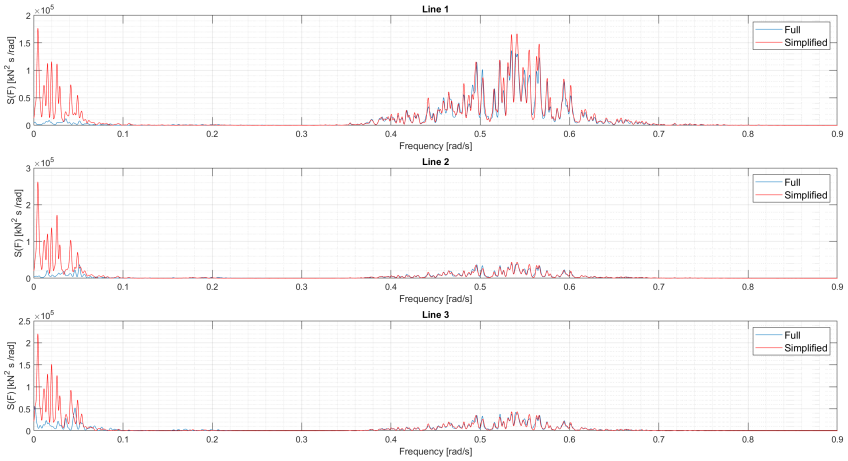

Figure 7.5: PSD of line tensions comparing the deepwater and simplified model - Load Case 2

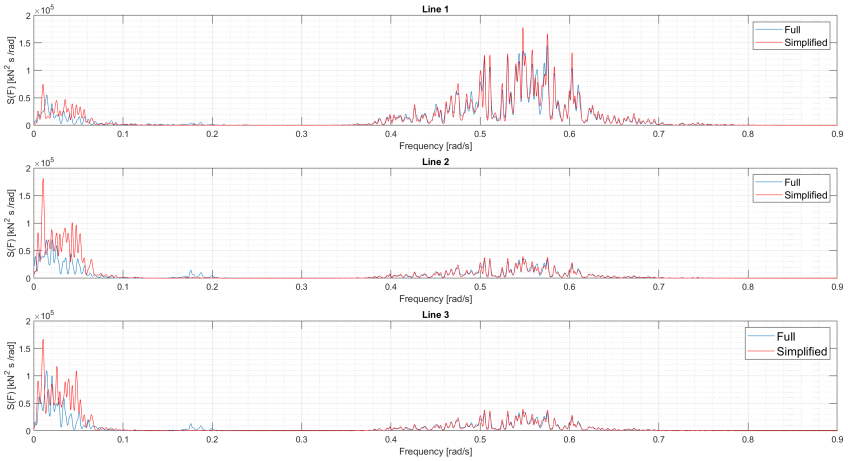

Figure 7.6: PSD of line tensions comparing the deepwater and simplified model - Load Case 3

Table 7.7: Percentage deviation of average line tensions and average surge and pitch offsets for simplified model

	LC1	**LC2**	**LC3**
Line 1	0.13%	0.10%	0.16%
Line 2	0.15%	0.11%	0.13%
Line 3	0.14%	0.10%	0.12%
Bridle 1	0.29%	0.25%	0.16%
Bridle 2	0.35%	0.27%	0.09%
Bridle 3	0.11%	0.07%	0.12%
Bridle 4	0.12%	0.08%	0.12%
Bridle 5	0.36%	0.26%	0.10%
Bridle 6	0.29%	0.25%	0.17%
Surge Offset	0.72%	0.80%	0.52%
Pitch Offset	0.82%	1.08%	0.53%

7.3 Further Comments

Although the coefficients of the simplified model are not perfect, the results of the environmental and decay analyses are considered close enough to be used for the park arrangement. In this case, the mooring system is being investigated and so the line tensions are the most important criteria for accuracy; thus, since the comparison of the line tension averages are within ±5% and the offsets are comparable albeit more conservative, these coefficients will be used. However, further work should be done on this simplified model to greater accuracy so that it can be readily used for future projects and studies. The coefficients that will affect the yaw $C6$ should also be calculated for greater simulation accuracy.

It is also noted that due to the larger time step of the simplified model, the processing time for the simulations is ~20 times shorter than for the full model. This means that the simplified model can be used for faster optimisation of the mooring lines.

CHAPTER 8

ARRANGEMENTS FOR SHARED ANCHOR POINTS

In this chapter, the results and analysis for turbines in an arrangement with shared anchor points are presented. Three possible arrangements were created in SIMA using the mooring lines developed in Chapter 6 and the simplified model developed in Chapter 7. These arrangements were then subjected to the same three load cases as the full deep-water model. The spars were checked to ensure they remained within the allowable offsets, and the mooring lines underwent ULS checks. The resultant force on the shared anchors is also checked.

8.1 Concept

For fixed bottom offshore structures, the foundation contributes to approximately 35% of the overall CAPEX [6]; however for FOWT the substructure also must incorporate the mooring and anchoring system. Since floating systems are a relatively new technology, there is no publicly available data on the cost of the mooring system compared to the cost of the wind turbine. It is estimated that mooring and anchoring system can cost over 10% of the overall CAPEX of a FOWT [26].

Unlike O&G floating platforms which are generally deployed in single units, offshore wind turbines are usually installed in multiples as a farm. In order to meet the world's growing demand for electricity, it will become necessary to install larger farms. In this project, the mooring design for a single turbine without shared anchors will need one anchor per mooring line per turbine. By creating these arrangements, the number of anchors used can be reduced, as well as the installation time due to the reduced anchors. This could greatly affect the reduction of the LCOE of a project. For deep water (as in this project), specialised installation equipment

will be required, resulting in higher installation costs. It is also likely that a location for such deep water will be further offshore, necessitating faster installations to reduce vessel hire costs. Therefore, it is reasonable to assume reducing the overall anchors will reduce the overall cost.

8.2 Methodology

For this section of the project the following process was implemented:

1. It was decided that three possible arrangements would be analysed.
2. The three arrangements were planned based on a park of approximately 5 turbines each (Hywind Scotland Pilot Park has 5 turbines [36]), with the intention to have as many 2-line, 180° anchor connections as possible for aesthetic reasons and so that the resulting anchor force will theoretically be 0 kN. Due to the layout of Arrangement 2 (Figure D.2), this configuration used 6 turbines instead of 5.
3. Once the basic design was conceived, the coordinates of the anchors and spars within the arrangements were found using basic geometry and then doubled checked in the software SACS.
4. Using these new coordinates, the spar and tower body with the simplified hub mass was copied so that an arrangement of 5 or 6 turbines was implemented in SIMA with the corresponding mooring lines.
5. For each model, the coefficients developed in Chapter 7 were applied, resulting in 3 different models (corresponding to each load case) for each arrangement (9 models total). In SIMA, different random wave and wind seeds were used for each run.
6. Four seeds for each of the three load cases were run for the 0° direction. The surge and pitch offsets were then extracted from these simulations, as well as the line tension time series. These results were then averaged.
7. The environment directions were then decided upon. Since it was found in Chapter 7 and in Step 6 above that there is very little variance between seeds, only 1 random wind and wave seed was analysed for each direction (other than 0°).

8.3 Arrangements Used For Analysis

Three possible arrangements are investigated using the simplified model. Figure 8.1 shows all three arrangements used. These diagrams can be seen in more detail in Appendix D. Table 8.1 compares the details for each arrangement in terms of the number of individual turbines included

in the farm, the total number of anchors, the number of shared anchors, the percentage reduction in number of anchors used overall for shared anchor points versus if the turbines had unshared anchor points, and the largest and smallest distances between two consecutive turbines in the arrangement.

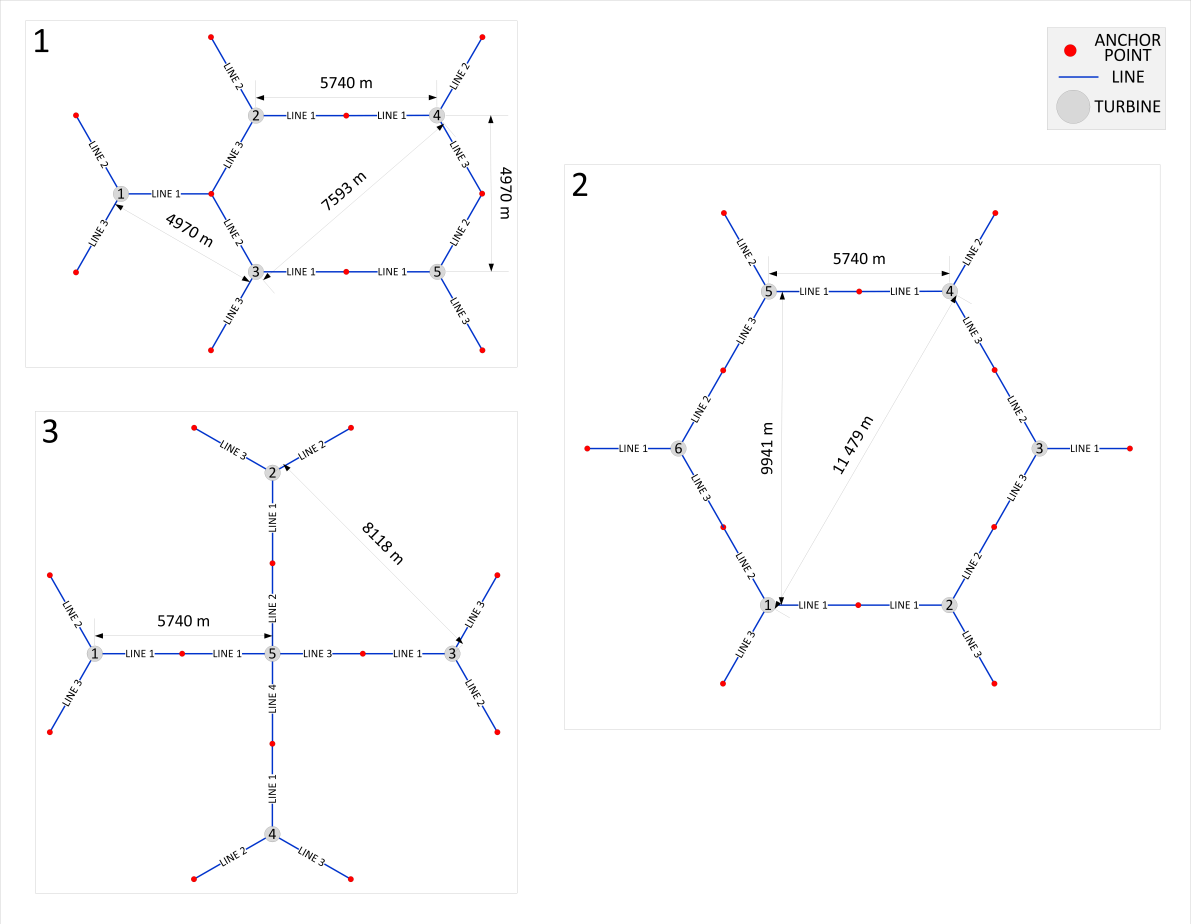

Figure 8.1: The three turbine mooring arrangements used in this project [Visio]

Table 8.1: Characteristics of the 3 arrangements

	Number of Turbines	**Number of Anchors**	**Number of Shared Anchors**	**Percentage Anchor Reduction**	**Distance between two consecutive turbines**		**Area Required** [km^2]	**Area per Turbine** [km^2]
					Largest [m]	**Smallest** [m]		
Arr. 1	5	10	4	33%	7 593	5 740	128.4	25.7
Arr. 2	6	12	6	33%	11 479	5 740	256.8	42.8
Arr. 3	5	12	4	20%	8 118	5 740	205.9	41.2

8.3.1 Arrangement 1

Arrangement 1 (Figure D.1) has 5 wind turbines, 4 shared anchors with 10 total anchors: 1 anchor with 3 lines at 120°, 2 anchors shared with 2 lines obliquely opposite each other, and 1 anchor

shared with two lines at a 120° angle to each other. This arrangement allows for 33% reduction in the number of anchors used.

8.3.2 Arrangement 2

Arrangement 2 (Figure D.2) has 6 wind turbines and 6 shared anchors out of 12 total anchors. Each shared anchor is subject to two lines in opposite directions. This arrangement also allows for a 33% reduction in the number of anchors used.

8.3.3 Arrangement 3

Arrangement 3 (Figure D.3) has 5 wind turbines and 4 shared anchors out of 12 total anchors. Each shared anchor is subject to two lines in opposite directions. This arrangement also allows for a 20% reduction in the number of anchors used. This arrangement is slightly different from the others as one of the turbines has 4 mooring lines and anchor points instead of three.

8.4 Analysis Procedure

After the layouts of the arrangements were decided upon, the coordinates of each anchor point, and wind turbine node were found. The arrangements were then implemented into SIMA using these coordinates. The 3 load cases were then applied to each arrangement in a variety of directions: 0-180° for Arrangement 1 and 0-90° for Arrangements 2 and 3. The results of this analysis were post processed to find the offsets of each spar, the line tensions, and the resulting forces on the shared anchors.

8.4.1 Wake Effects

The purpose of a wind turbine is to extract energy from the wind in order to generate electricity. As a result, the wind immediately leeward of the wind turbine rotor must have less energy than the windward side of the wind turbine, and the airflow of the incoming wind will become disturbed. Therefore, downwind of the wind turbine, the airflow will be turbulent and reduced in velocity. This downwind airflow is called the wake of the wind turbine. As the wake travels further downstream, the wake spreads and the dissipated energy is recovered until the airflow eventually returns to the free stream conditions [14].

Consequently, for wind turbine farms, wake effects are an important consideration when planning the layout of both offshore and onshore wind farms. As a rule of thumb, a spacing of at least ~6D is used for offshore wind farms [3]. For this project, the closest spacing is 5740 m or ~32D and according to Fontana et al. [11], wake effects can be ignored for spacings of more than 10D. If the wind turbines were closer where wake effects would have to be considered, then the wind coefficients derived would need to be adjusted in order to account for a reduction in wind velocity

and an increase in turbulence. Therefore, for these simulations, the wind coefficients are the same for each turbine in the arrangement regardless of the position in the arrangement with regards to the incoming wind flow. Additionally, the maximum surge offsets calculated will have little to no effect on the wake since change in position due to surge is significantly small when compared to the spacing.

Using general equations for the wind speed along a row of DTU 10MW RWT wind turbines, the velocity development for each spacing was plotted. It was shown that there is approximately no greater than 1.54% reduction in the wind velocity (Figure 8.2). This is based on the N.O. Jensen wake model [22] which is a simple single wake model, i.e. there is no interaction of the wake from adjacent turbine wakes. The N.O. Jensen model also assumes a linear wake expansion and disregards turbulence. This uses the assumption that the wind velocity v_1 at a distance x downstream of the turbine is related to the undisturbed upstream wind velocity v_0 by the turbine thrust coefficient C_T, the rotor radius r_0 and the radius r of the wind shadow cone as shown in Equation 8.1 [14]. The wake radius r is given by the radius of the area swept by the rotor r_0 (in this case the rotor diameter) and the entrainment factor α as shown in Equation 8.2 and Figure 8.3. The entrainment factor (Equation 8.3) thereby determines how fast the wake expands and is based on the hub height z and the surface roughness constant z_0. For this project, a simplified value of $\alpha = 0.1$ was used as this value was used in previous projects for the DTU 10MW RWT [4].

$$v_1 = v_0 + v_0\left(\sqrt{1-C_T}-1\right)\left(\frac{r_0}{r}\right)^2 \tag{8.1}$$

where

$$r = r_0 + \alpha x \tag{8.2}$$

and

$$\alpha = \frac{1}{2\ln\left(\frac{z}{z_0}\right)} \tag{8.3}$$

The N.O. Jensen wake model is a very simple model that is suitable for preliminary analysis. It does not consider the wake interactions for adjacent turbines or turbulent effects. For a more precise representation of wake interactions other wind resource models such as WAsP.dk, FAST Farm, and CFD should be used.

8.4.2 Directions

Each of the arrangements for each load case is subjected to in-line environmental loads for several directions. Only one seed per direction was used as it was found that there was very little variation in results when using seeds for the simplified model. Table 8.2 and Figure 8.4 show the directions applied for each arrangement. Since arrangements 2 and 3 are symmetric about

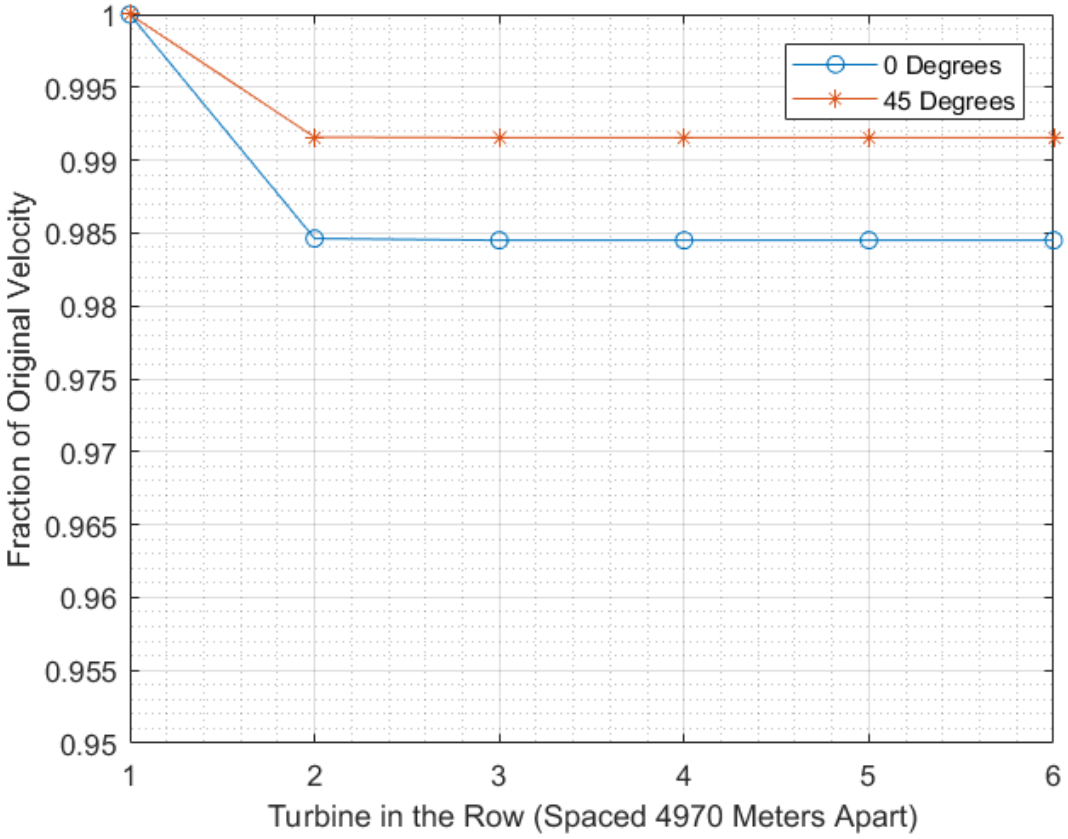

Figure 8.2: Plot of percentage of original free stream velocity versus consecutive number of turbines in a row

both the x- and y-axis, the loads were applied only from 0-90°. Since this project does not have an exact location, the wind, wave, and current loads are all in line with each other. If this were to be applied in an actual physical location, a wind rose for the area would need to be taken into account and the arrangements would be aligned with the dominant wind direction allowing for the most turbines exposed to undisturbed wind. Taking the loads in the same direction will theoretically give the most critical results.

8.5 Results Under Environmental Loading

This section presents the performance of the mooring system of the arrangement under environmental loading for three load cases: Rated Wind Speed, Cut-Out Wind Speed, and the 50-Year Wave and Wind condition. Each load case is then applied in several directions. Due to the large amount of results, only a select few are presented within the report. For the complete results, please refer to Appendices E through H.

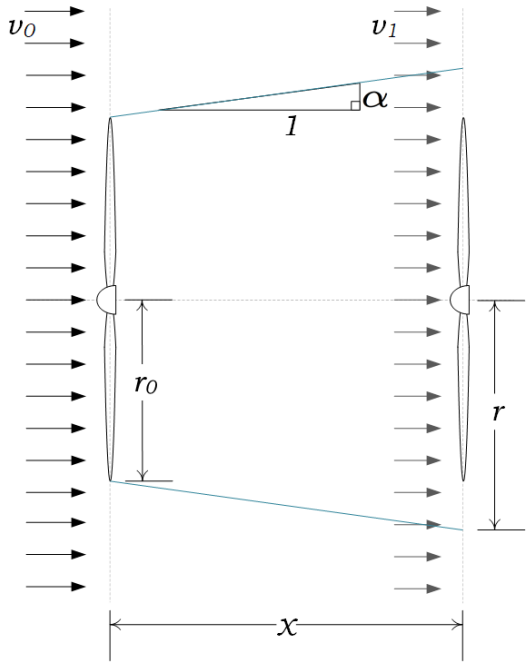

Figure 8.3: Graphic of the N.O. Jensen wake model concept [Visio]

Table 8.2: Directions for application of environmental loads

Direction Number	**Arrangement 1**	**Arrangement 2**	**Arrangement 3**
	Direction [°]		
0	0	0	0
1	30	30	30
2	45	45	45
3	60	60	60
4	75	75	75
5	90	90	90
6	105		
7	120		
8	135		
9	150		
10	180		

8.5.1 Offsets and Tensions

Table 8.3 presents the overall maxima and average tensions and surge offsets for each of the load cases in each arrangement over all the directions. The full results are found in Appendix E and Appendix F.

For the surge/sway offset checks, none of the spars exceeded the 10% of the water depth limit set by the aforementioned rule of thumb. The largest offset observed was 52.7 m in Arrangement 2,

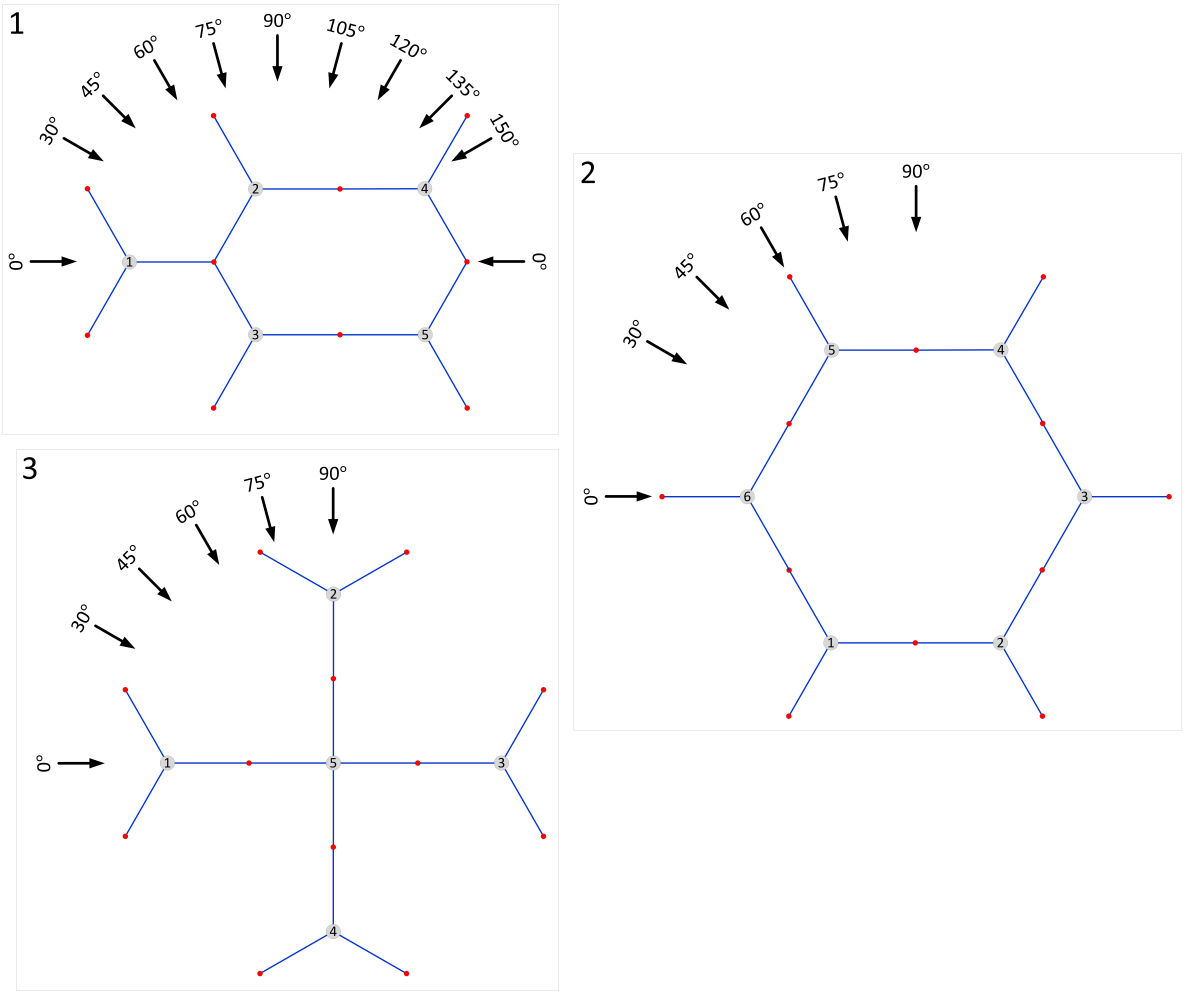

Figure 8.4: Graphic of environmental directions applied to arrays [Visio]

Load Case 1. Since the environmental loads were applied from many directions, the resultant offset from the surge and sway offset was calculated using the Pythagorean theorem to determine the maximum displacement from neutral in the xy-plane, These offsets were calculated in the time domain. The average offsets for all the arrangements are within 6% of each other. However, the maximum offsets are within 5% of each other for all arrangements in load cases 1 and 3, which cause the most severe conditions. The tensions for all the arrangements between the different load cases for both the overall maximum and average values are within 2% of each other

8.5.2 ULS Checks

Each load case for each direction in each line was checked at the ultimate limit state according to DNV-OS-J103 [10] as described in Section 6.6.1. All the arrangements failed the high safety class in at least one direction for all load cases, but easily passed for the normal safety class. The high

Table 8.3: Overall tensions and surge offsets for each load case in each arrangement

			LC1	**LC2**	**LC3**
Tensions [kN]	Arrangement 1	Avg	3042.9	2988.7	3070.1
		Max	4449.0	4178.9	4527.1
	Arrangement 2	Avg	3044.9	2988.6	3070.1
		Max	4409.6	4063.9	4432.4
	Arrangement 3	Avg	3019.8	2970.7	3048.1
		Max	4463.0	4110.9	4517.8
Surge Offset [m]	Arrangement 1	Avg	33.0	21.2	28.4
		Max	50.5	41.8	46.3
	Arrangement 2	Avg	33.5	21.3	28.5
		Max	52.7	35.4	44.8
	Arrangement 3	Avg	31.7	20.1	27.2
		Max	50.4	38.6	44.8

safety class was checked as this is the criteria needed for mooring systems without redundancy (i.e. without "extra" mooring lines). However, according to DNV [10], the normal safety class may be used if the turbines are not within collision distance of each other. This requirement is quite vague; however it may be argued that the spars are at least 5 km distance away from each other and that the normal safety class is acceptable. These conclusions are made without considering the limitations of the cabling system of the wind turbine. Ultimately, it is up to local regulations and the certifying body to determine whether the high safety class is needed.

All the ULS checks can be seen in Appendix H. For demonstrative reasons, the ULS checks for Arrangement 1, Load Case 1, Direction 0 are presented in Table 8.5; the average and maximum line tensions used for these calculations are shown in Table 8.4. “Line 1" is shortened to "L1" in these tables for brevity. When checked, the lines fail when there is only one line to windward and there is over a 50% increase in line tension (from pretension). The lines failed by no more than $\sim 13\%$ of the characteristic capacity S_C. In order to pass the high safety class the pretension can be slightly decreased or a line with a higher MBS can be used; this however will increase the weight of the line as well as the expense. Lowering the pretension should be done with care so as not to greatly increase the surge offset such that the system fails there instead.

Table 8.4: Average and maximum line tensions for Arrangement 1, Load Case 1, Direction 0 (0°)

	Turbine 1		**Turbine 2**		**Turbine 3**		**Turbine 4**		**Turbine 5**	
	Avg	**Max**	**Avg**	**Max**	**Avg**	**Max**	**Avg**	**Max**	**Avg**	**Max**
L1 [kN]	2556	2452	2289	2455	2289	2455	3822	4361	3822	4361
L2 [kN]	3165	3737	3437	3740	3437	3740	2612	2718	2612	2718
L3 [kN]	3165	3736	3437	3733	3437	3733	2612	2716	2612	2716

Table 8.5: ULS checks for Arrangement 1, Load Case 1, Direction 0 (0°)

	Turbine 1		**Turbine 2**		**Turbine 3**		**Turbine 4**		**Turbine 5**	
	T_d	$S_C > T_d$	T_d	$S_C > T_d$	T_d	$S_C > T_d$	T_d	$S_C > T_d$	T_d	$S_C > T_d$
High Safety Class										
L1 [kN]	9228	PASS	8834	PASS	8834	PASS	15326	FAIL	15326	FAIL
L2 [kN]	12969	PASS	13384	PASS	13384	PASS	9897	PASS	9897	PASS
L3 [kN]	12966	PASS	13368	PASS	13368	PASS	9894	PASS	9894	PASS
Normal Safety Class										
L1 [kN]	7613	PASS	7272	PASS	7272	PASS	12600	PASS	12600	PASS
L2 [kN]	10654	PASS	11014	PASS	11014	PASS	8151	PASS	8151	PASS
L3 [kN]	10652	PASS	11000	PASS	11000	PASS	8149	PASS	8149	PASS

8.5.3 Resultant Forces on Shared Anchors

For the shared anchors, the resultant forces are checked to determine which arrangement would be best in terms of the reduction of overall loading on the anchors. In theory, an anchor with a smaller capacity may be used for these shared anchors [11], [16], [12]. As such, anchor groups were created as shown in Figure 8.5. The lines and turbines for these groups are presented in Table 8.6. Figure 8.6 shows the time series of the resultant forces on the anchors for Arrangement 2. The LF influence can clearly be seen but the WF is more difficult to see in these plots since there is less influence from the waves in load case 1. The influence of the wave frequency can be seen in the PSD plots of Figure 8.7 which remain aproximately the same for all anchor groups. The low frequency influence is seen where the resultant tension in anchor group 4 is the highest due to the lines being in-line with the wind, waves and current. If the environment is in line with two mooring lines of opposing directions, the upwind line has a higher tension than the downwind line, and so the resultant is in the direction of the upwind line. This is caused by the displacement of the wind turbines stretching the upwind line and compressing the downwind line. Fontana et al. [11] also found up to 100% reductions on shared anchors for a three line system. The remaining PSD plots for all load cases in all arrangements for the shared anchors can be found in Appendix G,

8.6 General Discussion

In this project Arrangement 3 is the least favourable since it uses an additional line as well as has less anchor reduction. Arrangement 2 has higher average reduction in resultant anchor loads, without higher average tensions. The downfall of Arrangement 2 is the large amount of wasted real estate in the centre resulting in a high footprint.

Arrangement 1 also has a large empty area in the middle, and the configuration of anchor group 5 does not allow for any overall decrease in resultant force. However, the resultant force does not increase and the anchor design is governed by the highest individual loads, not the resultant

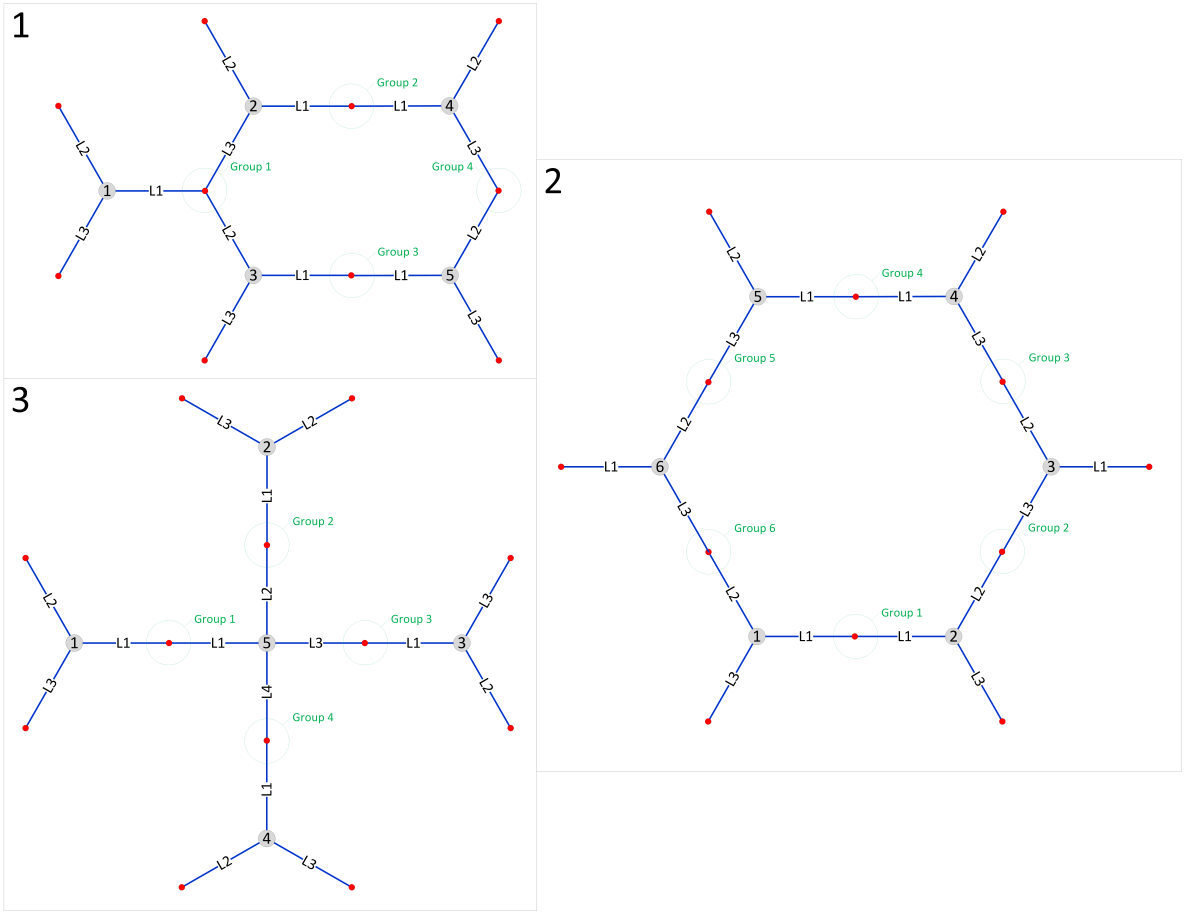

Figure 8.5: Line groups for shared anchors

loads [18]. This design also has the lowest footprint of the 3 arrangements

The arrangements presented here all pass the DNV ULS normal safety class check and remain within the 10% of the surge offset under environmental loading in a 50-Year storm condition. Since the turbines are spaced over 10D apart, there should be no issue regarding wake control. Suggestions for further work to improve the design are explained in Section 8.6.1 below.

8.6.1 Further Work

This section outlines suggested improvements to the arrangements.

8.6.1.1 Arrays

To improve the footprint of the mooring arrangement, the length of the mooring line can be reduced by creating floating mooring arrays. Figure 8.8 illustrates this concept. This is a combination of a tension leg and catenary mooring system where the catenary is attached to a floating

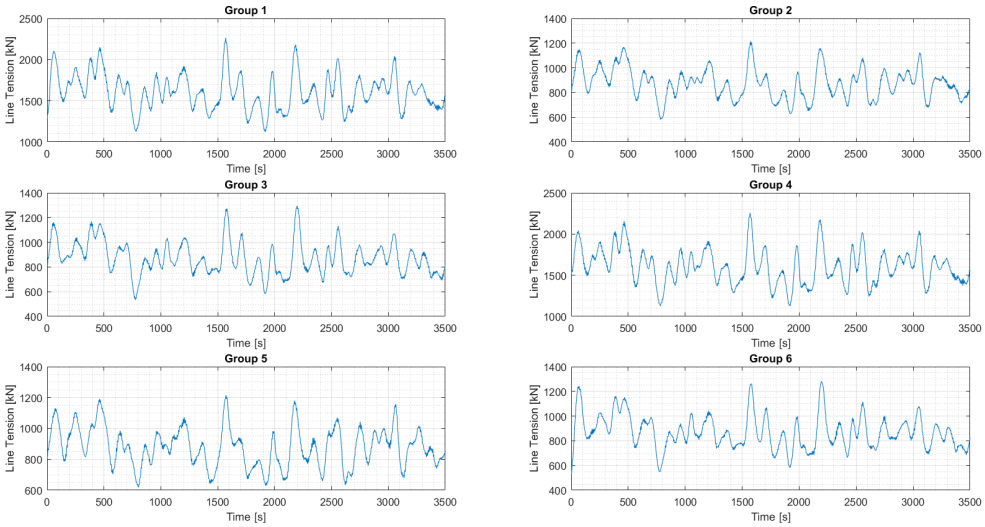

Figure 8.6: Time series of resultant anchor forces for Arrangement 2 Loadcase 1, Direction 0 (0°)

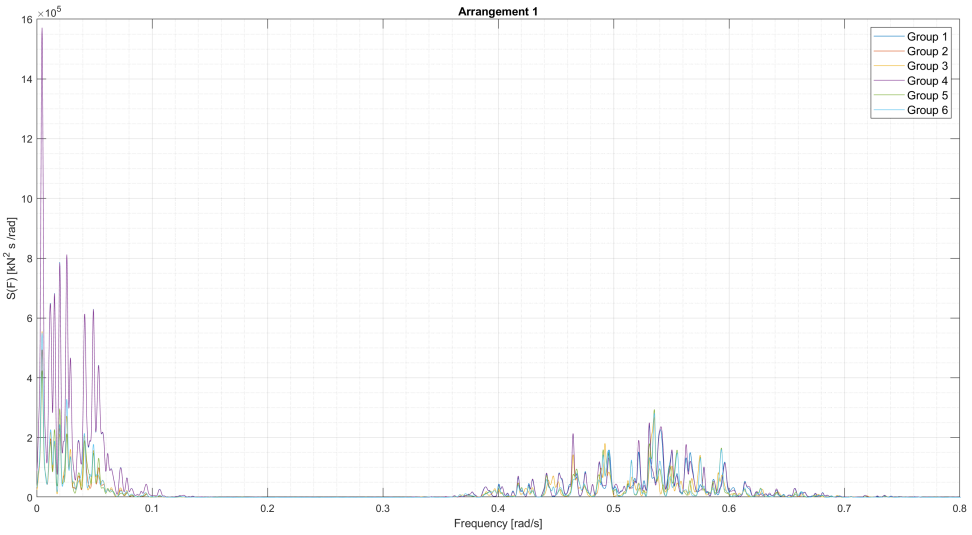

Figure 8.7: PSD for Arrangement 2 Loadcase 2, Direction 0 (0°)

"anchor" buoy.

Some research has been done on arrays with wave energy converters by Ringsberg et al [33]. However these devices have very different criteria for limitations with movement compared to FOWT, so the results from this study will not be directly applicable. The movements will also be coupled with the shared floaters and therefore the loading and analysis will be much more complex, leading to a computationally expensive project.

Table 8.6: Line groups for shared anchors

	Arrangement 1	**Arrangement 2**	**Arrangement 3**
Group 1	Turbine 1 Line 1 Turbine 2 Line 3 Turbine 3 Line 2	Turbine 1 Line 1 Turbine 2 Line 1	Turbine 1 Line 1 Turbine 5 Line 1
Group 2	Turbine 2 Line 1 Turbine 4 Line 1	Turbine 2 Line 2 Turbine 3 Line 3	Turbine 2 Line 1 Turbine 5 Line 2
Group 3	Turbine 3 Line 1 Turbine 5 Line 1	Turbine 3 Line 2 Turbine 4 Line 2	Turbine 3 Line 1 Turbine 5 Line 3
Group 4	Turbine 4 Line 3 Turbine 5 Line 2	Turbine 4 Line 1 Turbine 5 Line 1	Turbine 4 Line 1 Turbine 5 Line 3
Group 5		Turbine 5 Line 3 Turbine 6 Line 3	
Group 6		Turbine 6 Line 2 Turbine 1 Line 2	

Table 8.7: Overall reduction on anchor loads for each arrangement

	Arrangement 1			**Arrangement 2**			**Arrangement 3**		
	Max	**Min**	**Avg**	**Max**	**Min**	**Avg**	**Max**	**Min**	**Avg**
LC1	100.0%	0.7%	59.8%	100.0%	47.7%	78.2%	99.9%	21.9%	72.7%
LC2	100.0%	0.1%	62.9%	100.0%	51.6%	81.9%	99.9%	40.4%	78.6%
LC3	100.0%	0.1%	58.5%	100.0%	46.0%	76.6%	99.9%	14.9%	72.3%

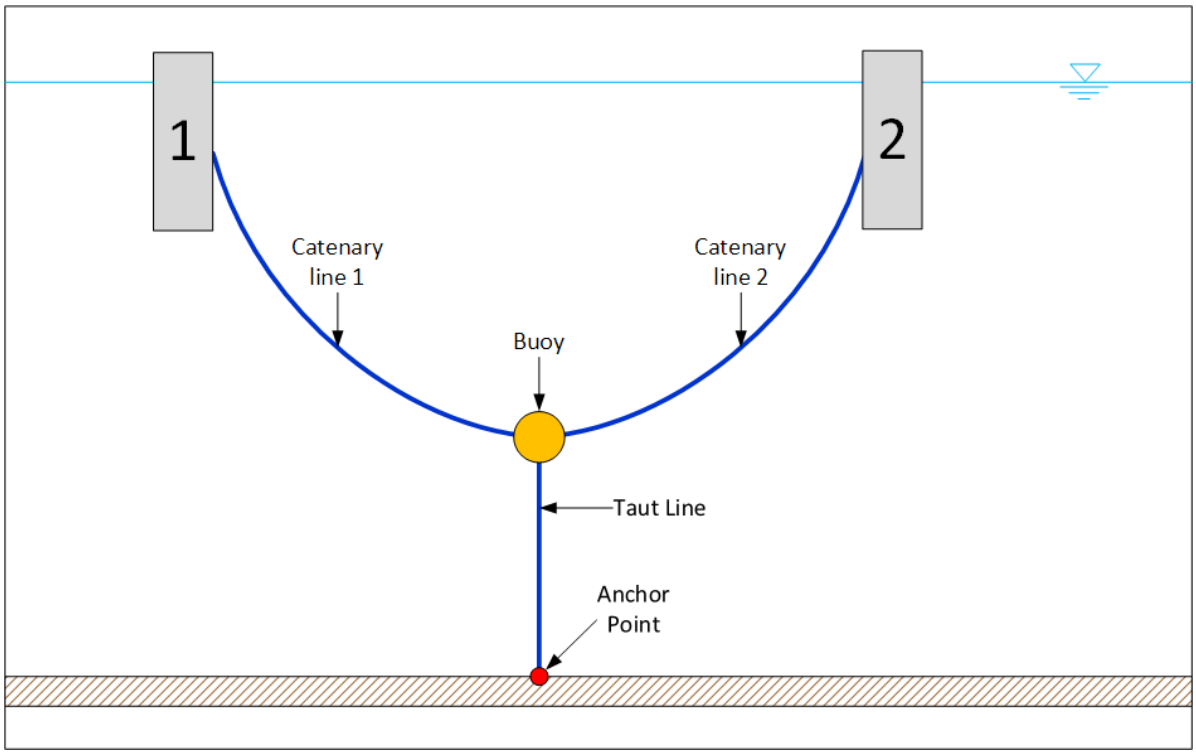

Figure 8.8: Floating Anchor Concept [Visio]

8.6.1.2 Taut Mooring

To reduce the line length and footprint, taut spread mooring (as shown in Figure 2.2) may also be investigated. This is usually done using purely synthetic line instead of a chain-poly-chain combination resulting in a simpler line and possibly simpler installations. The complication with taut mooring for shared anchors is that the anchor chosen will need to resist both vertical and horizontal loading in multiple directions, resulting in an even more complex loading scenario. Taut mooring is also sensitive to changes in the water depth since the lines are pretensioned. If there are large tidal changes or a storm surge, the lines maybe have to be tensioned and adjusted accordingly in order to maintain the correct waterline position of the floater.

8.6.1.3 Repeating Patterns

Figure 8.9 shows modified versions of Arrangements 1 (Figure D.1) and 2 (Figure D.2). These new patterns take up less real estate than their predecessors and allow for a greater reduction in anchor points. This comes at the loss of no lines at 180° in Arrangement A and a 6-line anchor in Arrangement B, which could potentially increase the load on the anchor points. Arrangement B also includes several shared anchors with 2 lines at 60°, a scenario which was not investigated in this project.

Still these arrangements are worth investigating as the layouts can be seen as “tiles” that can be used in repeating patterns for wind farms of larger sizes. That is, if the design is proven, it can be reused in different locations (within environmental/depth limitations) and in larger farms by repeating the pattern.

Table 8.8: Characteristics of arrangements for repetitive patterns

	Number of Turbines	**Number of Anchors**	**Number of Shared Anchors**	**Percentage Anchor Reduction**	**Distance between two consecutive turbines**		**Area Required** [km^2]	**Area per Turbine** [km^2]
					Largest [m]	**Smallest** [m]		
Arr. A	5	9	5	40%	8 586	4 970	128.4	25.7
Arr. B	6	7	7	44%	5 740	2 862	85.6	14.3

8.6.2 Challenges and Complications

While a reduction in anchors can contribute to a significant reduction in overall cost, the presence of multidirectional loading will result in a more complex loading scenario on the anchor. When anchors are shared, the loads will be cyclic in multiple directions which is not well understood in offshore geotechnics [18] since the industry standard for offshore anchors are with regards to unidirectional loading for O&G structures. According to research by Ringsberg et al. [33], the feasibility of shared anchors for mooring arrangements is greatly dependent on the LCOE, LCA, risk assessment of the entire project, not just the hydrodynamic and structure response analyses. Experiments by Herduin [18] also indicate that the capacity of a suction caisson anchor

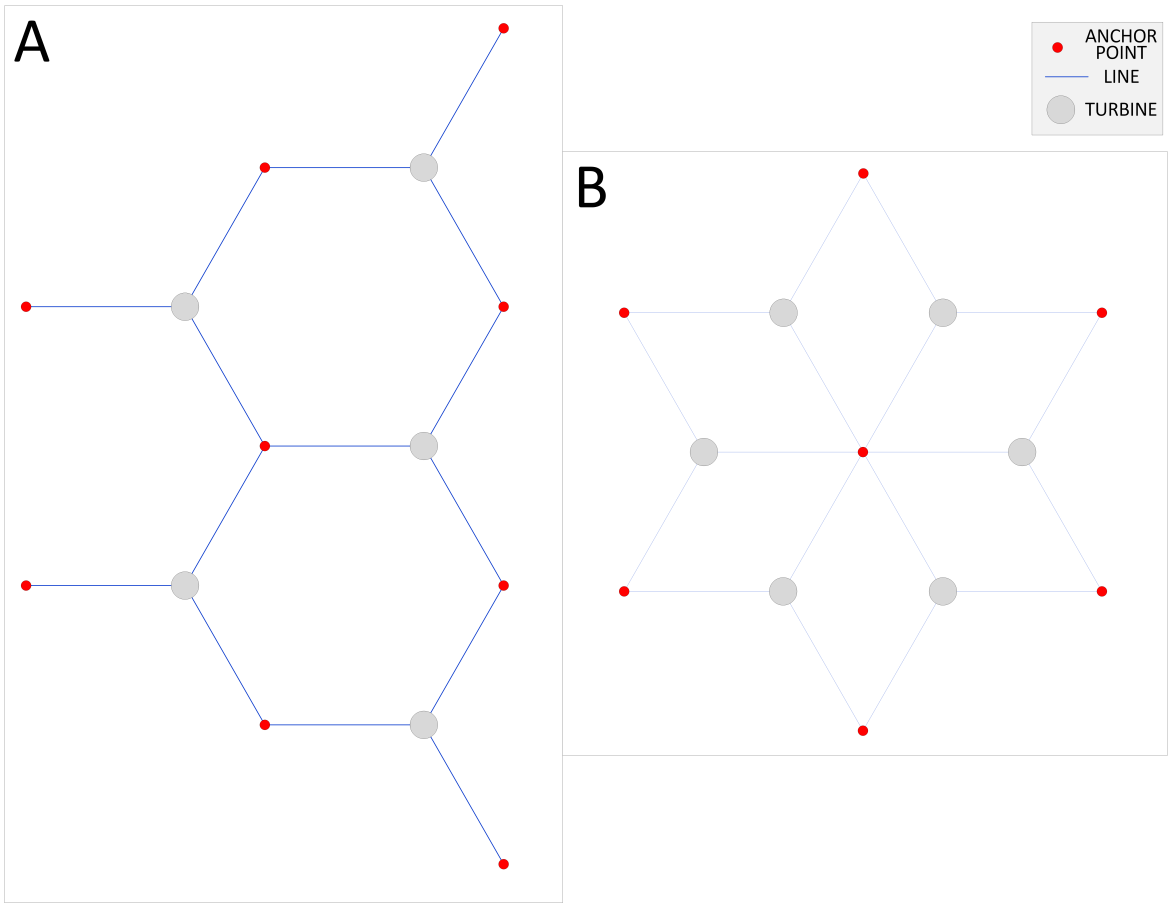

Figure 8.9: Wind turbine clusters for repetition [Visio]

is reduced by approximately 10% with just one multidirectional loading event. Multidirectional loading on different anchor types will need to be further researched before the implementation of mooring systems for FOWT with shared anchor points. It is not known whether multidirectional loading reduces the bearing capacity of the soil itself [18].

There is also the risk of a “domino-effect” of failure for shared anchors [17]: that is, a failure in the mooring system in one turbine can lead to the failure of the mooring system in another and can result in the whole park being out of commission. For anchors with multidirectional loads, especially those with the line loads distributed evenly around the anchor, it is unclear if one load is suddenly removed whether the anchor will remain intact or if the other lines attached will be affected; this is another topic of research regarding the feasibility of shared anchor points.

CHAPTER 9

CONCLUSIONS AND RECOMMENDATIONS

In this thesis, the mooring system was designed for the DTU 10MW RWT with a spar substructure at 600 m of water depth in the Norwegian North Sea. The response of the system under environmental loading was investigated for three load cases: rated wind speed, cut out wind speed, and the 50 year extreme conditions. The wind turbine was then adapted to a simplified model for use in a park arrangement with the same mooring system at a constant water depth. Three park arrangements were then formulated with shared anchors and the response of the wind turbines in these arrangements was examined. The resultant forces on the anchors from the tension on the mooring lines was then explored. The conclusions of this master thesis project are presented in this section. Recommendations for future work are also made so that research may continue if desired.

9.1 Conclusions

The main objective of this thesis was to design a realistic mooring design for the DTU 10MW RWT at 600 m water depth as stated in Section 1.2. Three sub questions were addressed to support this aim. The first was dealt with in Chapter 7, and the second and third in Chapter 8. The mooring design for a single turbine was developed in Chapter 6. It was found that the mooring line design kept the spar surge offset within 10% of the water depth as recommended by the rule of thumb. In reality, the allowable surge offset is dictated by the bend radius of the electrical cables and so it is possible that the allowable offset is higher. A higher allowable offset would allow lower pretension of the lines and shorter mooring lines and therefore a smaller overall footprint leading to a more cost-effective design. It is noted that when compared with the layout of the Hywind Scotland Pilot Park Wind turbines, the mooring length and footprint are

comparable for the water depth of 600 m.

The line tensions passed the DNV-OS-J103 ULS checks for the normal safety class. The line tensions did not pass the checks for the high safety class. The high safety class is necessary if the mooring design has no redundancy such as in this design, however the normal safety class is acceptable if the turbines are not at risk for collision if the mooring line fails. Since the turbines are at least 5 km away from each other in the arrangements, it is concluded that the normal safety class should be acceptable for this case. In retrospect, the single-turbine simulations should have been performed for varied directions where there is 1 mooring line to windward, since this is the most critical case.

The simplified model developed here, while not perfect, is a useful tool for analysis. The average, minimum, and maximum line tensions for all load cases and all lines were in $\pm 5\%$ of each other. The simplified model produced higher average surge offsets than the full model, but no more than 5% difference for the operational load cases. For the 50-Year extreme conditions, this difference was 13% greater but only amounted to ~ 5 m difference. The average pitch offsets had 0.3° difference between the two models. The simplified model does not give an accurate representation of the yaw rotation, so it is not recommended that this model be used in projects where this is a governing factor. The coefficients developed in this simplification as well as the simplified model can be used by other researchers for preliminary design and analysis if the main objective is to check mooring line tensions and offsets. Since the analysis time is much shorter than the full model, the simplified model can be used for optimisation purposes such as fine tuning the dimensions of the mooring line. To improve the design, the coefficients should be fine tuned and those which affect the yaw should be derived.

The arrangements investigated here can be used for a floating wind farm in 600 m water and is comparable to dimensioning of the Hywind Scotland system. Recommendations for improving the design are made in Section 9.2. The arrangements also depend on the suitability of anchors to multidirectional loads. In the simulations in this project it was found that resultant force on the anchor could be reduced up to 100% for anchors with two lines in opposing directions, however overall maximum load would govern the anchor design. The literature reviews conducted for this thesis indicated that further model testing is needed to test multidirectional loads on anchors as well as its effect on the soil bearing capacity. However, there is great interest in academia and industry regarding shared anchors for floating renewables as evidenced by recent articles published by [11], [12], [16], [17], [18], and [33]

Since the wind turbines were spread at least 5.7 km apart, wake control was not an issue in this project. The highest surge offset observed was 53 m which is only 0.9% of the separation. The surge offset would have little to no effect on the wake control.

9.2 Recommendations for Further Work

In addition to the recommendations made in Chapter 8, other recommendations for future work are explained here. It is recommended that further optimisation of the mooring lines be conducted with the simplified model to reduce the footprint of the layout for a single turbine. The arrangements of the turbines with shared anchor points also need to be optimised. The arrangements should maximise the space and not occupy more space than individually moored wind turbines.

The coefficients for the simplified wind turbine can be further developed so that the yaw displacement mimics that of the full model. A taut line mooring can also be tested for this deep water model, though it is not recommended for shared anchors due to the multiplane, multidirectional loading it would induce. The next step would be model testing of anchors and soil under multidirectional loading scenarios.

In this project the wind, wave, and current were aligned. A conservative, estimated current was also used. To optimise the design, the actual current profile and directional rose for wind and waves are needed. The misalignment of the environments may result in a less conservative and more feasible design.

In order to properly evaluate the feasibility of shared anchors, a full LCA (CAPEX + OPEX) analysis needs to be performed since the OPEX has greater influence on the LCOE than the CAPEX. This also means that a cost analysis of a wind park with shared anchors would need to be compared to one without. The following factors would need to be compared:

1. Cost of land area needed including the geotechnical survey.
2. Cost of anchors for each case: many simple unidirectional anchors vs fewer more complicated anchors for multidirectional loading.
3. Cost of installation.
4. Cost of decommissioning.

APPENDIX A

FINAL MOORING CONFIGURATION

For ease of reference, the final mooring configuration is presented here.

Table A.1: Properties of selected mooring lines

	Bridon Superline Polyester Line	**Ramnäs Bruk Studless Chain**
Unit Mass in Air [kg/m]	33.6	432.0
Axial Stiffness [MN]	296.1	6309.3
Diameter [m]	0.229	0.265
Tension Capacity (MBS) [MN]	14.715	14.700

Table A.2: Dimensions of selected mooring lines

Segment 1 (including Bridle Mid-length) - Chain [m]	450
Segment 2 - Polyester [m]	2129
Segment 3 - Chain [m]	350
Total Length [m]	2929
Footprint [m]	2862

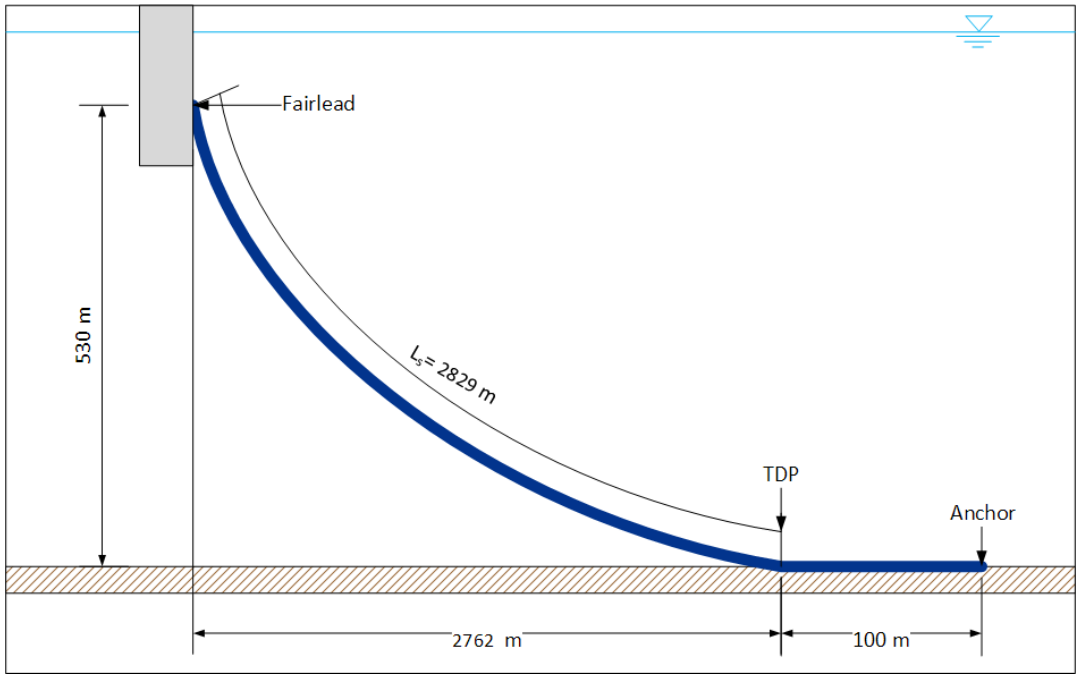

Figure A.1: Visual representation of catenary dimensioning [Visio]

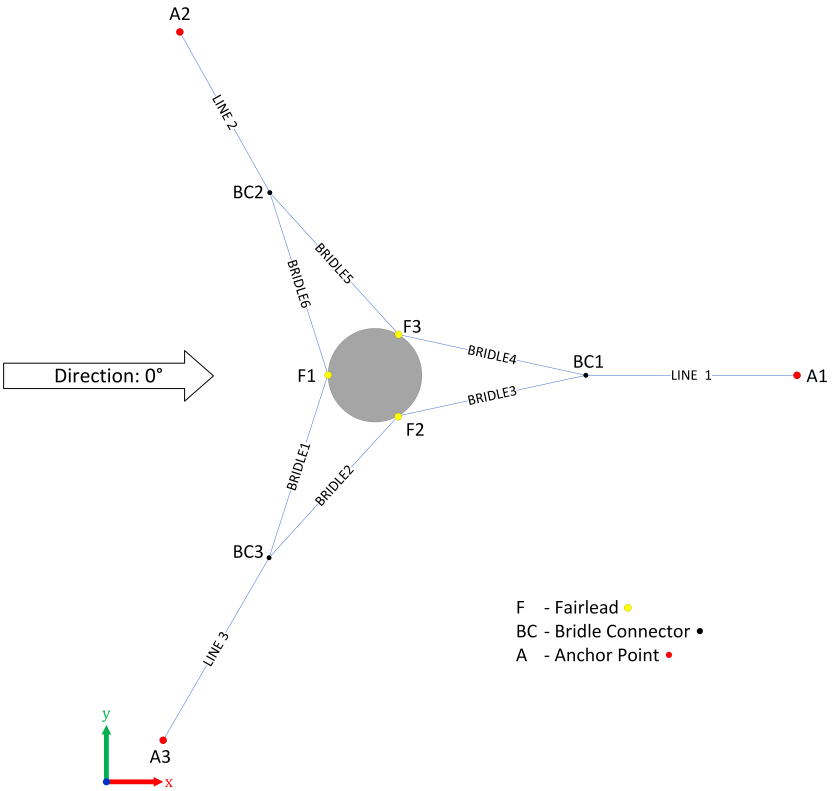

Figure A.2: Coordinate system used and new mooring configuration (with bridle) [Visio]

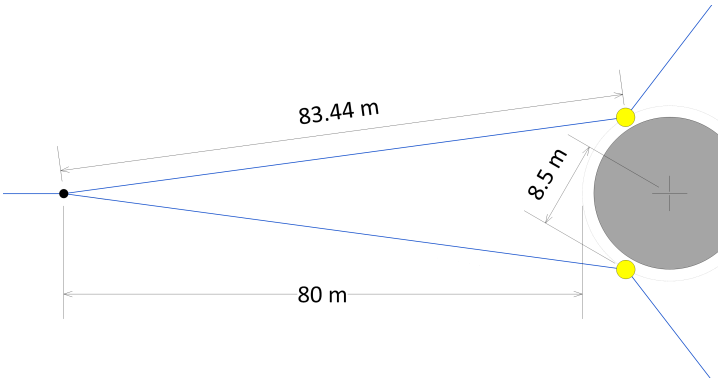

Figure A.3: Bridle dimensioning [Visio]

APPENDIX B

WIND COEFFICIENTS

The quadratic wind coefficients used in the simplified SIMA model are presented here in Tables B.1 to B.3

Table B.1: Wind coefficients and quadratic damping used in simplified model for Load Case 1

LC1: Rated Wind (U_{hub} = 11.0 m/s, U_{10} = 8.9 m/s)						
Direction	**C1**	**C2**	**C3**	**C4**	**C5**	**C6**
[°]	[Ns^2/m^2]			[Ns^2/m^2]		
0	16229.5	0.0	0.0	0.0	1694162.7	0.0
30	14055.1	8114.7	0.0	-847081.3	1467187.9	0.0
60	8114.7	14055.1	0.0	-1467187.9	847081.3	0.0
90	0.0	16229.5	0.0	-1694162.7	0.0	0.0
120	-8114.7	14055.1	0.0	-1467187.9	-847081.3	0.0
150	-14055.1	8114.7	0.0	-847081.3	-1467187.9	0.0
180	-16229.5	0.0	0.0	0.0	-1694162.7	0.0
210	-14055.1	-8114.7	0.0	847081.3	-1467187.9	0.0
240	-8114.7	-14055.1	0.0	1467187.9	-847081.3	0.0
270	0.0	-16229.5	0.0	1694162.7	0.0	0.0
300	8114.7	-14055.1	0.0	1467187.9	847081.3	0.0
330	14055.1	-8114.7	0.0	847081.3	1467187.9	0.0
360	16229.5	0.0	0.0	0.0	1694162.7	0.0
Quadratic damping = 2.92E + 10 Ns^2m^2						

Table B.2: Wind coefficients and quadratic damping used in simplified model for Load Case 2

LC2: Cutout Wind (U_{hub} = 25.0 m/s, U_{10} = 19.5 m/s)						
Direction	**C1**	**C2**	**C3**	**C4**	**C5**	**C6**
[°]		$[Ns^2/m^2]$			$[Ns^2/m^2]$	
0	2026.6	0.0	0.0	0.0	179349.8	0.0
30	1755.0	1013.3	0.0	89674.9	155321.5	0.0
60	1013.3	1755.0	0.0	155321.5	89674.9	0.0
90	0.0	2026.6	0.0	179349.8	0.0	0.0
120	-1013.3	1755.0	0.0	155321.5	-89674.9	0.0
150	-1755.0	1013.3	0.0	89674.9	-155321.5	0.0
180	-2026.6	0.0	0.0	0.0	-179349.8	0.0
210	-1755.0	-1013.3	0.0	-89674.9	-155321.5	0.0
240	-1013.3	-1755.0	0.0	-155321.5	-89674.9	0.0
270	0.0	-2026.6	0.0	-179349.8	0.0	0.0
300	1013.3	-1755.0	0.0	-155321.5	89674.9	0.0
330	1755.0	-1013.3	0.0	-89674.9	155321.5	0.0
360	2026.6	0.0	0.0	0.0	179349.8	0.0
Quadratic damping = 2.36E + 09 Ns^2m^2						

Table B.3: Wind coefficients and quadratic damping used in simplified model for Load Case 3

LC3: 50-Year Extreme Wind (U_{hub} = 42.9 m/s, U_{10} = 33.5 m/s)						
Direction	**C1**	**C2**	**C3**	**C4**	**C5**	**C6**
[°]		$[Ns^2/m^2]$			$[Ns^2/m^2]$	
0	724.3	0.0	0.0	0.0	44501.5	0.0
30	627.2	362.1	0.0	22250.8	38539.4	0.0
60	362.1	627.2	0.0	38539.4	22250.8	0.0
90	0.0	724.3	0.0	44501.5	0.0	0.0
120	-362.1	627.2	0.0	38539.4	-22250.8	0.0
150	-627.2	362.1	0.0	22250.8	-38539.4	0.0
180	-724.3	0.0	0.0	0.0	-44501.5	0.0
210	-627.2	-362.1	0.0	-22250.8	-38539.4	0.0
240	-362.1	-627.2	0.0	-38539.4	-22250.8	0.0
270	0.0	-724.3	0.0	-44501.5	0.0	0.0
300	362.1	-627.2	0.0	-38539.4	22250.8	0.0
330	627.2	-362.1	0.0	-22250.8	38539.4	0.0
360	724.3	0.0	0.0	0.0	44501.5	0.0
Quadratic damping = 5.46E + 08 Ns^2m^2						

APPENDIX C

SIMPLIFIED MODEL

The complete environmental results of the single simplified model are presented in this appendix

C.1 Line Tensions and Offset Averages

Table C.1: Line tension averages for simplified model under environmental loading

	LC1	**LC2**	**LC3**
Line 1 [kN]	2268.4	2365.8	2210.2
Line 2 [kN]	3471.6	3317.5	3540.8
Line 3 [kN]	3472.6	3317.0	3540.8
Bridle 1 [kN]	2837.4	2524.1	2789.9
Bridle 2 [kN]	1007.6	1176.9	1122.2
Bridle 3 [kN]	1372.2	1413.4	1343.1
Bridle 4 [kN]	1371.5	1413.2	1343.1
Bridle 5 [kN]	1006.9	1177.0	1122.3
Bridle 6 [kN]	2837.2	2524.4	2790.0
Overall Maximum [kN]	3472.6	3317.5	3540.8
Location	Line3	Line 2	Line2
Overall Minimum [kN]	1006.9	1176.9	1122.2
Location	Bridle 5	Bridle 2	Bridle 2

Table C.2: Surge and pitch offset averages

Load Case	**Surge Displacement** [m]	**% Offset**	**Pitch** [°]
1- Rated	37.0	6.17%	6.69
2- Cut Off	25.8	4.31%	3.59
3- 50 Year U_w	33.8	5.63%	3.14

C.2 Line Tensions and Offset Extreme Values

Table C.3: Line tension extrema

		LC1	**LC2**	**LC3**
Line 1 [kN]	**Max**	2451.8	2698.6	2545.3
	Min	2111.1	1980.7	1812.7
Line 2 [kN]	**Max**	3737.1	3568.7	3833.4
	Min	3236.5	3071.3	3278.8
Line 3 [kN]	**Max**	3735.6	3569.0	3820.2
	Min	3239.5	3057.6	3278.1
Bridle 1 [kN]	**Max**	3208.3	3029.4	3299.2
	Min	2357.3	1925.1	2057.8
Bridle 2 [kN]	**Max**	1460.2	1778.6	1914.9
	Min	713.3	761.2	696.0
Bridle 3 [kN]	**Max**	1591.0	1580.9	1499.4
	Min	1158.0	1219.4	1154.2
Bridle 4 [kN]	**Max**	1592.1	1573.6	1500.3
	Min	1137.0	1232.3	1158.7
Bridle 5 [kN]	**Max**	1419.4	1784.0	1913.5
	Min	718.0	761.3	693.2
Bridle 6 [kN]	**Max**	3210.1	3024.8	3296.2
	Min	2340.7	1926.9	2054.3
Overall Maximum [kN]		3737.1	3569.0	3833.4
Location		Line 2	Line 3	Line 2
Overall Minimum [kN]		713.3	761.2	693.2
Location		Bridle 2	Bridle 2	Bridle 5

Table C.4: Maximum offsets of simplified model

Load Case	**Surge Displacement** [m]	**% Offset**	**Pitch** [°]	**Yaw** [°]
1- Rated	48.5	8.09%	10.3	0.7
2- Cut Off	36.9	6.15%	8.1	0.3
3- 50 Year U_w	45.4	7.57%	8.1	0.2

C.3 Line Tension Plots from Environmental Analysis

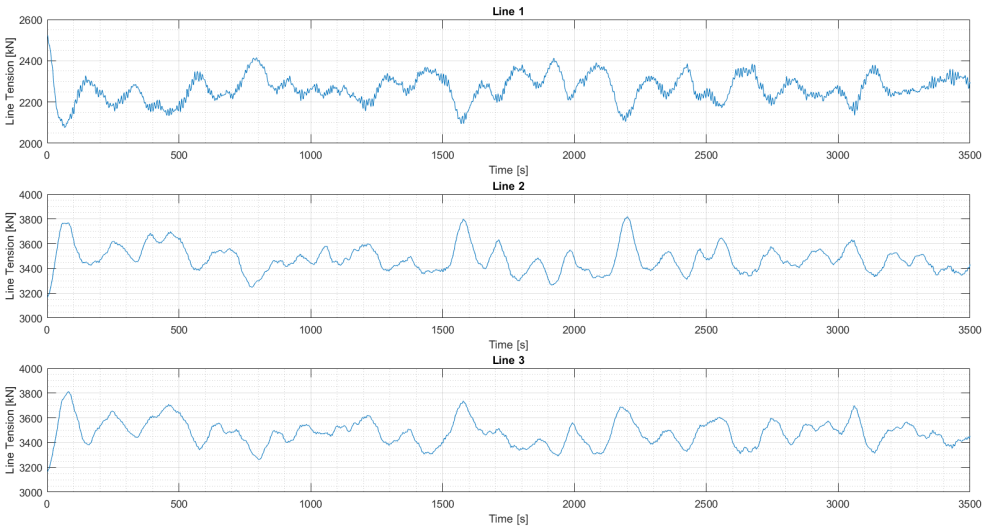

Figure C.1: Time series of line tensions for simplified deepwater model - Load Case 1

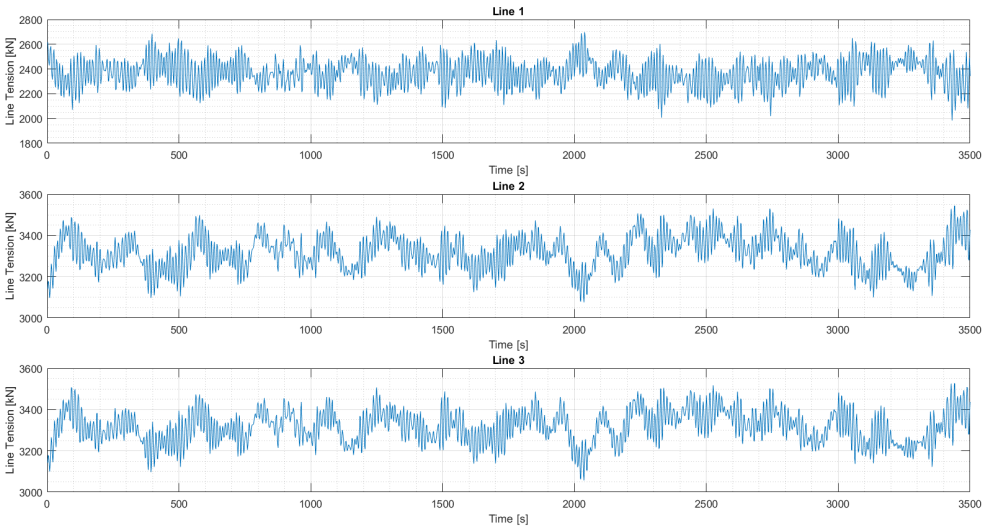

Figure C.2: Time series of line tensions for simplified deepwater model - Load Case 2

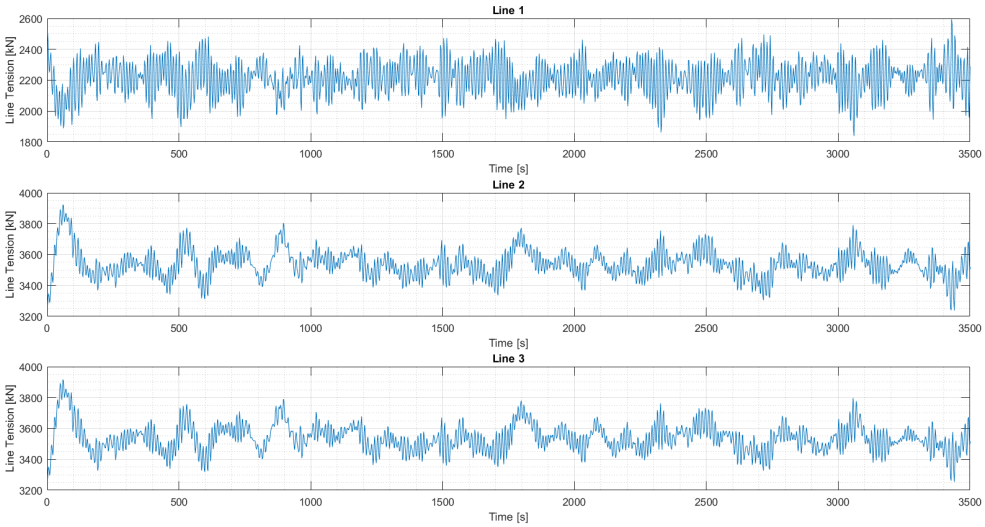

Figure C.3: Time series of line tensions for simplified deepwater model - Load Case 3

C.4 Offset Comparisons from Environmental Analysis

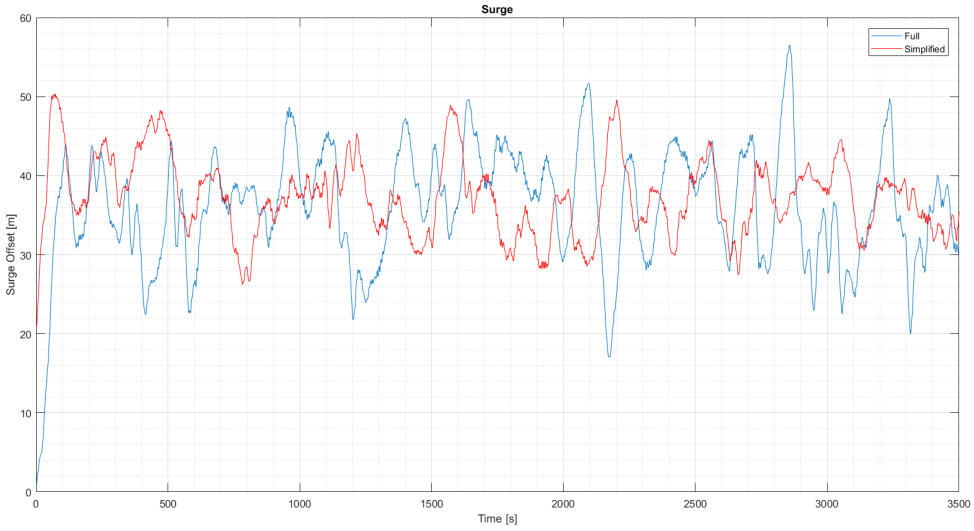

Figure C.4: Time series comparison of surge offset for full and simplified model - LC1

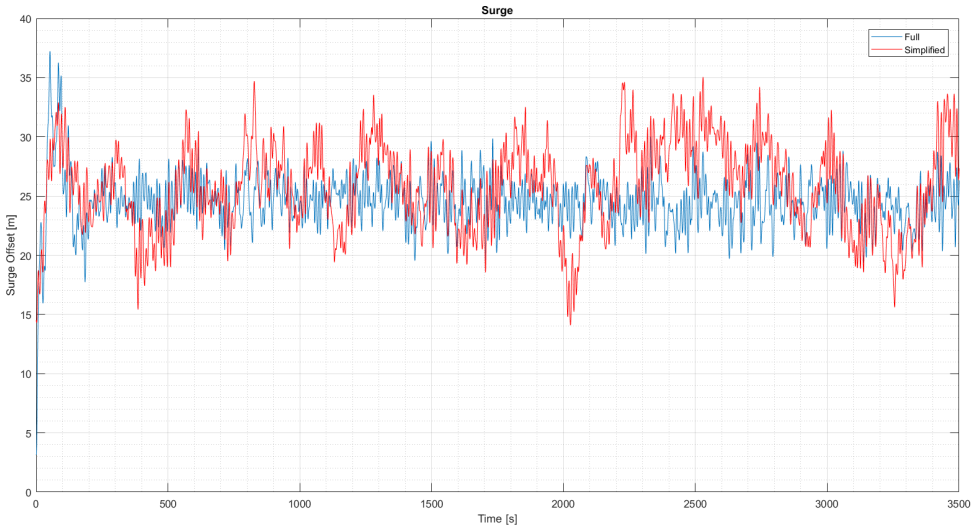

Figure C.5: Time series comparison of surge offset for full and simplified model - LC2

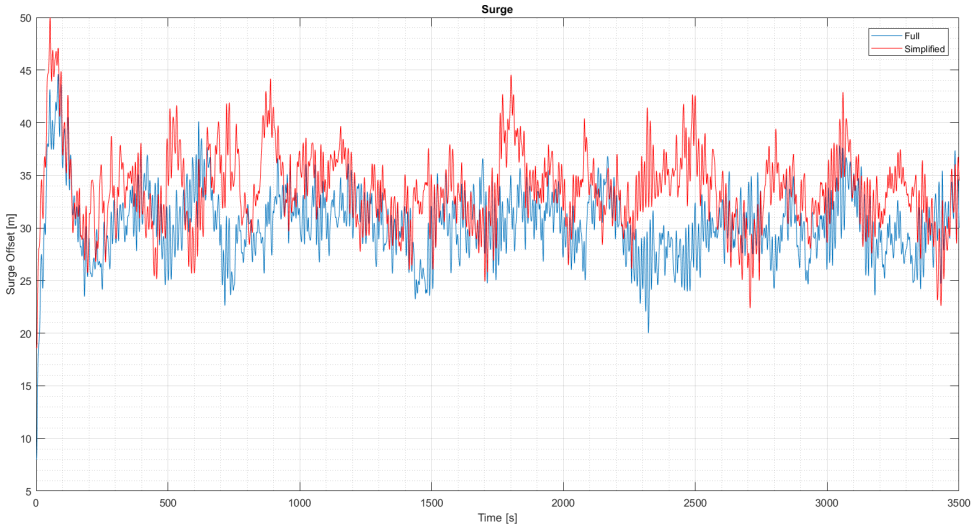

Figure C.6: Time series comparison of surge offset for full and simplified model - LC3

APPENDIX D

ARRANGEMENT LAYOUTS

Here the individual diagrams of the arrangements are presented for ease of referencing. Please note that these diagrams are not to scale and are for illustrative purposes only

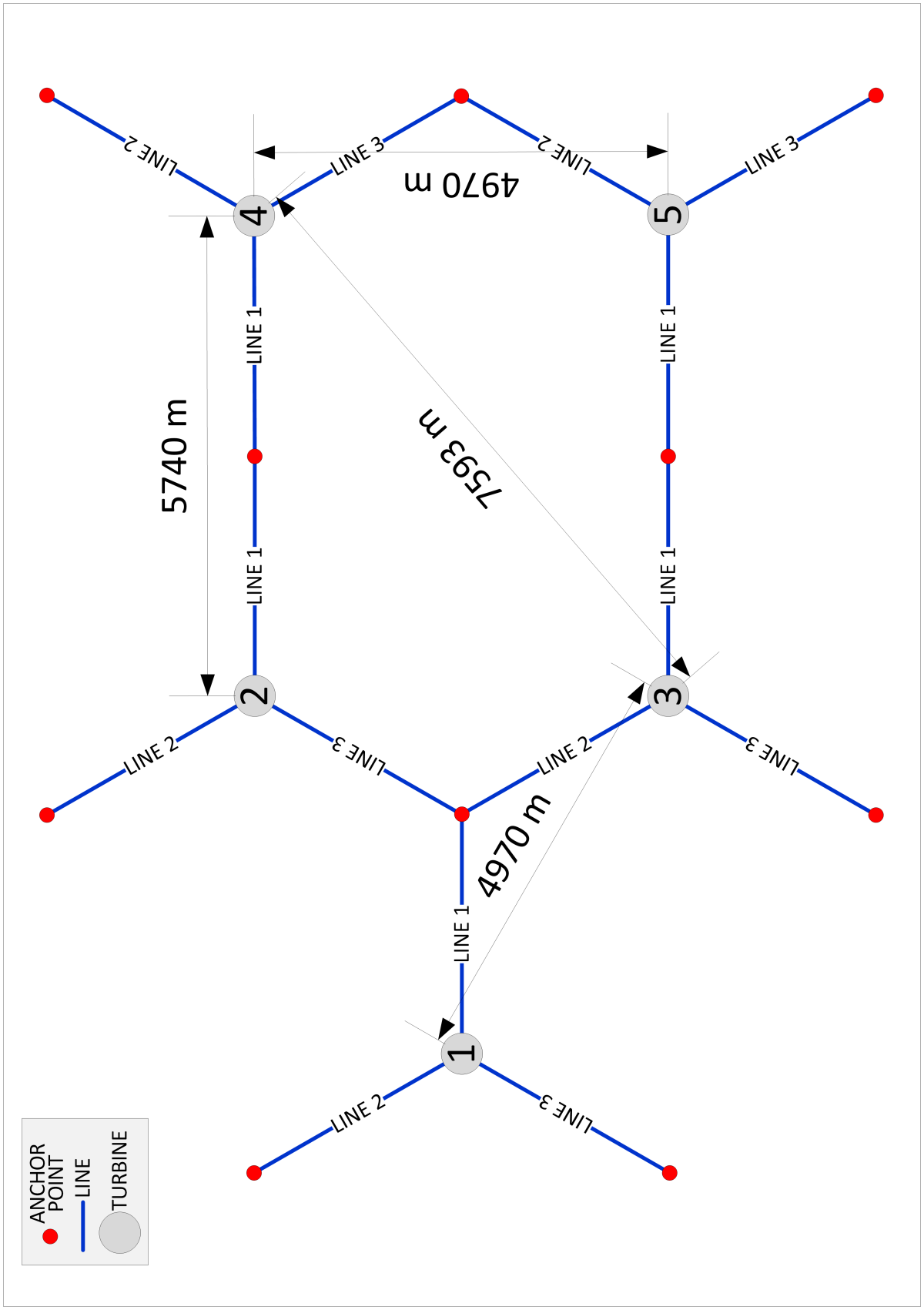

Figure D.1: Arrangement 1

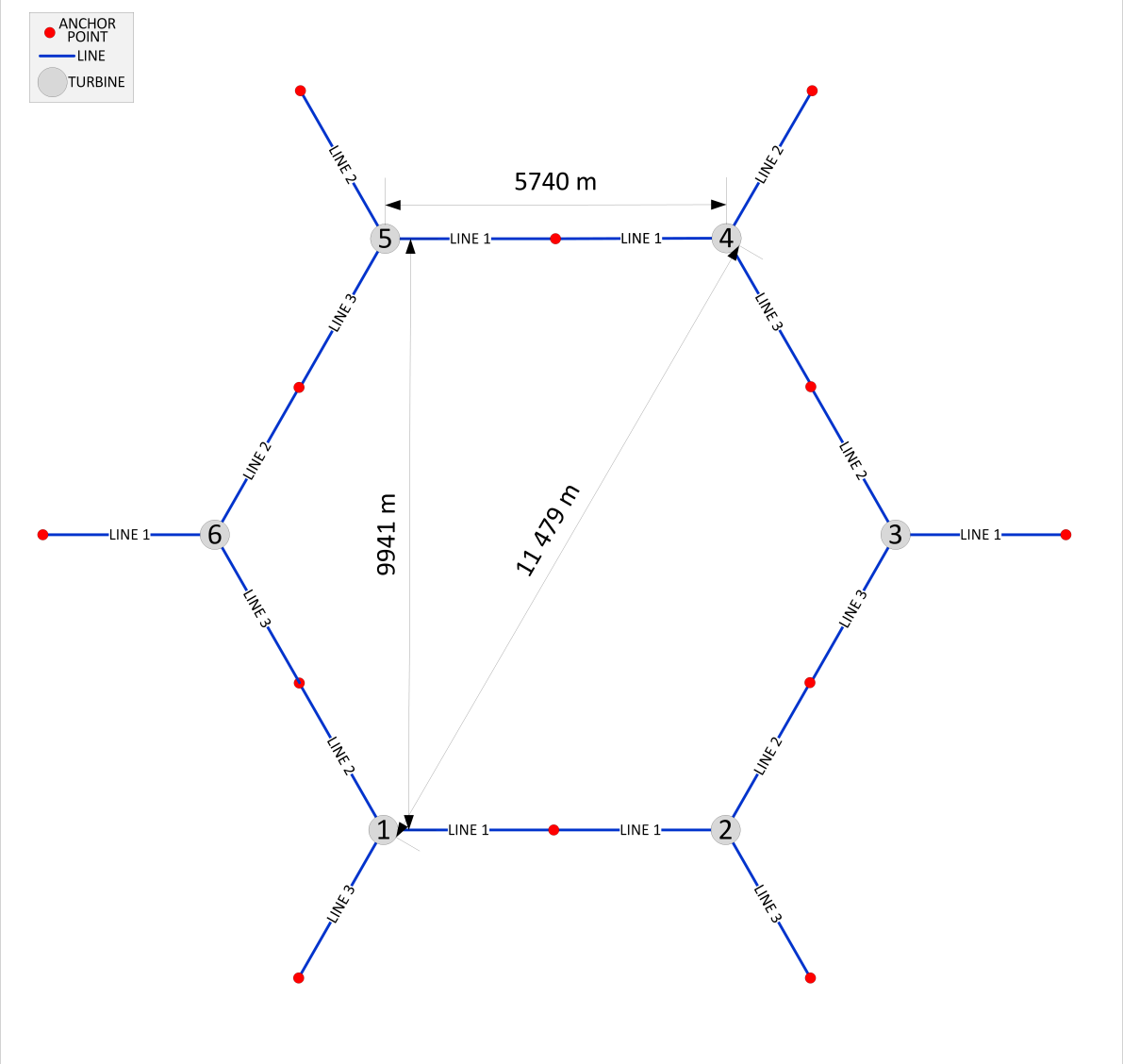

Figure D.2: Arrangement 2

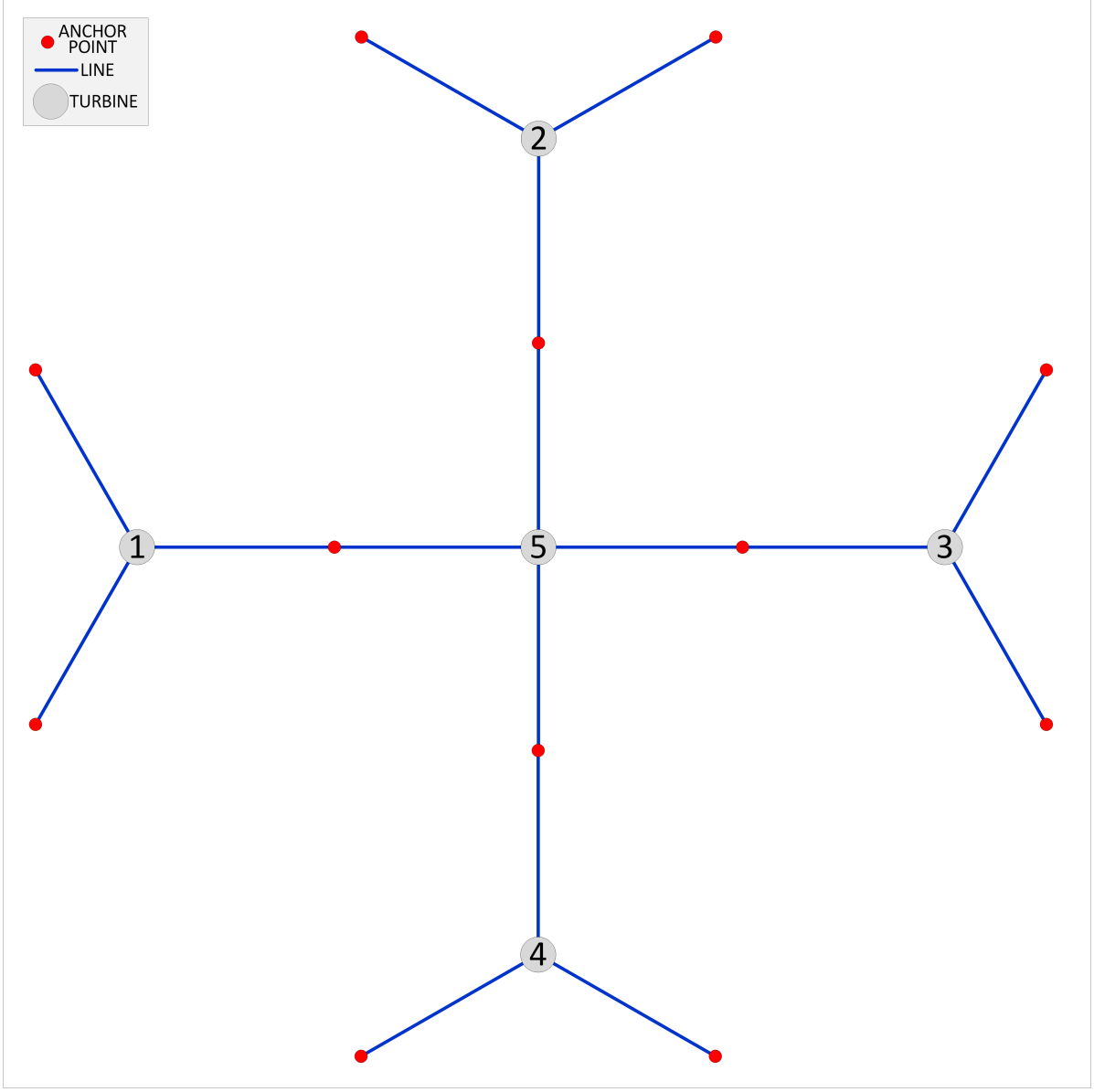

Figure D.3: Arrangement 3

APPENDIX E

ARRANGEMENT ENVIRONMENTAL RESULTS - OFFSETS

The tables for the offsets of the turbines of the arrangements under environmental loading are presented here.

E.1 Arrangement 1

Table E.1: Pitch Results for Arrangement 1, Direction 0 (0°)

		Turbine 1	Turbine 2	Turbine 3	Turbine 4	Turbine 5
LC1	**Maximum** [°]	10.2	10.2	10.2	10.4	10.4
	Average [°]	6.68	6.68	6.68	6.73	6.73
LC2	**Maximum** [°]	8.15	8.32	8.32	8.51	8.51
	Average [°]	3.59	3.59	3.59	3.61	3.61
LC3	**Maximum** [°]	8.14	7.96	7.96	8.11	8.11
	Average [°]	3.14	3.14	3.14	3.15	3.15

Table E.2: Horizontal offsets for Arrangement 1, Load Case 1, all directions

		Turbine 1	Turbine 2	Turbine 3	Turbine 4	Turbine 5
0	**Maximum [m]**	48.4	48.5	48.5	39.0	39.0
	Average [m]	37.0	36.9	36.9	30.0	30.0
1	**Maximum [m]**	46.4	46.3	46.5	46.9	46.8
	Average [m]	32.7	32.7	32.7	32.8	32.7
2	**Maximum [m]**	43.1	43.0	43.5	49.7	49.2
	Average [m]	29.9	29.9	29.9	34.5	34.5
3	**Maximum [m]**	41.7	41.7	41.7	50.7	50.8
	Average [m]	29.3	29.3	29.3	35.8	35.8
4	**Maximum [m]**	40.9	40.9	41.1	47.2	47.1
	Average [m]	30.7	30.7	30.7	35.3	35.3
5	**Maximum [m]**	45.5	45.3	45.5	45.7	45.8
	Average [m]	33.3	33.3	33.3	33.3	33.3
6	**Maximum [m]**	46.8	47.0	46.9	40.9	40.8
	Average [m]	35.1	35.1	35.1	30.5	30.5
7	**Maximum [m]**	49.1	49.2	49.0	41.3	41.0
	Average [m]	36.2	36.2	36.2	29.6	29.6
8	**Maximum [m]**	48.4	48.3	48.4	41.9	41.8
	Average [m]	35.5	35.4	35.4	30.8	30.8
9	**Maximum [m]**	45.4	45.2	45.7	45.3	45.5
	Average [m]	33.2	33.2	33.2	33.2	33.2
10	**Maximum [m]**	39.9	39.5	39.5	48.4	48.4
	Average [m]	30.1	30.1	30.1	36.9	36.9

Table E.3: Horizontal offsets for Arrangement 1, Load Case 2, all directions

		Turbine 1	Turbine 2	Turbine 3	Turbine 4	Turbine 5
0	**Maximum [m]**	36.9	37.0	37.0	32.5	32.5
	Average [m]	25.8	25.8	25.8	22.0	22.0
1	**Maximum [m]**	31.6	32.6	31.9	32.3	32.0
	Average [m]	23.0	23.0	23.0	22.7	22.7
2	**Maximum [m]**	29.6	30.1	28.5	31.2	31.9
	Average [m]	19.9	19.9	19.9	22.4	22.4
3	**Maximum [m]**	27.8	27.7	28.0	34.4	34.5
	Average [m]	18.4	18.4	18.4	22.5	22.5
4	**Maximum [m]**	26.5	26.0	27.2	29.9	31.3
	Average [m]	17.4	17.4	17.4	20.2	20.2
5	**Maximum [m]**	27.4	28.7	26.3	28.6	26.2
	Average [m]	19.1	19.1	19.1	19.1	19.0
6	**Maximum [m]**	29.3	29.3	29.9	25.8	25.9
	Average [m]	20.5	20.5	20.6	17.6	17.7
7	**Maximum [m]**	31.0	31.1	32.1	26.6	26.8
	Average [m]	22.1	22.1	22.1	18.2	18.2
8	**Maximum [m]**	34.2	33.8	34.4	30.4	31.1
	Average [m]	22.4	22.4	22.4	19.9	19.9
9	**Maximum [m]**	36.6	36.9	35.9	35.5	36.2
	Average [m]	22.6	22.6	22.6	22.9	22.9
10	**Maximum [m]**	34.3	35.2	35.2	41.8	41.8
	Average [m]	21.9	21.9	21.9	25.9	25.9

Table E.4: Horizontal offsets for Arrangement 1, Load Case 3, all directions

		Turbine 1	Turbine 2	Turbine 3	Turbine 4	Turbine 5
0	**Maximum [m]**	45.4	45.1	45.1	37.5	37.5
	Average [m]	33.8	33.8	33.8	27.0	27.0
1	**Maximum [m]**	40.5	40.7	40.2	40.7	40.0
	Average [m]	29.9	29.8	29.8	29.6	29.6
2	**Maximum [m]**	39.5	39.9	39.9	46.1	44.5
	Average [m]	26.1	26.1	26.0	30.4	30.5
3	**Maximum [m]**	34.9	33.5	35.0	43.0	43.1
	Average [m]	24.5	24.5	24.5	31.1	31.1
4	**Maximum [m]**	33.6	33.9	32.9	38.5	39.2
	Average [m]	24.4	24.4	24.3	29.0	29.0
5	**Maximum [m]**	37.1	36.8	36.1	36.9	36.1
	Average [m]	26.8	26.8	26.8	26.8	26.8
6	**Maximum [m]**	38.5	39.3	39.4	33.3	33.0
	Average [m]	29.1	29.0	29.1	24.4	24.4
7	**Maximum [m]**	44.8	44.8	43.0	35.5	35.0
	Average [m]	31.2	31.2	31.1	24.5	24.5
8	**Maximum [m]**	41.9	42.0	42.8	38.0	37.3
	Average [m]	30.4	30.4	30.4	26.1	26.0
9	**Maximum [m]**	42.1	43.5	42.4	40.9	42.4
	Average [m]	29.7	29.7	29.7	29.9	29.9
10	**Maximum [m]**	38.3	37.6	37.6	46.3	46.3
	Average [m]	27.3	27.3	27.3	33.9	33.9

E.2 Arrangement 2

The section presents the horizontal offsets for all directions of Arrangement 2 and the pitch of Direction 0 for all turbines.

Table E.5: Pitch Results for Arrangement 2, Direction 0 (0°)

		Turbine 1	Turbine 2	Turbine 3	Turbine 4	Turbine 5	Turbine 6
LC1	**Maximum [°]**	10.3	10.4	10.3	10.4	10.3	10.3
	Average [°]	6.69	6.74	6.69	6.74	6.69	6.58
LC2	**Maximum [°]**	8.15	8.13	8.01	8.13	8.12	8.26
	Average [°]	3.59	3.61	3.60	3.60	3.60	3.40
LC3	**Maximum [°]**	8.14	8.08	7.88	8.08	8.23	8.09
	Average [°]	3.14	3.15	3.14	3.14	3.14	3.01

Table E.6: Horizontal offsets for Arrangement 2, Load Case 1, all directions

		Turbine 1	Turbine 2	Turbine 3	Turbine 4	Turbine 5	Turbine 6
0	**Maximum [m]**	48.5	39.0	48.5	38.9	48.7	38.8
	Average [m]	37.0	30.1	37.0	30.1	37.1	29.8
1	**Maximum [m]**	44.4	44.0	44.5	44.2	44.3	45.2
	Average [m]	34.0	34.1	34.0	34.1	34.0	35.1
2	**Maximum [m]**	40.7	46.4	40.9	46.2	41.1	47.9
	Average [m]	30.2	34.8	30.2	34.9	30.3	36.2
3	**Maximum [m]**	41.2	52.3	41.1	52.8	41.2	53.1
	Average [m]	30.4	37.3	30.4	37.4	30.4	38.6
4	**Maximum [m]**	43.6	48.7	43.6	48.7	43.8	50.5
	Average [m]	30.0	34.4	30.0	34.5	30.1	36.5
5	**Maximum [m]**	42.9	42.8	43.0	42.7	42.7	44.2
	Average [m]	33.4	33.4	33.4	33.5	33.4	35.0

Table E.7: Horizontal offsets for Arrangement 2, Load Case 2, all directions

		Turbine 1	Turbine 2	Turbine 3	Turbine 4	Turbine 5	Turbine 6
0	**Maximum [m]**	36.9	31.8	37.0	31.7	37.0	31.8
	Average [m]	25.8	21.9	25.8	21.8	25.9	21.5
1	**Maximum [m]**	33.5	33.9	36.0	35.9	33.4	34.4
	Average [m]	23.1	22.8	23.0	22.7	23.1	23.7
2	**Maximum [m]**	29.8	34.8	31.2	33.6	30.9	35.3
	Average [m]	20.0	22.5	19.9	22.4	20.0	24.1
3	**Maximum [m]**	26.9	32.2	26.0	33.3	26.1	34.2
	Average [m]	18.4	22.5	18.4	22.5	18.4	24.2
4	**Maximum [m]**	25.6	29.9	25.6	29.8	26.8	32.6
	Average [m]	17.5	20.4	17.5	20.4	17.5	22.8
5	**Maximum [m]**	29.7	29.7	27.7	27.5	27.5	29.7
	Average [m]	19.1	19.1	19.0	19.1	19.1	21.1

Table E.8: Horizontal offsets for Arrangement 2, Load Case 3, all directions

		Turbine 1	Turbine 2	Turbine 3	Turbine 4	Turbine 5	Turbine 6
0	**Maximum [m]**	45.4	37.6	44.8	37.6	45.4	36.5
	Average [m]	33.8	27.2	33.7	27.2	33.8	26.9
1	**Maximum [m]**	43.0	41.3	42.9	41.9	42.3	43.7
	Average [m]	29.6	29.4	29.5	29.4	29.6	30.3
2	**Maximum [m]**	38.9	43.9	38.4	43.9	38.6	45.4
	Average [m]	26.0	30.4	26.0	30.4	26.1	32.1
3	**Maximum [m]**	32.6	41.8	34.0	43.6	34.1	43.4
	Average [m]	24.6	31.2	24.6	31.3	24.6	32.8
4	**Maximum [m]**	34.4	40.2	32.5	39.3	35.2	42.7
	Average [m]	24.5	29.1	24.5	29.2	24.5	31.5
5	**Maximum [m]**	35.5	35.1	36.0	35.4	35.6	37.6
	Average [m]	26.9	26.8	26.9	26.9	26.9	28.9

E.3 Arrangement 3

The section presents the horizontal offsets for all directions of Arrangement 3 and the pitch of Direction 0 for all turbines.

Table E.9: Pitch Results for Arrangement 3, Direction 0 (0°)

		Turbine 1	Turbine 2	Turbine 3	Turbine 4	Turbine 5	Turbine 6
LC1	**Maximum [°]**	10.3	10.4	10.3	10.4	10.3	10.3
	Average [°]	6.69	6.74	6.69	6.74	6.69	6.58
LC2	**Maximum [°]**	8.15	8.13	8.01	8.13	8.12	8.26
	Average [°]	3.59	3.61	3.60	3.60	3.60	3.40
LC3	**Maximum [°]**	8.14	8.08	7.88	8.08	8.23	8.09
	Average [°]	3.14	3.15	3.14	3.14	3.14	3.01

Table E.10: Horizontal offsets for Arrangement 3, Load Case 1, all directions

		Turbine 1	Turbine 2	Turbine 3	Turbine 4	Turbine 5
0	**Maximum [m]**	48.5	43.8	39.3	43.7	34.8
	Average [m]	37.0	33.6	30.0	33.6	26.6
1	**Maximum [m]**	43.4	47.7	43.5	38.6	34.2
	Average [m]	32.6	35.6	32.6	29.2	25.7
2	**Maximum [m]**	40.3	46.3	46.2	40.9	35.1
	Average [m]	30.4	34.9	35.0	30.5	26.0
3	**Maximum [m]**	42.9	47.0	50.6	47.1	38.5
	Average [m]	29.8	33.3	36.5	33.4	26.3
4	**Maximum [m]**	42.4	42.9	48.4	48.0	36.4
	Average [m]	30.0	30.0	34.4	34.4	25.4
5	**Maximum [m]**	45.4	40.6	45.3	48.9	36.4
	Average [m]	34.4	30.6	34.4	37.7	26.9

Table E.11: Horizontal offsets for Arrangement 3, Load Case 2, all directions

		Turbine 1	Turbine 2	Turbine 3	Turbine 4	Turbine 5
0	**Maximum [m]**	36.9	34.1	31.8	34.1	28.7
	Average [m]	25.8	23.8	22.0	23.8	19.2
1	**Maximum [m]**	35.3	38.6	34.7	31.6	27.9
	Average [m]	22.9	24.7	22.7	20.8	18.1
2	**Maximum [m]**	29.5	33.5	33.0	29.6	25.2
	Average [m]	19.8	22.5	22.3	19.6	16.5
3	**Maximum [m]**	26.8	29.2	30.2	30.4	23.7
	Average [m]	18.1	20.3	22.1	20.0	15.7
4	**Maximum [m]**	26.0	25.3	30.4	30.6	23.6
	Average [m]	17.5	17.6	20.4	20.3	14.7
5	**Maximum [m]**	27.6	23.7	27.7	30.3	21.4
	Average [m]	19.0	16.9	19.0	20.9	14.7

Table E.12: Horizontal offsets for Arrangement 3, Load Case 3, all directions

		Turbine 1	Turbine 2	Turbine 3	Turbine 4	Turbine 5
0	**Maximum [m]**	45.4	41.4	37.5	41.4	34.8
	Average [m]	33.8	30.3	27.0	30.3	24.8
1	**Maximum [m]**	41.7	45.0	41.2	36.1	35.9
	Average [m]	30.0	33.1	29.8	26.5	23.7
2	**Maximum [m]**	38.2	42.7	42.5	37.6	33.6
	Average [m]	26.0	30.6	30.4	25.9	22.1
3	**Maximum [m]**	35.1	38.4	41.4	38.8	29.5
	Average [m]	24.8	28.3	31.5	28.1	22.1
4	**Maximum [m]**	34.9	34.7	42.0	41.5	30.6
	Average [m]	24.5	24.6	29.3	29.0	21.3
5	**Maximum [m]**	40.0	33.1	40.0	42.6	31.8
	Average [m]	26.9	23.5	26.9	30.2	21.4

APPENDIX F

ARRANGEMENT ENVIRONMENTAL RESULTS - TENSIONS

The tables for the line tensions of Arrangements 1-3 under environmental loading are presented here. This section presents the maximum and average line tensions for each line in Arrangements 1-3. Also included are the line tension time series plots for Direction 0 for each turbine in each arrangement.

F.1 Arrangement 1

F.1.1 Load Case 1

Table F.1: Maximum and average line tensions for each line in each turbine in Arrangement 1, under Load Case 1

		Turbine 1		**Turbine 2**		**Turbine 3**		**Turbine 4**		**Turbine 5**	
		Max	**Avg**	**Max**	**Avg**	**Max**	**Avg**	**Max**	**Avg**	**Max**	**Avg**
0	**L1**	2452	2268	2455	2269	2455	2269	4361	3865	4361	3865
	L2	3737	3472	3740	3471	3740	3471	2718	2605	2718	2605
	L3	3736	3473	3733	3472	3733	3472	2716	2606	2716	2606
1	**L1**	2565	2363	2560	2363	2566	2363	4228	3738	4218	3738
	L2	3208	3021	3205	3020	3206	3020	2558	2362	2559	2362
	L3	4315	3738	4324	3738	4315	3739	3273	3023	3273	3023
2	**L1**	2593	2470	2594	2470	2600	2470	4056	3604	4041	3604
	L2	2893	2800	2892	2800	2894	2800	2472	2308	2483	2308
	L3	4403	3795	4396	3795	4425	3795	3554	3242	3545	3242
3	**L1**	2711	2615	2710	2615	2709	2615	3783	3448	3785	3449
	L2	2716	2610	2713	2610	2715	2610	2443	2283	2445	2283
	L3	4443	3833	4449	3833	4442	3833	3773	3454	3775	3454
4	**L1**	2899	2804	2905	2804	2899	2804	3455	3249	3453	3248
	L2	2633	2460	2650	2460	2628	2460	2514	2298	2521	2298
	L3	4221	3819	4221	3819	4231	3819	3904	3629	3892	3628
5	**L1**	3177	3027	3177	3026	3177	3026	3180	3024	3184	3024
	L2	2510	2354	2505	2355	2507	2354	2530	2355	2520	2355
	L3	4190	3753	4197	3753	4188	3753	4162	3755	4172	3755
6	**L1**	3453	3245	3459	3245	3460	3245	2919	2805	2922	2805
	L2	2529	2301	2543	2301	2533	2301	2622	2462	2625	2462
	L3	3944	3622	3950	3622	3943	3622	4174	3812	4173	3812
7	**L1**	3755	3458	3756	3458	3757	3458	2700	2611	2704	2611
	L2	2461	2278	2459	2278	2454	2278	2747	2610	2747	2610
	L3	3742	3458	3743	3458	3736	3458	4433	3845	4434	3845
8	**L1**	3973	3629	3967	3628	3964	3629	2597	2460	2600	2460
	L2	2461	2296	2455	2296	2463	2296	2910	2801	2910	2801
	L3	3502	3252	3506	3251	3504	3252	4323	3823	4316	3824
9	**L1**	4171	3750	4164	3750	4173	3750	2522	2357	2507	2357
	L2	2512	2355	2520	2355	2521	2355	3180	3021	3179	3021
	L3	3216	3026	3218	3026	3219	3026	4204	3752	4208	3752
10	**L1**	4349	3863	4320	3863	4320	3863	2440	2269	2440	2269
	L2	2713	2605	2715	2605	2715	2605	3693	3469	3693	3469
	L3	2730	2607	2731	2607	2731	2607	3744	3471	3744	3471
***All values shown in kilonewtons [kN]**											

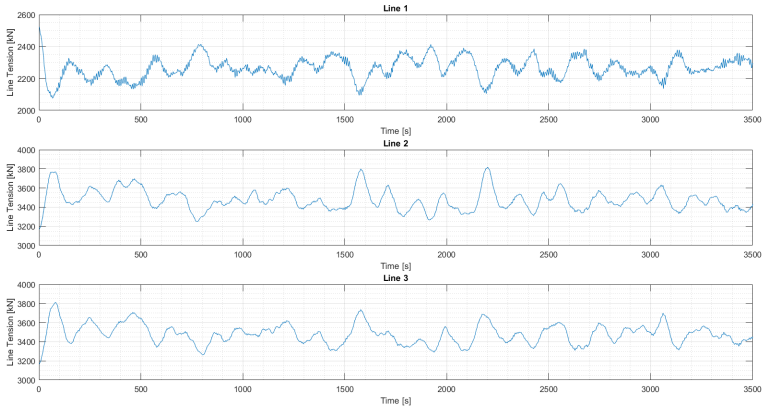

Figure F.1: Line Tensions Arrangement 1, Load Case 1, Turbine 1

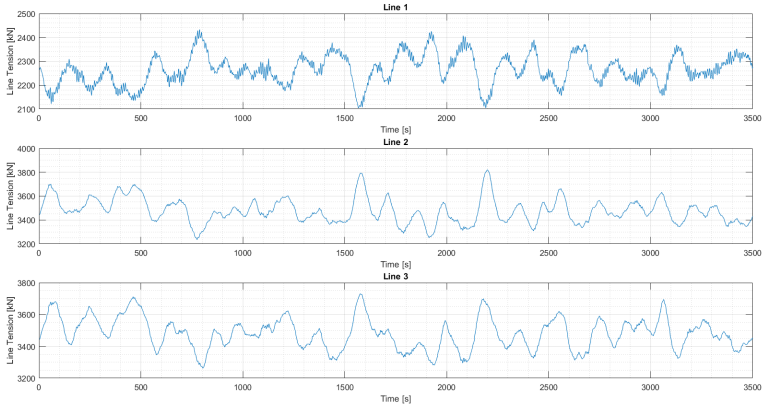

Figure F.2: Line Tensions Arrangement 1, Load Case 1, Turbine 2

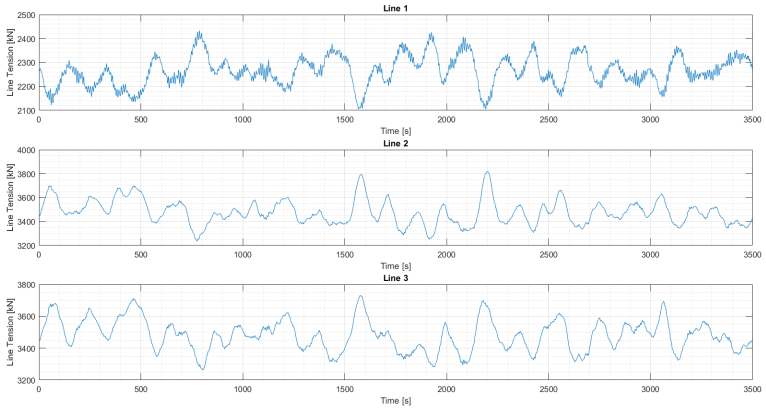

Figure F.3: Line Tensions Arrangement 1, Load Case 1, Turbine 3

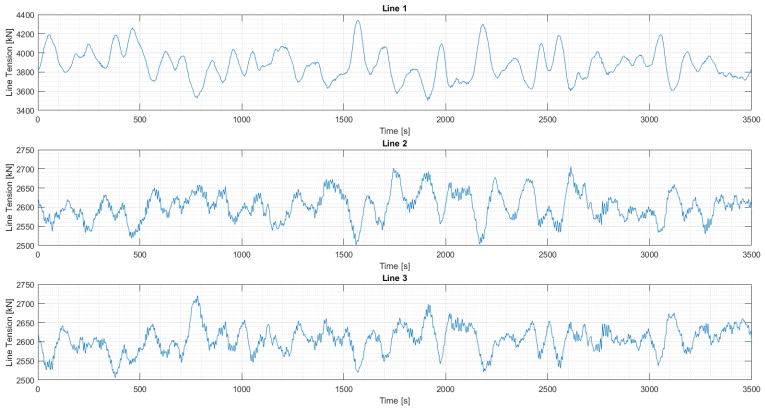

Figure F.4: Line Tensions Arrangement 1, Load Case 1, Turbine 4

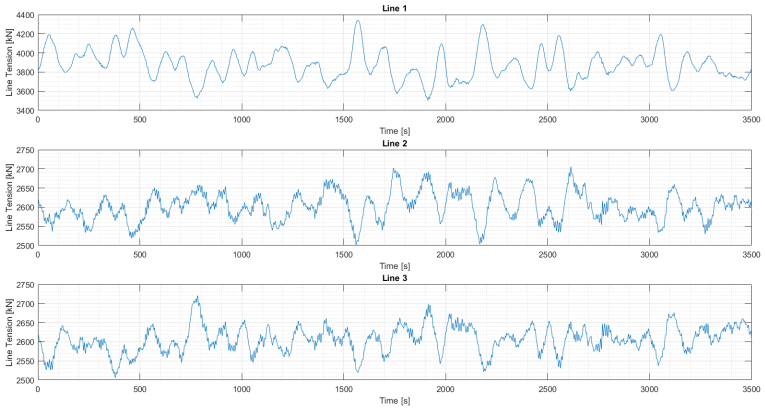

Figure F.5: Line Tensions Arrangement 1, Load Case 1, Turbine 5

F.1.2 Load Case 2

Table F.2: Maximum and average line tensions for each line in each turbine in Arrangement 1, under Load Case 2

		Turbine 1		Turbine 2		Turbine 3		Turbine 4		Turbine 5	
		Max	**Avg**	**Max**	**Avg**	**Max**	**Avg**	**Max**	**Avg**	**Max**	**Avg**
0	**L1**	2699	2366	2713	2366	2713	2366	4040	3634	4040	3634
	L2	3569	3318	3576	3317	3576	3318	2913	2652	2913	2652
	L3	3569	3317	3579	3317	3579	3317	2896	2652	2896	2652
1	**L1**	2735	2439	2718	2439	2731	2439	3864	3553	3836	3552
	L2	3198	2972	3169	2972	3170	2972	2746	2434	2771	2435
	L3	3910	3558	3863	3557	3891	3558	3168	2982	3166	2982
2	**L1**	2735	2439	2718	2439	2731	2439	3864	3553	3836	3552
	L2	3198	2972	3169	2972	3170	2972	2746	2434	2771	2435
	L3	3910	3558	3863	3557	3891	3558	3168	2982	3166	2982
3	**L1**	2905	2656	2917	2657	2905	2656	3599	3316	3607	3316
	L2	2912	2645	2907	2645	2908	2645	2729	2363	2643	2363
	L3	4103	3640	4052	3639	4099	3640	3652	3325	3671	3324
4	**L1**	3017	2809	3018	2809	3036	2810	3404	3141	3409	3141
	L2	2764	2534	2810	2535	2819	2534	2731	2397	2678	2396
	L3	4056	3590	4002	3588	4050	3590	3744	3434	3740	3435
5	**L1**	3219	2978	3184	2978	3174	2978	3178	2978	3184	2977
	L2	2733	2437	2702	2437	2752	2437	2711	2437	2752	2437
	L3	3864	3553	3936	3553	3849	3552	3937	3553	3850	3552
6	**L1**	3348	3148	3353	3148	3380	3148	3026	2808	3046	2807
	L2	2716	2389	2674	2389	2705	2389	2841	2531	2822	2531
	L3	3755	3444	3707	3444	3781	3444	3951	3601	3966	3602
7	**L1**	3543	3311	3535	3310	3563	3311	2928	2657	2936	2657
	L2	2697	2369	2698	2369	2699	2370	2939	2650	2914	2650
	L3	3560	3316	3571	3316	3596	3315	4010	3628	4018	3629
8	**L1**	3733	3438	3762	3437	3752	3438	2832	2537	2789	2537
	L2	2712	2391	2677	2391	2668	2390	3029	2800	3052	2800
	L3	3381	3151	3371	3151	3380	3152	4008	3601	4012	3601
9	**L1**	3975	3550	4010	3550	3993	3550	2822	2440	2712	2440
	L2	2751	2437	2776	2437	2766	2437	3235	2972	3268	2973
	L3	3203	2981	3189	2982	3255	2981	4053	3556	4000	3556
10	**L1**	4132	3634	4179	3636	4179	3636	2694	2366	2694	2366
	L2	2899	2653	2893	2652	2894	2652	3664	3319	3664	3319
	L3	2915	2652	2890	2651	2890	2651	3672	3318	3672	3318
***All values shown in kilonewtons [kN]**											

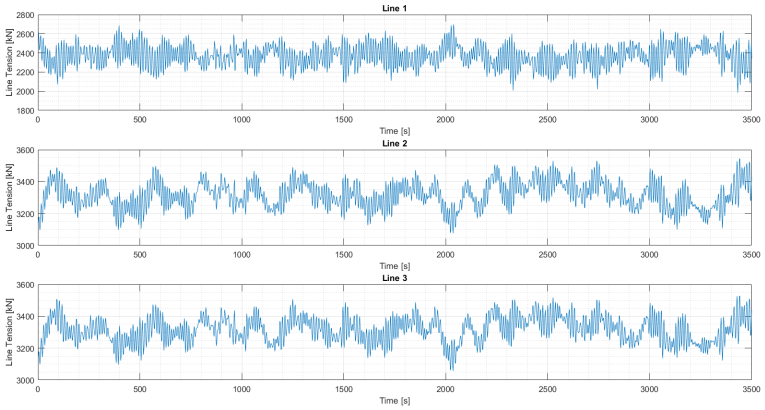

Figure F.6: Line Tensions Arrangement 1, Load Case 2, Turbine 1

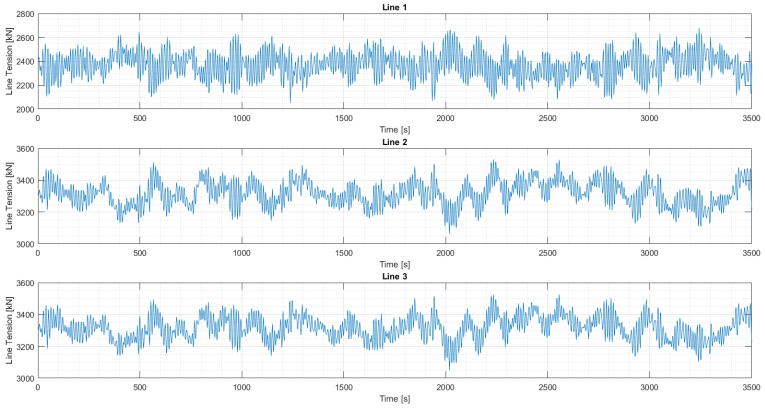

Figure F.7: Line Tensions Arrangement 1, Load Case 2, Turbine 2

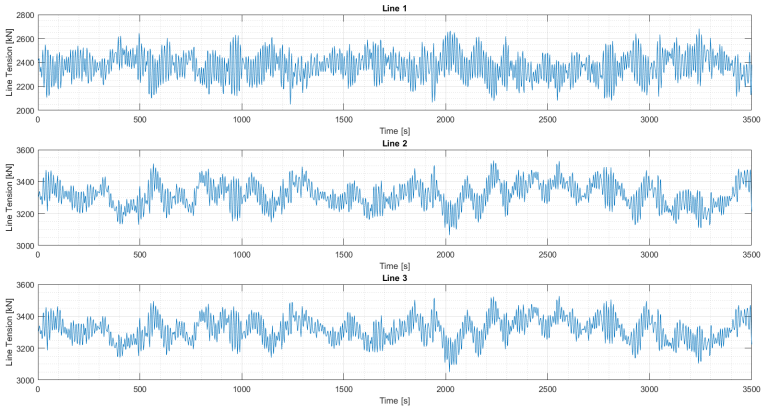

Figure F.8: Line Tensions Arrangement 1, Load Case 2, Turbine 3

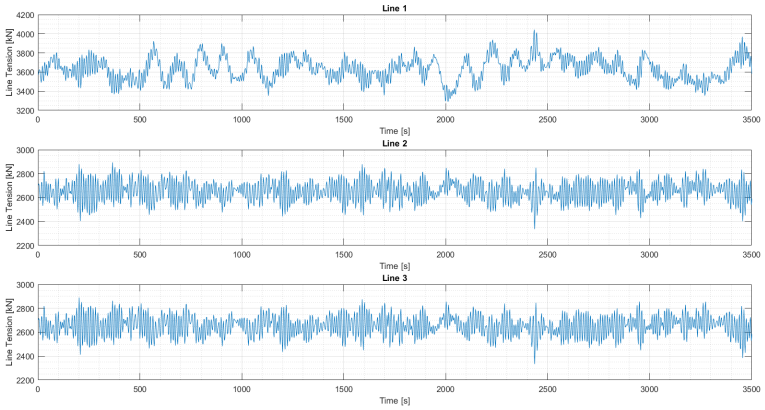

Figure F.9: Line Tensions Arrangement 1, Load Case 2, Turbine 4

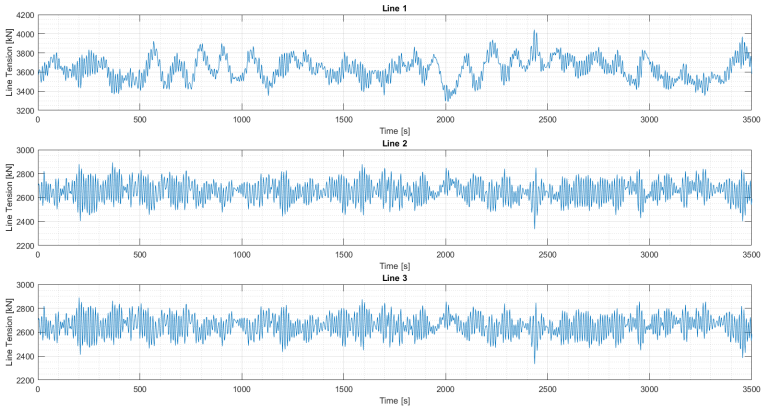

Figure F.10: Line Tensions Arrangement 1, Load Case 2, Turbine 5

F.1.3 Load Case 3

Table F.3: Maximum and average line tensions for each line in each turbine in Arrangement 1, under Load Case 3

		Turbine 1		**Turbine 2**		**Turbine 3**		**Turbine 4**		**Turbine 5**	
		Max	**Avg**	**Max**	**Avg**	**Max**	**Avg**	**Max**	**Avg**	**Max**	**Avg**
0	**L1**	2545	2210	2529	2211	2529	2211	4442	3968	4442	3968
	L2	3833	3541	3814	3540	3814	3541	2849	2588	2849	2588
	L3	3820	3541	3806	3540	3805	3540	2857	2588	2857	2588
1	**L1**	2670	2300	2656	2301	2670	2301	4222	3859	4267	3861
	L2	3253	3043	3273	3043	3281	3043	2612	2298	2638	2297
	L3	4213	3872	4244	3871	4203	3871	3272	3057	3272	3058
2	**L1**	2724	2429	2733	2430	2743	2430	4163	3707	4125	3709
	L2	3032	2795	3048	2794	3026	2794	2560	2240	2554	2239
	L3	4444	3927	4527	3927	4467	3926	3636	3304	3532	3305
3	**L1**	2829	2594	2873	2595	2838	2595	3867	3535	3863	3535
	L2	2821	2580	2872	2580	2830	2580	2525	2210	2558	2211
	L3	4457	3970	4336	3969	4455	3969	3878	3544	3896	3544
4	**L1**	3071	2806	3045	2806	3114	2806	3532	3295	3535	3295
	L2	2747	2423	2720	2422	2721	2423	2609	2241	2602	2242
	L3	4287	3920	4379	3921	4326	3919	4034	3712	3994	3711
5	**L1**	3293	3051	3280	3050	3301	3050	3303	3049	3293	3049
	L2	2590	2302	2582	2303	2657	2303	2579	2303	2655	2303
	L3	4260	3857	4253	3855	4267	3855	4259	3855	4271	3856
6	**L1**	3517	3298	3515	3297	3588	3298	3039	2805	3037	2805
	L2	2558	2240	2557	2240	2533	2239	2712	2423	2765	2422
	L3	4069	3713	4036	3713	4047	3715	4328	3923	4315	3926
7	**L1**	3879	3539	3870	3538	3808	3537	2885	2593	2899	2593
	L2	2558	2210	2611	2210	2546	2211	2904	2583	2888	2583
	L3	3903	3545	3892	3544	3824	3543	4476	3969	4488	3968
8	**L1**	4049	3706	4078	3705	4038	3707	2725	2429	2702	2429
	L2	2515	2243	2568	2242	2614	2240	3027	2795	3027	2795
	L3	3525	3300	3542	3301	3532	3302	4439	3926	4450	3926
9	**L1**	4323	3865	4314	3864	4290	3863	2599	2301	2584	2301
	L2	2628	2297	2597	2297	2573	2298	3242	3046	3270	3046
	L3	3327	3055	3325	3056	3256	3056	4230	3869	4370	3869
10	**L1**	4445	3974	4352	3972	4352	3972	2581	2209	2581	2209
	L2	2816	2587	2839	2587	2839	2587	3795	3543	3795	3543
	L3	2821	2587	2839	2587	2839	2587	3813	3543	3813	3543
***All values shown in kilonewtons [kN]**											

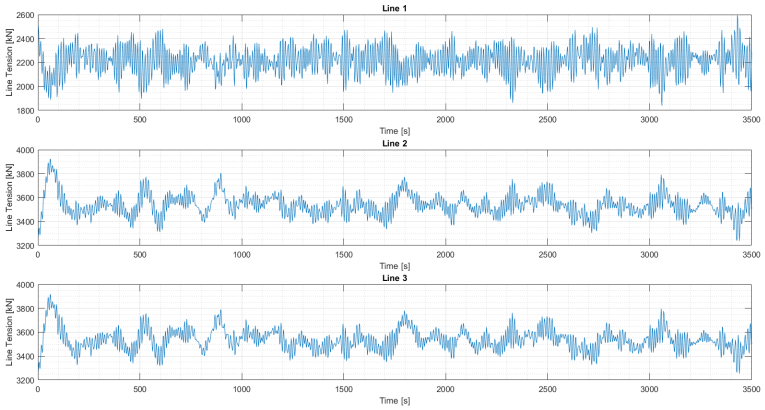

Figure F.11: Line Tensions Arrangement 1, Load Case 3, Turbine 1

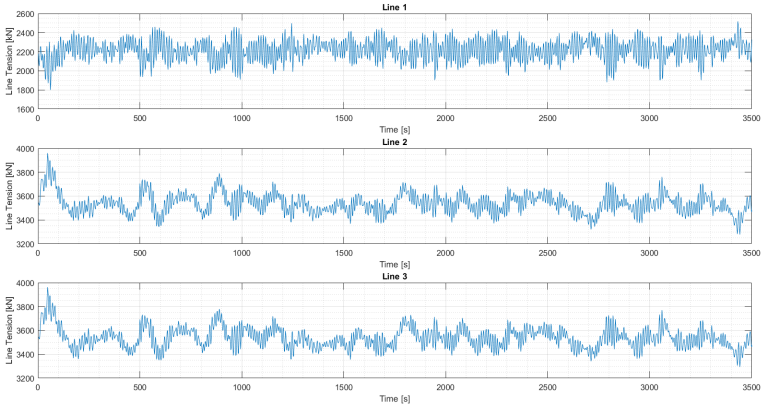

Figure F.12: Line Tensions Arrangement 1, Load Case 3, Turbine 2

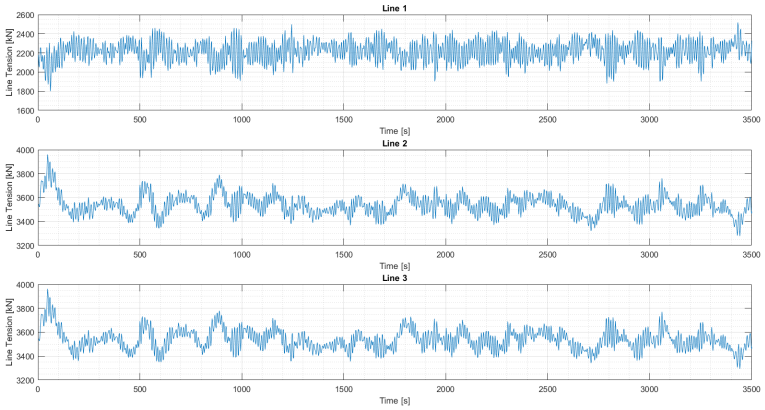

Figure F.13: Line Tensions Arrangement 1, Load Case 3, Turbine 3

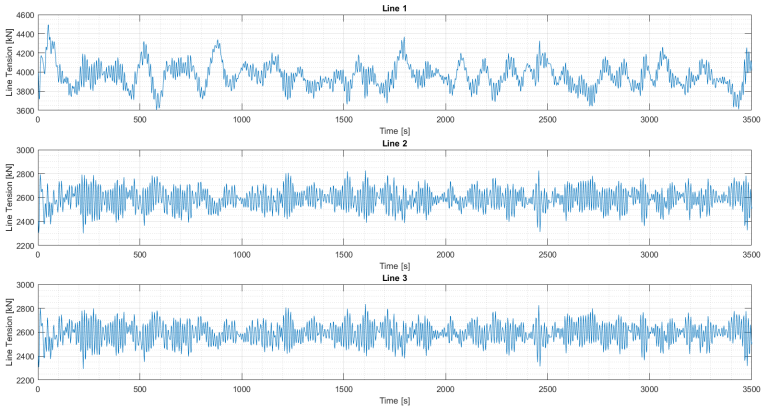

Figure F.14: Line Tensions Arrangement 1, Load Case 3, Turbine 4

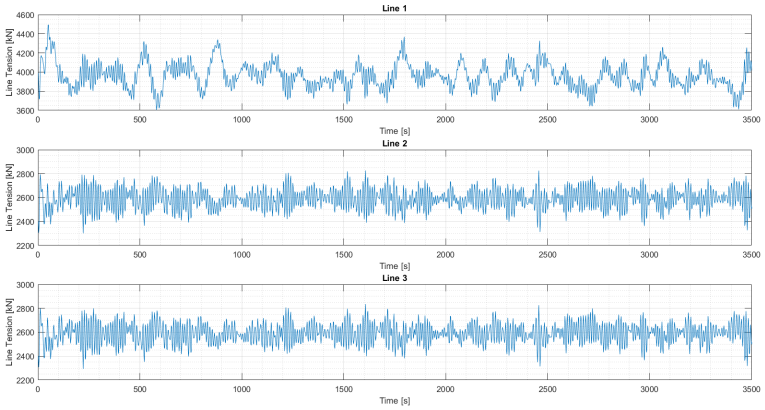

Figure F.15: Line Tensions Arrangement 1, Load Case 3, Turbine 5

F.2 Arrangement 2

F.2.1 Load Case 1

Table F.4: Maximum and average line tensions for each line in each turbine in Arrangement 2, under Load Case 1

		Turbine 1		Turbine 2		Turbine 3		Turbine 4		Turbine 5		Turbine 6	
		Max	**Avg**	**Max**	**Avg**	**Max**	**Avg**	**Max**	**Avg**	**Max**	**Avg**	**Max**	**Avg**
0	**L1**	2452	2268	4362	3866	2452	2269	4360	3864	2450	2268	4354	3859
	L2	3737	3472	2717	2606	3737	3472	2715	2605	3736	3470	2714	2605
	L3	3736	3473	2716	2606	3732	3473	2714	2604	3733	3471	2717	2601
1	**L1**	2491	2347	4086	3773	2498	2347	4088	3772	2494	2346	4086	3773
	L2	3203	3026	3186	3034	3204	3026	3181	3032	3208	3024	3187	3036
	L3	4099	3776	2506	2345	4109	3777	2495	2343	4096	3775	2499	2346
2	**L1**	2617	2467	3953	3612	2621	2467	3946	3612	2615	2465	3965	3619
	L2	2917	2800	3436	3246	2915	2800	3435	3245	2913	2798	3437	3248
	L3	4283	3805	2491	2303	4284	3806	2489	2301	4279	3804	2490	2304
3	**L1**	2717	2607	3848	3475	2726	2608	3861	3474	2724	2607	3832	3475
	L2	2706	2601	3786	3483	2704	2601	3775	3481	2703	2600	3782	3483
	L3	4410	3873	2431	2265	4403	3874	2419	2264	4401	3873	2438	2271
4	**L1**	2913	2805	3472	3236	2911	2805	3473	3235	2913	2804	3476	3249
	L2	2624	2467	3986	3608	2613	2467	3994	3606	2616	2466	4013	3617
	L3	4329	3795	2488	2309	4325	3795	2481	2308	4339	3793	2496	2309
5	**L1**	3213	3025	3169	3026	3215	3025	3165	3025	3213	3023	3157	3030
	L2	2505	2353	4109	3757	2495	2354	4106	3755	2508	2352	4101	3746
	L3	4112	3757	2490	2353	4119	3758	2492	2352	4112	3756	2487	2365
***All values shown in kilonewtons [kN]**													

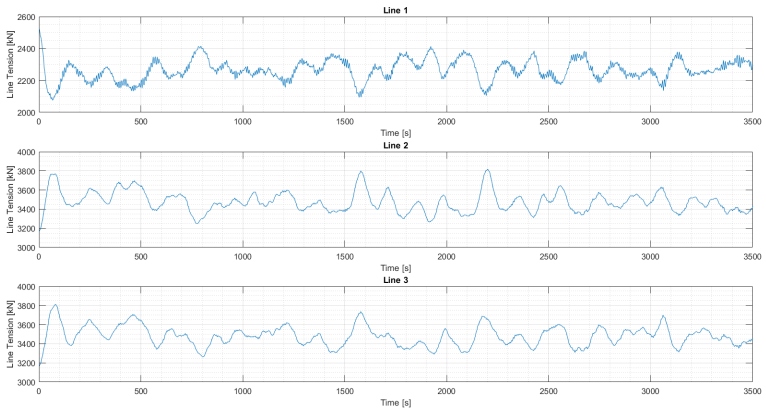

Figure F.16: Line Tensions Arrangement 2, Load Case 1, Turbine 1

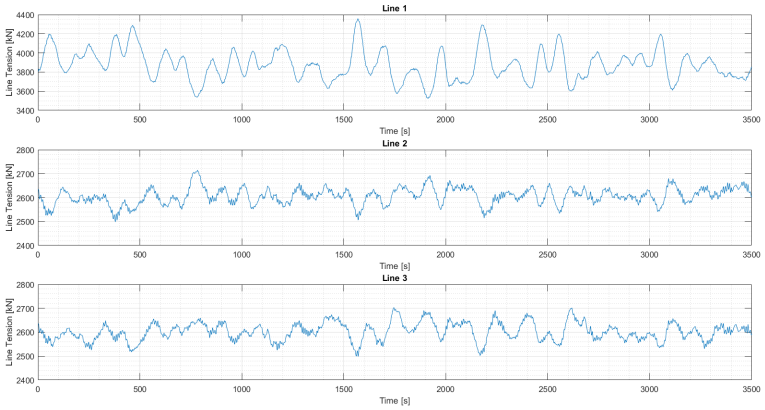

Figure F.17: Line Tensions Arrangement 2, Load Case 1, Turbine 2

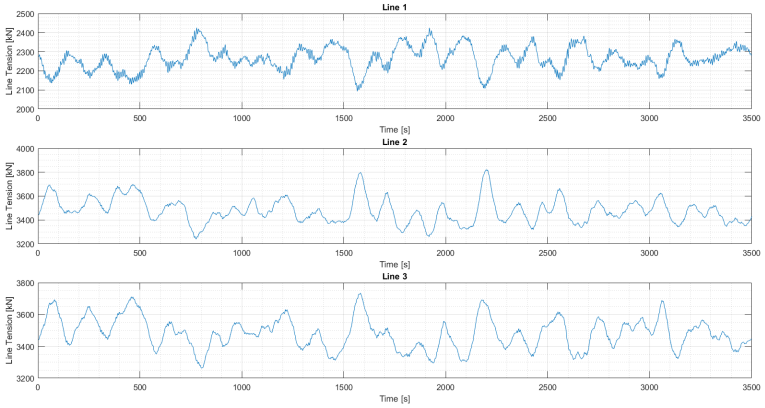

Figure F.18: Line Tensions Arrangement 2, Load Case 1, Turbine 3

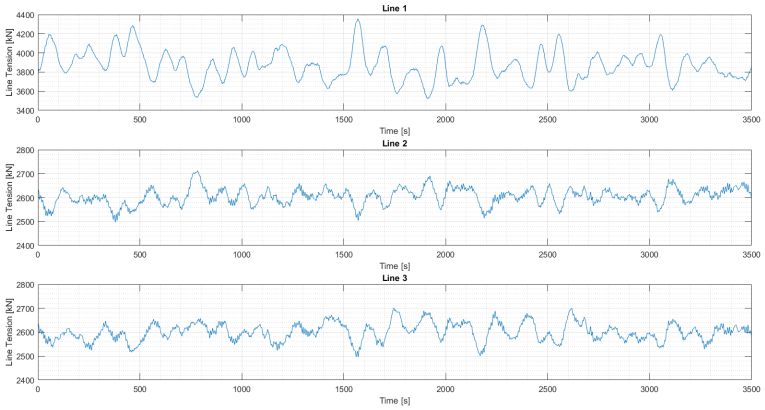

Figure F.19: Line Tensions Arrangement 2, Load Case 1, Turbine 4

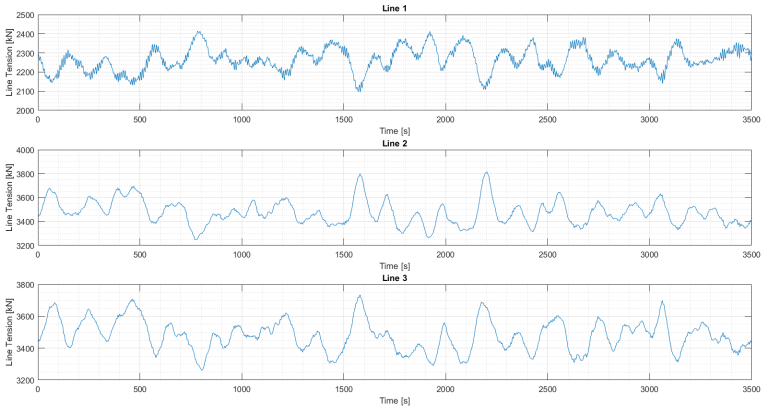

Figure F.20: Line Tensions Arrangement 2, Load Case 1, Turbine 5

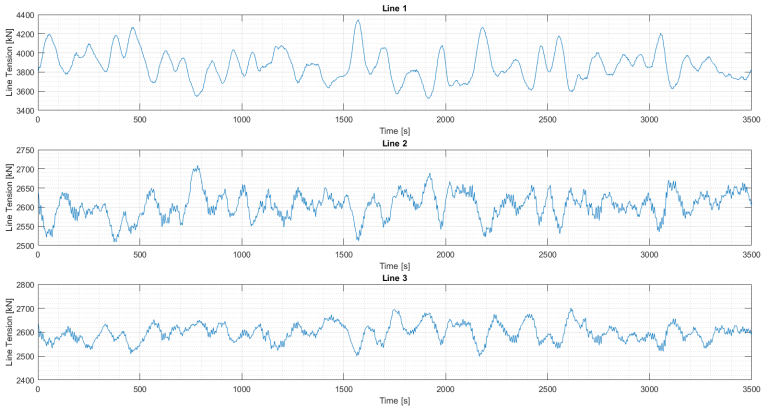

Figure F.21: Line Tensions Arrangement 2, Load Case 1, Turbine 6

F.2.2 Load Case 2

Table F.5: Maximum and average line tensions for each line in each turbine in Arrangement 2, under Load Case 2

		Turbine 1		Turbine 2		Turbine 3		Turbine 4		Turbine 5		Turbine 6	
		Max	**Avg**	**Max**	**Avg**	**Max**	**Avg**	**Max**	**Avg**	**Max**	**Avg**	**Max**	**Avg**
0	**L1**	2699	2366	4064	3634	2697	2366	4062	3632	2710	2365	4028	3631
	L2	3569	3318	2915	2652	3581	3318	2913	2651	3574	3316	2894	2645
	L3	3569	3317	2920	2653	3580	3317	2919	2651	3573	3315	2922	2653
1	**L1**	2727	2437	3894	3555	2791	2439	3968	3552	2750	2436	3901	3555
	L2	3183	2973	3193	2982	3179	2974	3188	2980	3160	2973	3184	2979
	L3	3924	3560	2745	2435	4002	3558	2783	2435	3933	3559	2734	2435
2	**L1**	2910	2536	3785	3440	2846	2536	3764	3438	2871	2535	3809	3451
	L2	3037	2801	3421	3152	3003	2802	3425	3149	3017	2800	3390	3153
	L3	4020	3603	2731	2391	3974	3603	2742	2390	4000	3602	2773	2387
3	**L1**	2904	2655	3590	3317	2890	2656	3584	3316	2888	2654	3567	3320
	L2	2888	2647	3595	3322	2891	2648	3616	3321	2889	2646	3621	3322
	L3	4022	3638	2640	2365	3987	3637	2647	2363	3985	3635	2638	2367
4	**L1**	3007	2809	3364	3145	3014	2809	3373	3144	3031	2808	3399	3153
	L2	2810	2533	3728	3439	2821	2533	3695	3438	2809	2532	3824	3454
	L3	3995	3595	2701	2394	3983	3596	2699	2392	4016	3593	2701	2389
5	**L1**	3207	2978	3203	2978	3200	2978	3180	2976	3184	2977	3173	2971
	L2	2746	2436	3972	3554	2723	2438	3902	3550	2728	2437	3959	3556
	L3	3968	3554	2743	2437	3885	3552	2729	2437	3910	3550	2740	2448
***All values shown in kilonewtons [kN]**													

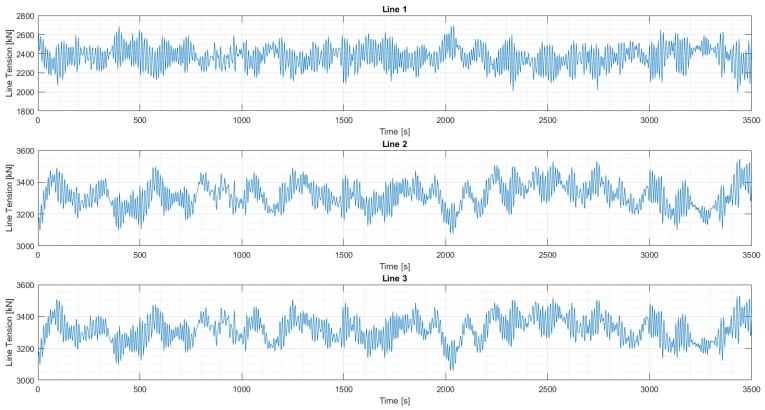

Figure F.22: Line Tensions Arrangement 2, Load Case 2, Turbine 1

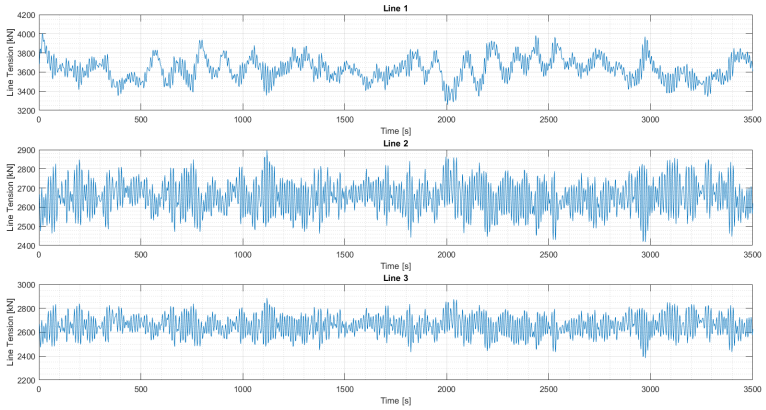

Figure F.23: Line Tensions Arrangement 2, Load Case 2, Turbine 2

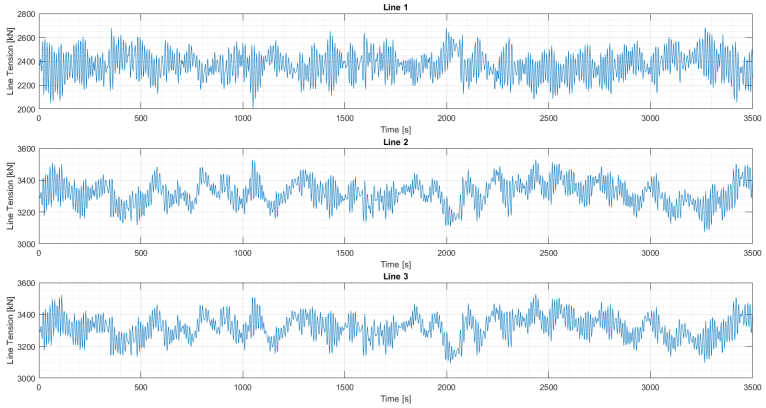

Figure F.24: Line Tensions Arrangement 2, Load Case 2, Turbine 3

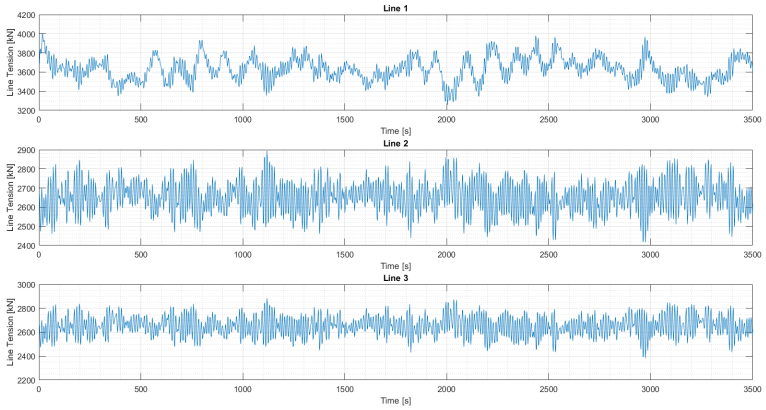

Figure F.25: Line Tensions Arrangement 2, Load Case 2, Turbine 4

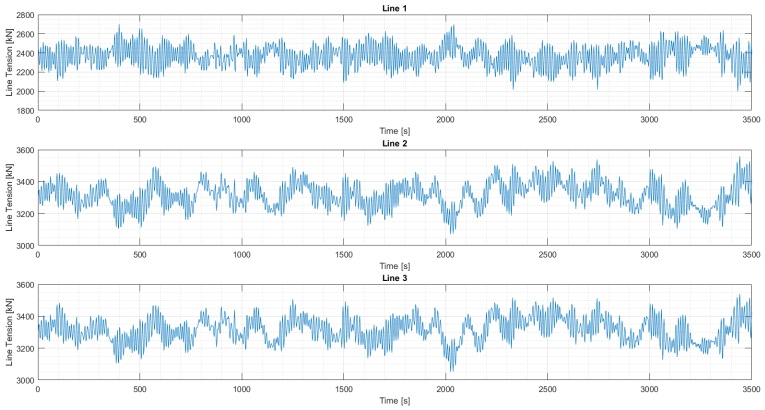

Figure F.26: Line Tensions Arrangement 2, Load Case 2, Turbine 5

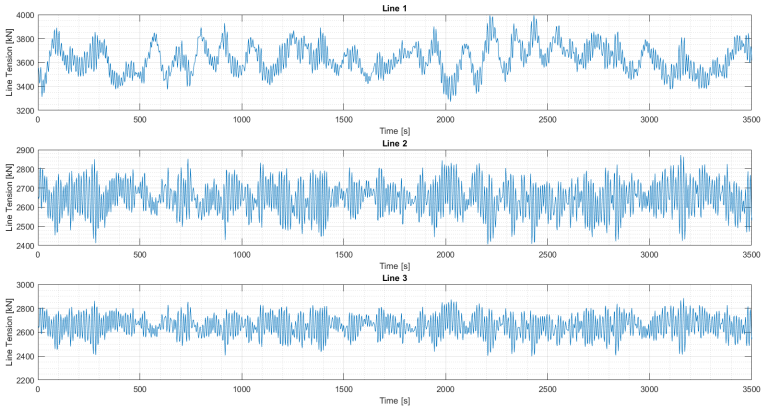

Figure F.27: Line Tensions Arrangement 2, Load Case 2, Turbine 6

F.2.3 Load Case 3

Table F.6: Maximum and average line tensions for each line in each turbine in Arrangement 2, under Load Case 3

		Turbine 1		Turbine 2		Turbine 3		Turbine 4		Turbine 5		Turbine 6	
		Max	**Avg**	**Max**	**Avg**	**Max**	**Avg**	**Max**	**Avg**	**Max**	**Avg**	**Max**	**Avg**
0	**L1**	2545	2210	4428	3969	2545	2211	4426	3967	2548	2210	4392	3965
	L2	3833	3541	2844	2588	3821	3541	2843	2586	3834	3539	2829	2581
	L3	3820	3541	2838	2588	3819	3541	2836	2586	3819	3539	2857	2588
1	**L1**	2662	2306	4241	3853	2661	2306	4262	3851	2634	2305	4316	3850
	L2	3277	3042	3288	3055	3242	3042	3263	3053	3263	3040	3284	3054
	L3	4319	3860	2633	2302	4266	3860	2648	2300	4264	3859	2642	2303
2	**L1**	2692	2430	4099	3705	2691	2430	4070	3704	2689	2429	4018	3713
	L2	2990	2795	3550	3302	3025	2797	3527	3300	3003	2795	3558	3310
	L3	4333	3924	2542	2243	4301	3922	2536	2241	4355	3920	2543	2240
3	**L1**	2844	2592	3843	3538	2834	2593	3858	3538	2833	2592	3854	3538
	L2	2810	2581	3818	3545	2840	2581	3884	3546	2839	2580	3801	3548
	L3	4402	3973	2510	2212	4432	3974	2557	2208	4430	3972	2513	2216
4	**L1**	3019	2806	3562	3299	3072	2807	3506	3297	3061	2805	3597	3309
	L2	2690	2421	4109	3716	2708	2421	4092	3716	2718	2420	4107	3734
	L3	4393	3927	2539	2240	4299	3928	2547	2238	4390	3925	2562	2240
5	**L1**	3268	3051	3282	3049	3288	3052	3337	3048	3318	3050	3308	3046
	L2	2581	2300	4223	3858	2629	2300	4189	3857	2629	2300	4230	3865
	L3	4209	3858	2598	2302	4184	3859	2623	2301	4195	3856	2663	2313
***All values shown in kilonewtons [kN]**													

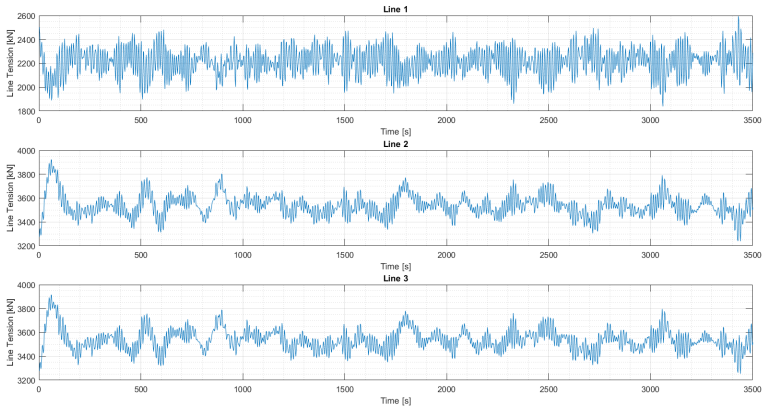

Figure F.28: Line Tensions Arrangement 2, Load Case 3, Turbine 1

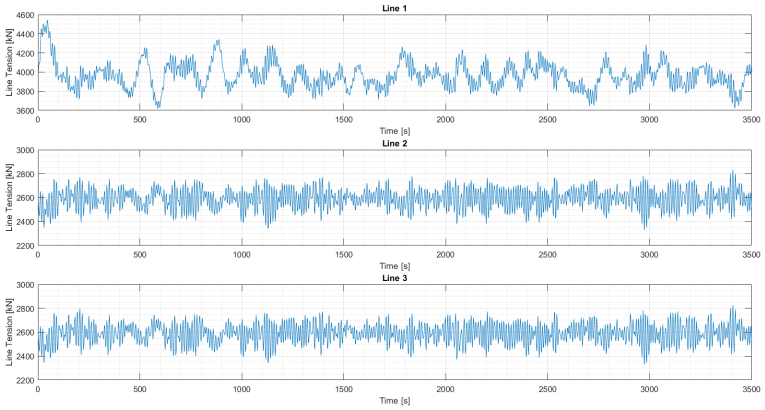

Figure F.29: Line Tensions Arrangement 2, Load Case 3, Turbine 2

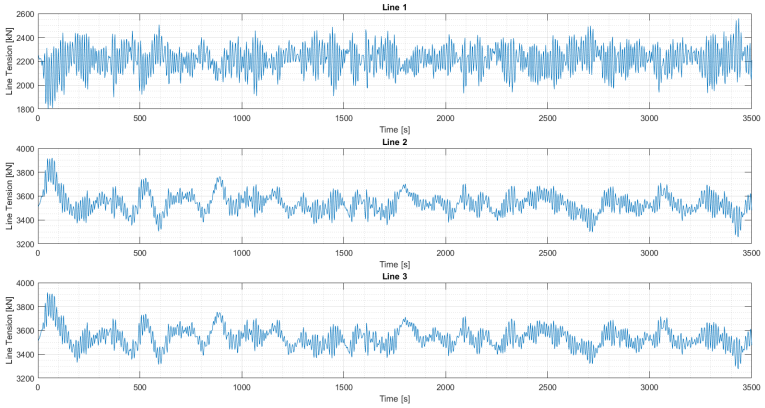

Figure F.30: Line Tensions Arrangement 2, Load Case 3, Turbine 3

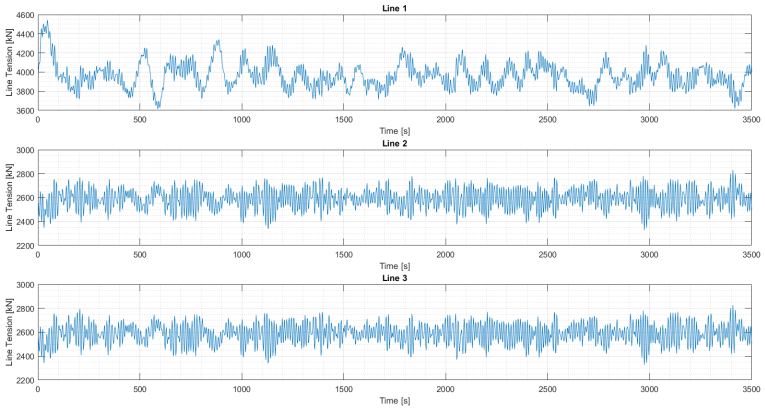

Figure F.31: Line Tensions Arrangement 2, Load Case 3, Turbine 4

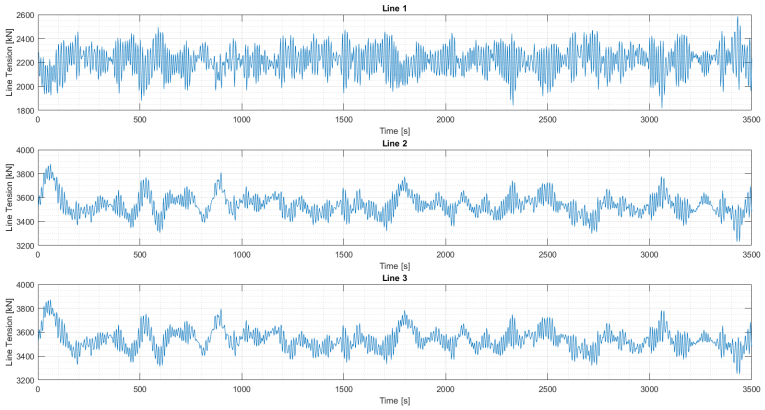

Figure F.32: Line Tensions Arrangement 2, Load Case 3, Turbine 5

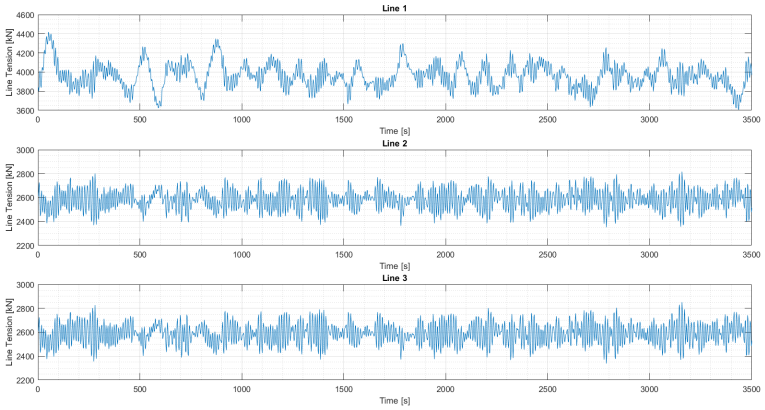

Figure F.33: Line Tensions Arrangement 2, Load Case 3, Turbine 6

F.3 Arrangement 3

F.3.1 Load Case 1

Table F.7: Maximum and average line tensions for each line in each turbine in Arrangement 3, under Load Case 1

		Turbine 1		**Turbine 2**		**Turbine 3**		**Turbine 4**		**Turbine 5**	
		Max	**Avg**	**Max**	**Avg**	**Max**	**Avg**	**Max**	**Avg**	**Max**	**Avg**
0	**L1**	2452	2268	3172	3028	4366	3865	3190	3027	4079	3652
	L2	3737	3472	2517	2348	2713	2606	4182	3769	2930	2870
	L3	3736	3473	4198	3769	2716	2605	2514	2348	2555	2408
	L4									2925	2871
1	**L1**	2542	2364	3723	3447	4119	3732	2714	2612	3824	3499
	L2	3133	3017	2485	2286	3202	3021	4278	3827	2708	2612
	L3	4099	3734	3686	3443	2541	2363	2723	2615	2608	2467
	L4									3367	3206
2	**L1**	2563	2466	3936	3622	3905	3614	2566	2460	3579	3366
	L2	2879	2797	2417	2303	3440	3250	4162	3808	2616	2523
	L3	4196	3811	3430	3239	2425	2300	2906	2807	2608	2526
	L4									3605	3374
3	**L1**	2724	2611	4276	3758	3778	3460	2569	2354	3397	3212
	L2	2727	2607	2575	2356	3822	3465	4224	3755	2619	2459
	L3	4463	3851	3189	3022	2508	2276	3250	3028	2722	2609
	L4									3950	3520
4	**L1**	2923	2804	4301	3795	3511	3236	2477	2309	3174	3031
	L2	2592	2468	2598	2470	3932	3605	4025	3604	2551	2435
	L3	4333	3795	2939	2801	2469	2309	3483	3239	2802	2730
	L4									4008	3581
5	**L1**	3213	3035	4376	3884	3214	3031	2450	2260	2931	2869
	L2	2508	2340	2696	2604	4224	3788	3729	3484	2536	2403
	L3	4186	3786	2706	2601	2502	2342	3764	3488	2946	2872
	L4									4093	3667
***All values shown in kilonewtons [kN]**											

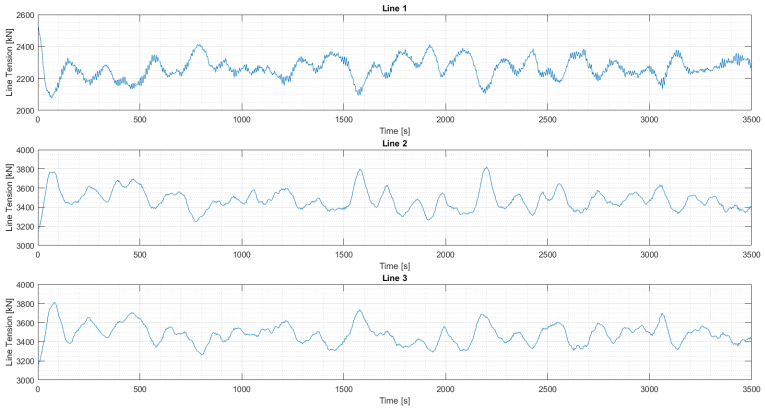

Figure F.34: Line Tensions Arrangement 3, Load Case 1, Turbine 1

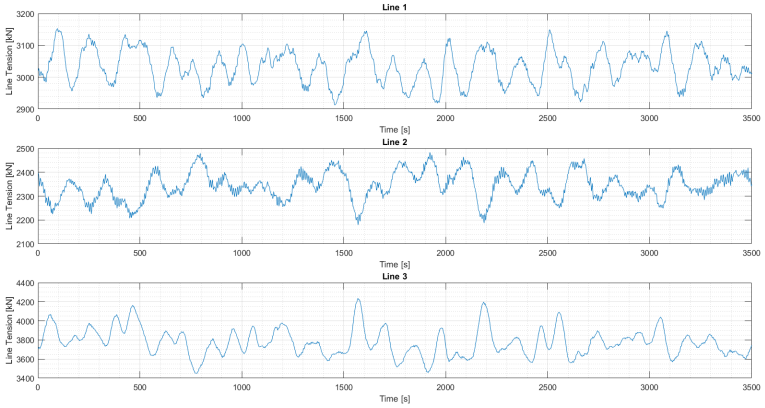

Figure F.35: Line Tensions Arrangement 3, Load Case 1, Turbine 2

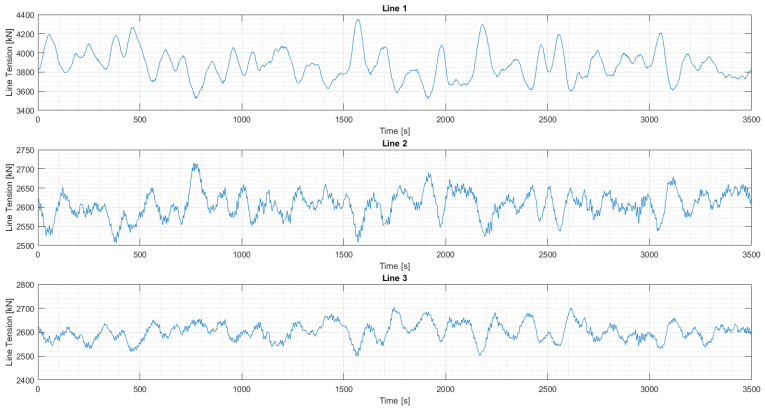

Figure F.36: Line Tensions Arrangement 3, Load Case 1, Turbine 3

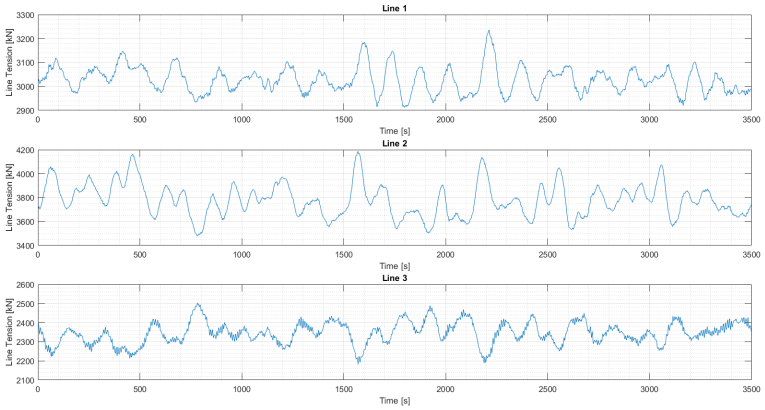

Figure F.37: Line Tensions Arrangement 3, Load Case 1, Turbine 4

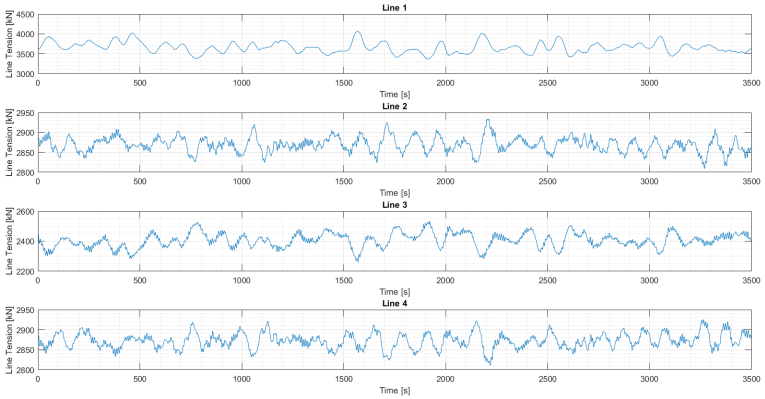

Figure F.38: Line Tensions Arrangement 3, Load Case 1, Turbine 5

F.3.2 Load Case 2

Table F.8: Maximum and average line tensions for each line in each turbine in Arrangement 3, under Load Case 2

		Turbine 1		**Turbine 2**		**Turbine 3**		**Turbine 4**		**Turbine 5**	
		Max	**Avg**	**Max**	**Avg**	**Max**	**Avg**	**Max**	**Avg**	**Max**	**Avg**
0	**L1**	2699	2366	3179	2975	4006	3634	3167	2976	3858	3473
	L2	3569	3318	2778	2439	2900	2652	3933	3554	3063	2878
	L3	3569	3317	3935	3554	2907	2652	2768	2439	2788	2460
	L4									3061	2877
1	**L1**	2782	2439	3629	3320	3909	3552	2902	2647	3760	3376
	L2	3225	2973	2698	2365	3167	2982	4111	3636	2884	2652
	L3	3995	3556	3603	3315	2755	2435	2914	2657	2797	2509
	L4									3397	3144
2	**L1**	2882	2538	3736	3440	3741	3434	2874	2530	3525	3257
	L2	3053	2800	2725	2393	3391	3150	3959	3594	2827	2574
	L3	3960	3598	3390	3142	2726	2391	3065	2812	2831	2576
	L4									3553	3261
3	**L1**	2932	2659	3909	3548	3560	3308	2784	2440	3348	3136
	L2	2904	2649	2730	2443	3529	3315	3964	3541	2781	2511
	L3	3989	3625	3187	2972	2771	2370	3229	2981	2887	2657
	L4									3682	3370
4	**L1**	3042	2809	3957	3596	3392	3145	2718	2392	3192	3002
	L2	2825	2534	2824	2537	3792	3439	3767	3437	2754	2480
	L3	3964	3594	3010	2804	2783	2394	3377	3150	2985	2761
	L4									3797	3432
5	**L1**	3171	2978	3977	3630	3162	2976	2688	2369	3070	2876
	L2	2721	2439	2901	2653	3879	3549	3563	3312	2753	2463
	L3	3863	3548	2896	2652	2730	2440	3558	3314	3061	2878
	L4									3776	3468
	***All values shown in kilonewtons [kN]**										

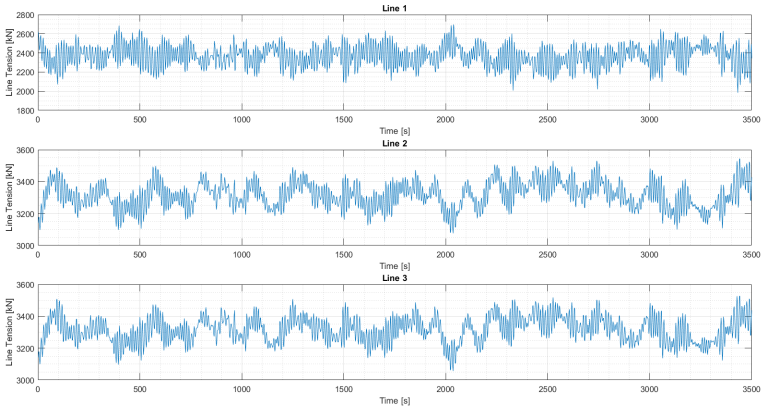

Figure F.39: Line Tensions Arrangement 3, Load Case 2, Turbine 1

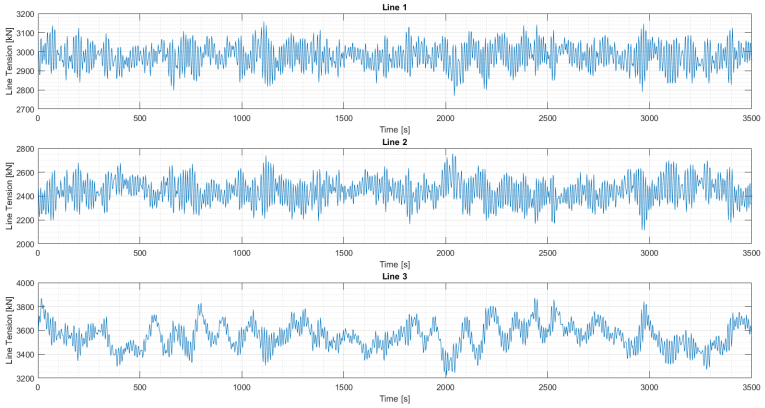

Figure F.40: Line Tensions Arrangement 3, Load Case 2, Turbine 2

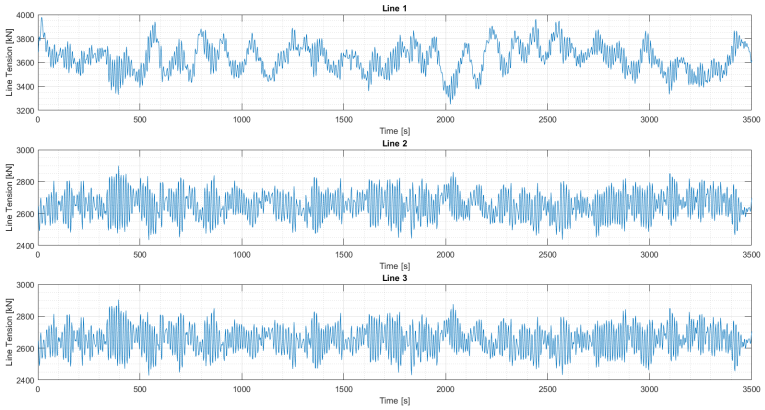

Figure F.41: Line Tensions Arrangement 3, Load Case 2, Turbine 3

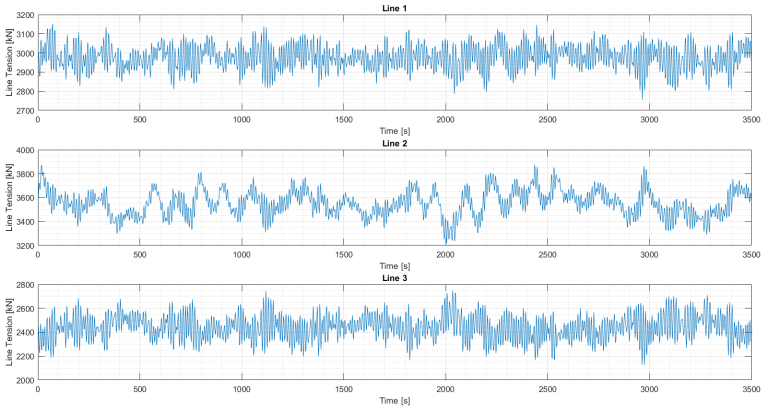

Figure F.42: Line Tensions Arrangement 3, Load Case 2, Turbine 4

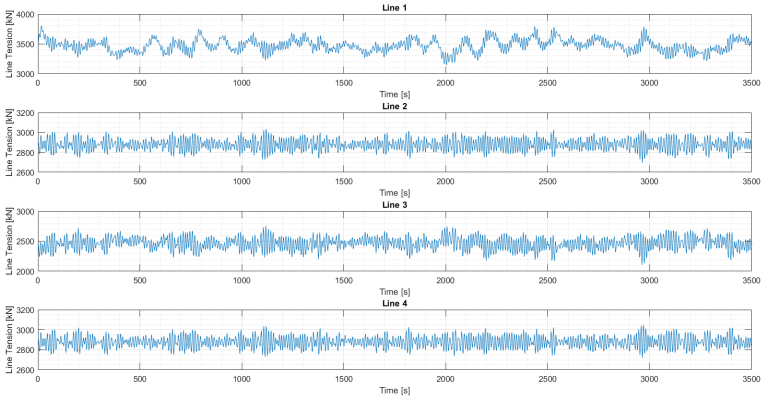

Figure F.43: Line Tensions Arrangement 3, Load Case 2, Turbine 5

F.3.3 Load Case 3

Table F.9: Maximum and average line tensions for each line in each turbine in Arrangement 3, under Load Case 3

		Turbine 1		**Turbine 2**		**Turbine 3**		**Turbine 4**		**Turbine 5**	
		Max	**Avg**	**Max**	**Avg**	**Max**	**Avg**	**Max**	**Avg**	**Max**	**Avg**
0	**L1**	2545	2210	3262	3048	4452	3968	3261	3049	4216	3793
	L2	3833	3541	2618	2301	2836	2588	4259	3863	3091	2911
	L3	3820	3541	4268	3863	2838	2588	2622	2301	2632	2329
	L4									3093	2911
1	**L1**	2617	2300	3807	3548	4223	3865	2824	2579	3982	3640
	L2	3266	3045	2505	2207	3266	3058	4355	3977	2836	2591
	L3	4232	3874	3780	3539	2574	2295	2847	2593	2681	2388
	L4									3554	3286
2	**L1**	2752	2430	4046	3713	4063	3705	2733	2422	3767	3452
	L2	2982	2796	2541	2245	3556	3304	4409	3918	2749	2481
	L3	4408	3923	3549	3293	2539	2244	3038	2810	2752	2483
	L4									3806	3457
3	**L1**	2888	2592	4274	3879	3793	3544	2582	2292	3489	3281
	L2	2854	2577	2613	2297	3797	3554	4315	3871	2683	2385
	L3	4486	3986	3285	3046	2521	2203	3290	3062	2846	2594
	L4									3964	3648
4	**L1**	3033	2806	4420	3933	3555	3300	2527	2240	3273	3085
	L2	2728	2421	2739	2425	4179	3721	4128	3712	2629	2346
	L3	4459	3929	3113	2798	2563	2237	3586	3304	2960	2747
	L4									4210	3743
5	**L1**	3288	3052	4518	3963	3289	3051	2520	2214	3076	2910
	L2	2598	2303	2872	2589	4385	3857	3884	3539	2628	2331
	L3	4392	3857	2864	2589	2611	2303	3892	3540	3084	2911
	L4									4322	3788
	***All values shown in kilonewtons [kN]**										

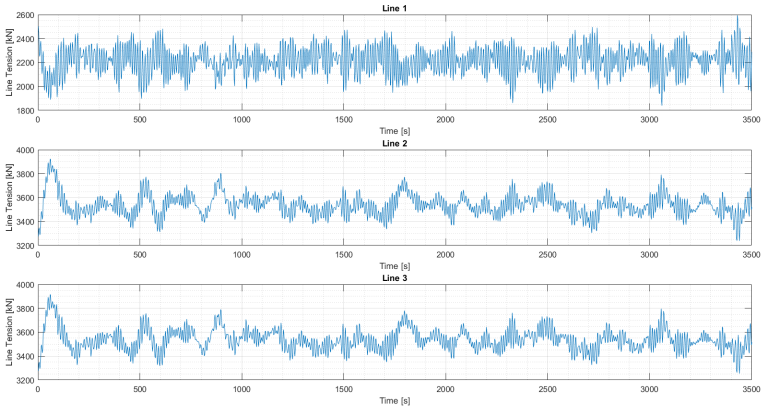

Figure F.44: Line Tensions Arrangement 3, Load Case 3, Turbine 1

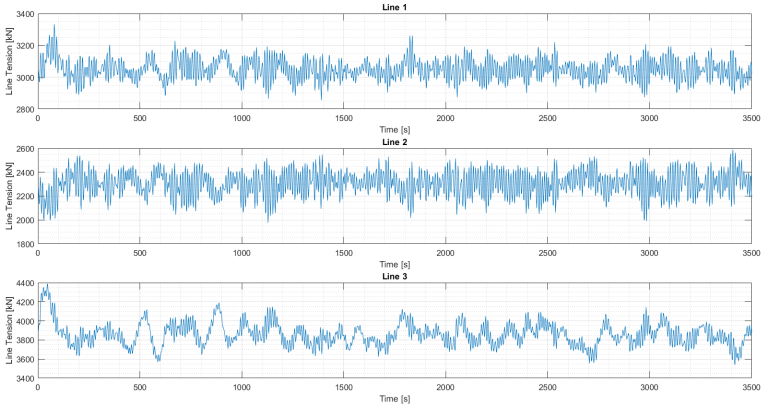

Figure F.45: Line Tensions Arrangement 3, Load Case 3, Turbine 2

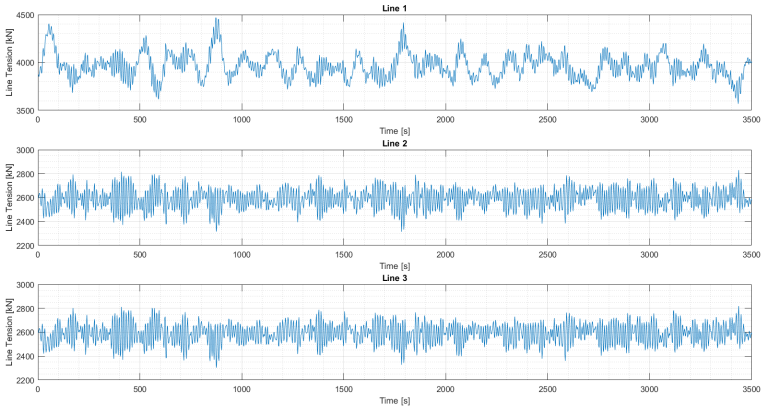

Figure F.46: Line Tensions Arrangement 3, Load Case 3, Turbine 3

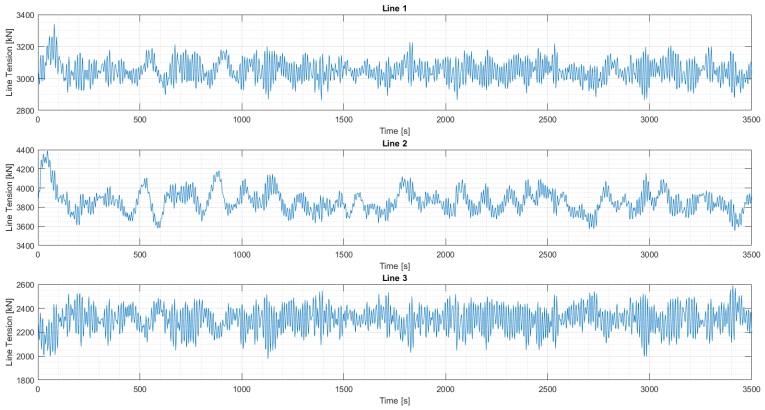

Figure F.47: Line Tensions Arrangement 3, Load Case 3, Turbine 4

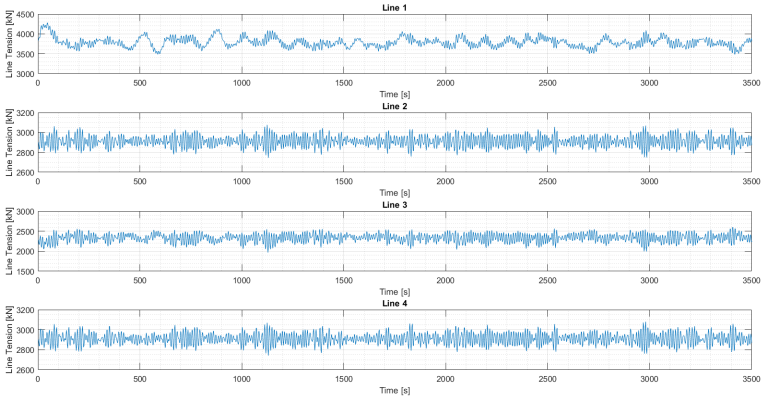

Figure F.48: Line Tensions Arrangement 3, Load Case 3, Turbine 5

APPENDIX G

RESULTANT FORCES ON SHARED ANCHORS

The full results for the resultant forces on the shared anchors are presented here for all the load cases of all the arrangements. The “Overall Maximum Tension” is the maximum tension this anchor group experiences from a single line. The reduction is the percentage reduction from this overall maximum.

G.1 Arrangement 1

Table G.1: Resultant Forces on anchor groups for Arrangement 1, Load Case 1

Direction	Group	Overall Maximum Tension [kN]	Minimum Resultant Tension [kN]	Reduction	Maximum Resultant Tension [kN]	Reduction	Average Resultant Tension [kN]	Reduction
0	**1**	3763	818	78%	1532	59%	1193	68%
	2	4356	1040	76%	2229	49%	1582	64%
	3	4356	1040	76%	2229	49%	1582	64%
	4	2723	2511	8%	2704	1%	2608	4%
1	**1**	4324	694	84%	1850	57%	1194	72%
	2	4227	788	81%	2040	52%	1375	67%
	3	4218	799	81%	2040	52%	1375	67%
	4	3273	2674	18%	2895	12%	2754	16%
2	**1**	4396	775	82%	1899	57%	1195	73%
	2	4056	782	81%	1735	57%	1133	72%
	3	4040	765	81%	1721	57%	1133	72%
	4	3554	2787	22%	3099	13%	2893	19%
3	**1**	4449	786	82%	1939	56%	1220	73%
	2	3783	525	86%	1254	67%	833	78%
	3	3785	524	86%	1257	67%	833	78%
	4	3773	2914	23%	3274	13%	3045	19%
4	**1**	4303	657	85%	1697	61%	1225	72%
	2	3469	254	93%	632	82%	445	87%
	3	3453	251	93%	637	82%	444	87%
	4	3950	2952	25%	3389	14%	3182	19%
5	**1**	4197	822	80%	1708	59%	1213	71%
	2	3180	0	100%	122	96%	37	99%
	3	3183	0	100%	120	96%	37	99%
	4	4162	3075	26%	3608	13%	3290	21%
6	**1**	3950	658	83%	1573	60%	1180	70%
	2	3459	192	94%	705	80%	440	87%
	3	3460	193	94%	716	79%	440	87%
	4	4174	3058	27%	3625	13%	3351	20%
7	**1**	3755	791	79%	1623	57%	1181	69%
	2	3756	518	86%	1242	67%	847	77%
	3	3757	526	86%	1236	67%	847	77%
	4	4433	3144	29%	3848	13%	3403	23%
8	**1**	3973	783	80%	1661	58%	1191	70%
	2	3967	728	82%	1620	59%	1168	71%
	3	3964	713	82%	1629	59%	1169	71%
	4	4323	3177	27%	3792	12%	3430	21%
9	**1**	4171	817	80%	1708	59%	1210	71%
	2	4164	926	78%	1962	53%	1393	67%
	3	4173	941	77%	1961	53%	1393	67%
	4	4203	3225	23%	3746	11%	3446	18%
10	**1**	4349	714	84%	1821	58%	1257	71%
	2	4320	1031	76%	2192	49%	1594	63%
	3	4320	1031	76%	2192	49%	1594	63%
	4	3744	3255	13%	3719	1%	3470	7%

Table G.2: Resultant Forces on anchor groups for Arrangement 1, Load Case 2

Direction	Group	Overall Maximum Tension [kN]	Minimum Resultant Tension [kN]	Reduction	Maximum Resultant Tension [kN]	Reduction	Average Resultant Tension [kN]	Reduction
0	**1**	3532	434	88%	1434	59%	946	73%
	2	4043	636	84%	1799	56%	1261	69%
	3	4043	636	84%	1799	56%	1261	69%
	4	2894	2334	19%	2885	0%	2653	8%
1	**1**	3873	564	85%	1426	63%	973	75%
	2	4013	557	86%	1686	58%	1113	72%
	3	3843	618	84%	1707	56%	1113	71%
	4	3178	2561	19%	2926	8%	2752	13%
2	**1**	4032	593	85%	1464	64%	965	76%
	2	3709	508	86%	1411	62%	900	76%
	3	3916	491	87%	1434	63%	899	77%
	4	3364	2681	20%	3014	10%	2851	15%
3	**1**	4052	415	90%	1559	62%	989	76%
	2	3599	177	95%	1129	69%	659	82%
	3	3607	289	92%	1099	70%	660	82%
	4	3652	2788	24%	3174	13%	2967	19%
4	**1**	4048	579	86%	1516	63%	953	76%
	2	3404	11	100%	649	81%	331	90%
	3	3409	15	100%	741	78%	332	90%
	4	3743	2858	24%	3287	12%	3053	18%
5	**1**	3936	492	88%	1372	65%	971	75%
	2	3184	0	100%	45	99%	12	100%
	3	3228	0	100%	47	99%	12	100%
	4	3937	2969	25%	3438	13%	3150	20%
6	**1**	3996	559	86%	1393	65%	946	76%
	2	3416	47	99%	649	81%	340	90%
	3	3380	27	99%	641	81%	341	90%
	4	3951	2985	24%	3466	12%	3206	19%
7	**1**	3571	474	87%	1378	61%	944	74%
	2	3535	248	93%	1039	71%	653	82%
	3	3563	293	92%	1060	70%	654	82%
	4	4010	3017	25%	3524	12%	3254	19%
8	**1**	3732	538	86%	1413	62%	942	75%
	2	3762	425	89%	1424	62%	900	76%
	3	3752	476	87%	1351	64%	901	76%
	4	4274	3041	29%	3557	17%	3277	23%
9	**1**	3975	555	86%	1556	61%	968	76%
	2	4010	537	87%	1861	54%	1110	72%
	3	3993	613	85%	1750	56%	1110	72%
	4	4053	3087	24%	3642	10%	3305	18%
10	**1**	4132	470	89%	1722	58%	982	76%
	2	4179	668	84%	1957	53%	1270	70%
	3	4179	668	84%	1957	53%	1270	70%
	4	3672	3079	16%	3667	0%	3318	10%

Table G.3: Resultant Forces on anchor groups for Arrangement 1, Load Case 3

Direction	Group	Overall Maximum Tension [kN]	Minimum Resultant Tension [kN]	Reduction	Maximum Resultant Tension [kN]	Reduction	Average Resultant Tension [kN]	Reduction
0	**1**	3963	699	82%	1927	51%	1320	67%
	2	4494	1183	74%	2526	44%	1745	61%
	3	4494	1183	74%	2526	44%	1745	61%
	4	2835	2297	19%	2831	0%	2589	9%
1	**1**	4244	810	81%	1894	55%	1365	68%
	2	4899	1014	79%	2117	57%	1558	68%
	3	4267	1015	76%	2144	50%	1560	63%
	4	3395	2604	23%	2957	13%	2759	19%
2	**1**	4527	835	82%	2118	53%	1357	70%
	2	4163	787	81%	1968	53%	1277	69%
	3	4125	755	82%	1974	52%	1279	69%
	4	3636	2763	24%	3162	13%	2924	20%
3	**1**	4496	922	79%	1985	56%	1382	69%
	2	3867	477	88%	1482	62%	940	76%
	3	4244	593	86%	1432	66%	940	78%
	4	3878	2913	25%	3364	13%	3103	20%
4	**1**	4379	928	79%	1902	57%	1352	69%
	2	3532	176	95%	847	76%	489	86%
	3	3535	181	95%	784	78%	489	86%
	4	4034	3031	25%	3505	13%	3241	20%
5	**1**	4271	862	80%	1939	55%	1348	68%
	2	3303	0	100%	35	99%	10	100%
	3	3301	0	100%	35	99%	11	100%
	4	4272	3135	27%	3688	14%	3363	21%
6	**1**	4036	915	77%	1845	54%	1319	67%
	2	3515	141	96%	835	76%	493	86%
	3	3588	190	95%	835	77%	493	86%
	4	4328	3131	28%	3752	13%	3432	21%
7	**1**	3892	857	78%	1811	53%	1330	66%
	2	3870	549	86%	1575	59%	945	76%
	3	3808	502	87%	1400	63%	944	75%
	4	4786	3153	34%	3881	19%	3492	27%
8	**1**	4049	755	81%	1812	55%	1313	68%
	2	4078	750	82%	1836	55%	1276	69%
	3	4038	799	80%	1802	55%	1278	68%
	4	4439	3232	27%	3872	13%	3503	21%
9	**1**	4323	836	81%	1939	55%	1360	69%
	2	4314	1044	76%	2198	49%	1563	64%
	3	4290	1024	76%	2248	48%	1562	64%
	4	4230	3313	22%	3816	10%	3531	17%
10	**1**	4468	841	81%	1993	55%	1387	69%
	2	4389	1139	74%	2385	46%	1763	60%
	3	4389	1139	74%	2385	46%	1763	60%
	4	3860	3264	15%	3804	1%	3543	8%

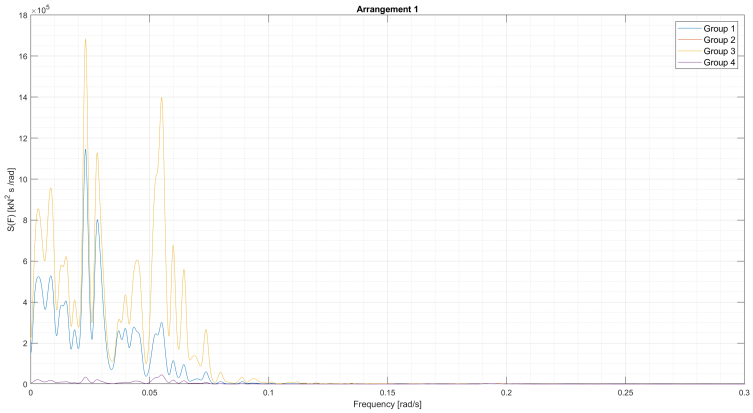

Figure G.1: PSD of resultant anchor forces for Arrangement 1 Load Case 1

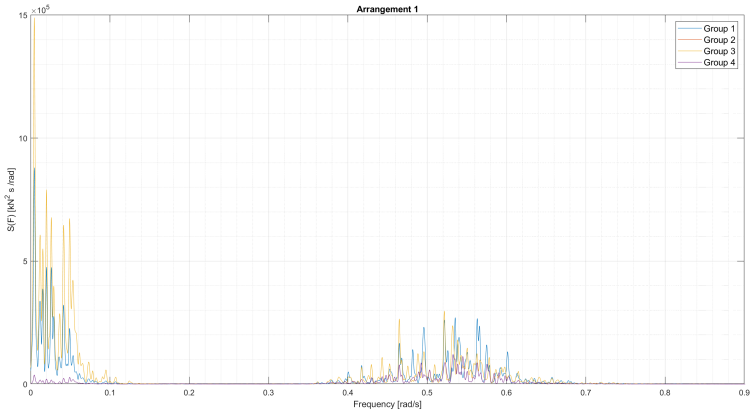

Figure G.2: PSD of resultant anchor forces for Arrangement 1 Load Case 2

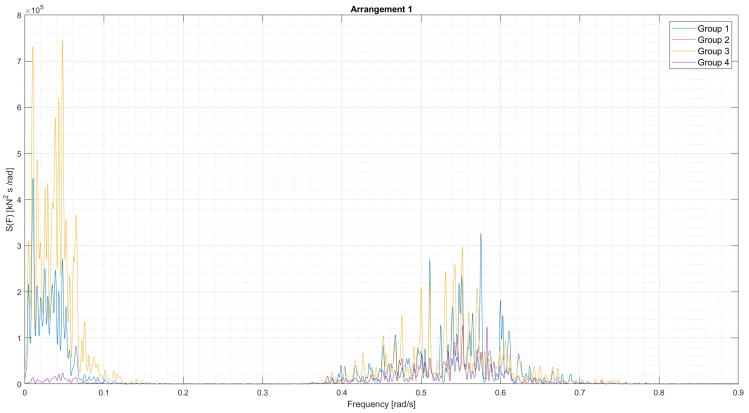

Figure G.3: PSD of resultant anchor forces for Arrangement 1 Load Case 3

G.2 Arrangement 2

Table G.4: Resultant Forces on anchor groups for Arrangement 2, Load Case 1

Direction	Group	Overall Maximum Tension [kN]	Minimum Resultant Tension [kN]	Reduction	Maximum Resultant Tension [kN]	Reduction	Average Resultant Tension [kN]	Reduction
0	1	4357	1125	74%	2263	48%	1605	63%
	2	3735	581	84%	1215	67%	872	77%
	3	3822	533	86%	1295	66%	870	77%
	4	4356	1123	74%	2255	48%	1604	63%
	5	3735	1125	83%	1215	67%	877	77%
	6	3819	581	86%	1281	66%	870	77%
1	1	4102	990	76%	1840	55%	1426	65%
	2	4177	466	89%	1058	75%	743	82%
	3	3204	0	100%	150	95%	39	99%
	4	4109	976	76%	1851	55%	1426	65%
	5	4171	990	78%	1854	56%	1429	66%
	6	3227	466	100%	163	95%	40	99%
2	1	3953	714	82%	1599	60%	1146	71%
	2	4284	312	93%	924	78%	561	87%
	3	3435	261	92%	725	79%	445	87%
	4	3946	706	82%	1597	60%	1146	71%
	5	4279	714	77%	2114	51%	1500	65%
	6	3437	312	92%	708	79%	448	87%
3	1	3848	586	85%	1329	65%	868	77%
	2	4403	184	96%	675	85%	391	91%
	3	3775	557	85%	1269	66%	880	77%
	4	3861	584	85%	1333	65%	867	78%
	5	4401	586	75%	2303	48%	1601	64%
	6	3782	184	85%	1267	67%	882	77%
4	1	3472	273	92%	637	82%	431	88%
	2	4325	52	99%	392	91%	187	96%
	3	3994	704	82%	1662	58%	1139	71%
	4	3473	254	93%	637	82%	431	88%
	5	4339	273	78%	2192	49%	1484	66%
	6	4013	52	83%	1698	58%	1150	71%
5	1	3213	0	100%	116	96%	37	99%
	2	4119	0	100%	105	97%	27	99%
	3	4106	961	77%	1852	55%	1401	66%
	4	3213	0	100%	113	96%	37	99%
	5	4112	0	76%	1844	55%	1391	66%
	6	4101	0	76%	1861	55%	1392	66%

Table G.5: Resultant Forces on anchor groups for Arrangement 2, Load Case 2

Direction	Group	Overall Maximum Tension [kN]	Minimum Resultant Tension [kN]	Reduction	Maximum Resultant Tension [kN]	Reduction	Average Resultant Tension [kN]	Reduction
0	1	4006	678	83%	1836	54%	1261	69%
	2	3529	255	93%	1052	70%	661	81%
	3	3529	261	93%	1056	70%	662	81%
	4	4004	680	83%	1863	53%	1260	69%
	5	3540	678	93%	1021	71%	661	81%
	6	3544	255	91%	1053	70%	668	81%
1	1	3894	577	85%	1683	57%	1118	71%
	2	4002	246	94%	1039	74%	576	86%
	3	3188	0	100%	111	97%	20	99%
	4	3968	632	84%	1738	56%	1116	72%
	5	3933	577	84%	1721	56%	1123	71%
	6	3203	246	100%	152	95%	29	99%
2	1	3785	380	90%	1417	63%	904	76%
	2	3974	54	99%	815	79%	451	89%
	3	3425	7	100%	700	80%	348	90%
	4	3764	355	91%	1448	62%	903	76%
	5	4000	380	85%	1882	53%	1214	70%
	6	3390	54	99%	650	81%	352	90%
3	1	3590	260	93%	1032	71%	661	82%
	2	3987	59	99%	639	84%	315	92%
	3	3616	285	92%	1073	70%	673	81%
	4	3584	332	91%	1021	71%	661	82%
	5	3985	260	81%	1929	52%	1268	68%
	6	3621	59	92%	1108	69%	676	81%
4	1	3387	19	99%	677	80%	336	90%
	2	4023	0	100%	431	89%	160	96%
	3	4090	402	90%	1357	67%	905	78%
	4	3464	26	99%	655	81%	336	90%
	5	4046	19	83%	1767	56%	1204	70%
	6	3907	0	88%	1531	61%	921	76%
5	1	3207	0	100%	73	98%	17	99%
	2	4082	0	100%	351	91%	73	98%
	3	3902	632	84%	1700	56%	1112	71%
	4	3184	0	100%	54	98%	13	100%
	5	3910	0	84%	1678	57%	1102	72%
	6	3959	0	87%	1682	58%	1120	72%

Table G.6: Resultant Forces on anchor groups for Arrangement 2, Load Case 3

Direction	Group	Overall Maximum Tension [kN]	Minimum Resultant Tension [kN]	Reduction	Maximum Resultant Tension [kN]	Reduction	Average Resultant Tension [kN]	Reduction
0	1	4543	1143	75%	2453	46%	1745	62%
	2	3918	499	87%	1361	65%	945	76%
	3	3920	475	88%	1394	64%	946	76%
	4	4541	1153	75%	2431	46%	1744	62%
	5	3873	1143	86%	1348	65%	945	76%
	6	3924	499	88%	1399	64%	953	76%
1	1	4282	1021	76%	2250	47%	1547	64%
	2	4266	438	90%	1289	70%	805	81%
	3	3263	0	100%	95	97%	18	99%
	4	4262	1007	76%	2215	48%	1547	64%
	5	4313	1021	77%	2225	48%	1555	64%
	6	3284	438	100%	115	96%	27	99%
2	1	4099	845	79%	1813	56%	1275	69%
	2	4301	303	93%	969	77%	620	86%
	3	3527	165	95%	826	77%	503	86%
	4	4070	876	78%	1813	55%	1274	69%
	5	4355	845	73%	2196	50%	1680	61%
	6	3558	303	94%	895	75%	515	86%
3	1	3843	542	86%	1409	63%	946	75%
	2	4501	98	98%	743	84%	429	90%
	3	3884	539	86%	1376	65%	965	75%
	4	3858	561	85%	1416	63%	946	75%
	5	4500	542	73%	2430	46%	1756	61%
	6	3801	98	84%	1390	63%	967	75%
4	1	3562	173	95%	833	77%	492	86%
	2	4299	0	100%	531	88%	212	95%
	3	4092	735	82%	1929	53%	1295	68%
	4	3506	165	95%	839	76%	492	86%
	5	4390	173	75%	2290	48%	1685	62%
	6	4107	0	80%	1876	54%	1313	68%
5	1	3293	0	100%	69	98%	19	99%
	2	4670	0	100%	352	92%	76	98%
	3	4189	1015	76%	2080	50%	1557	63%
	4	3337	0	100%	41	99%	12	100%
	5	4195	0	76%	2035	51%	1544	63%
	6	4230	0	76%	2113	50%	1565	63%

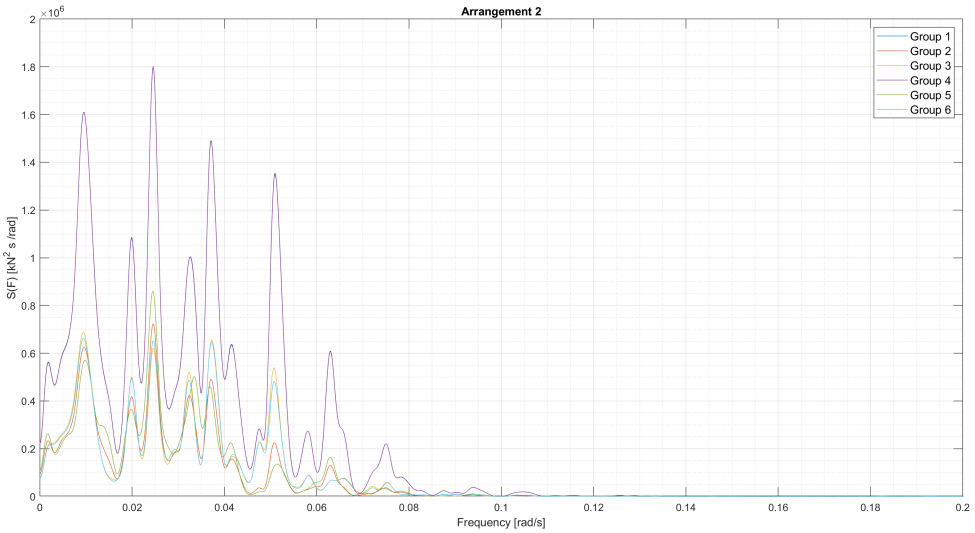

Figure G.4: PSD of resultant anchor forces for Arrangement 2 Load Case 1

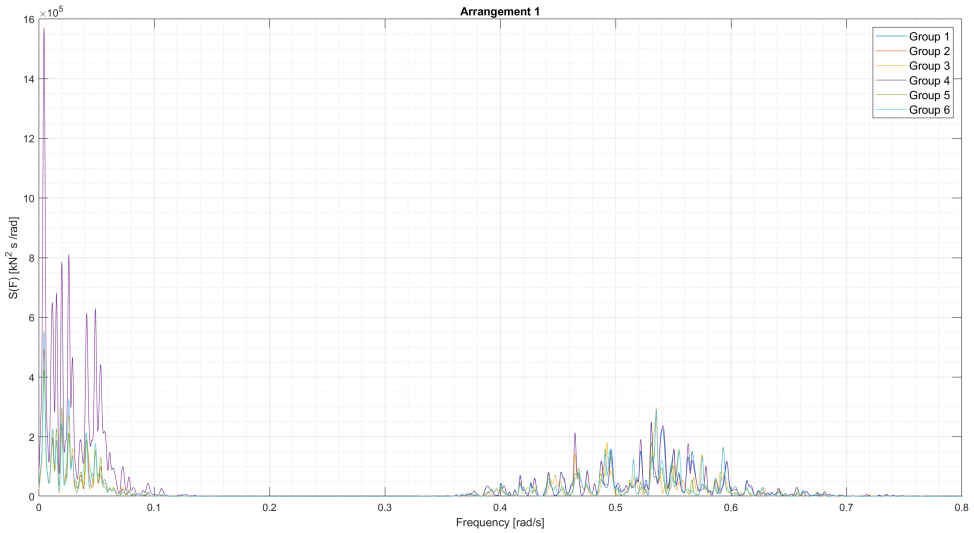

Figure G.5: PSD of resultant anchor forces for Arrangement 2 Load Case 2

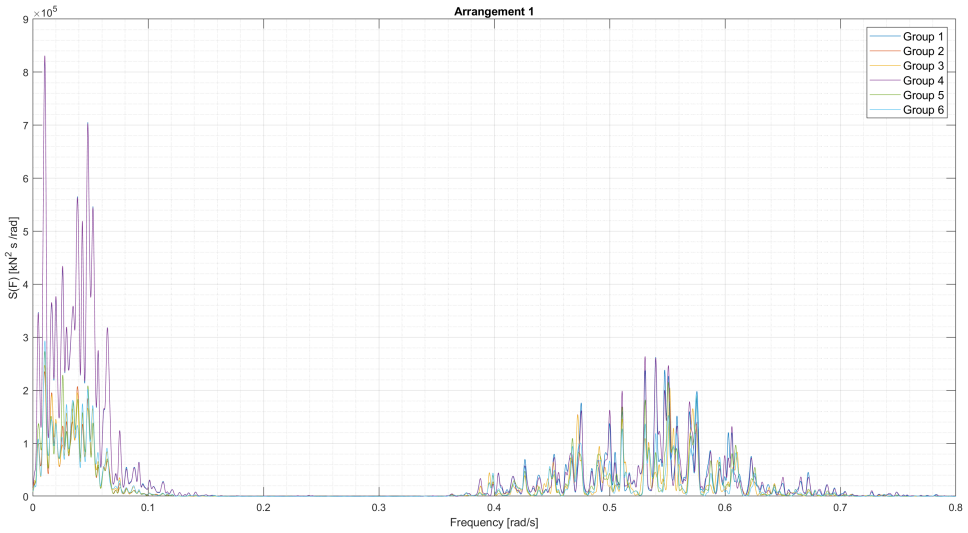

Figure G.6: PSD of resultant anchor forces for Arrangement 2 Load Case 3

G.3 Arrangement 3

Table G.7: Resultant Forces on anchor groups for Arrangement 3, Load Case 1

Direction	Group	Overall Maximum Tension [kN]	Minimum Resultant Tension [kN]	Reduction	Maximum Resultant Tension [kN]	Reduction	Average Resultant Tension [kN]	Reduction
0	**1**	3179	882	72%	1923	40%	1370	57%
	2	2725	22	99%	306	89%	157	94%
	3	4176	911	78%	2085	50%	1444	65%
	4	4082	0	100%	300	93%	153	96%
1	**1**	3723	682	82%	1579	58%	1135	70%
	2	2541	505	80%	1198	53%	835	67%
	3	4278	773	82%	1775	59%	1265	70%
	4	3824	364	90%	831	78%	594	84%
2	**1**	3936	668	83%	1214	69%	900	77%
	2	2425	788	67%	1510	38%	1099	55%
	3	4162	843	80%	1466	65%	1088	74%
	4	3579	656	82%	1248	65%	914	74%
3	**1**	4276	304	93%	913	79%	601	86%
	2	2575	730	72%	1974	23%	1299	50%
	3	4224	489	88%	1252	70%	851	80%
	4	3397	641	81%	1765	48%	1166	66%
4	**1**	4301	68	98%	452	89%	227	95%
	2	2598	949	63%	2016	22%	1360	48%
	3	4025	303	92%	864	79%	506	87%
	4	3174	904	72%	1861	41%	1272	60%
5	**1**	4376	1	100%	394	91%	166	96%
	2	2696	966	64%	2105	22%	1480	45%
	3	4224	0	100%	357	92%	158	96%
	4	2931	918	69%	1943	34%	1407	52%

Table G.8: Resultant Forces on anchor groups for Arrangement 3, Load Case 2

Direction	Group	Overall Maximum Tension [kN]	Minimum Resultant Tension [kN]	Reduction	Maximum Resultant Tension [kN]	Reduction	Average Resultant Tension [kN]	Reduction
0	**1**	3158	882	72%	1923	40%	1370	57%
	2	2725	22	99%	306	89%	157	94%
	3	4176	911	78%	2085	50%	1444	65%
	4	4082	0	100%	300	93%	153	96%
1	**1**	3723	682	82%	1579	58%	1135	70%
	2	2541	505	80%	1198	53%	835	67%
	3	4278	773	82%	1775	59%	1265	70%
	4	3824	364	90%	831	78%	594	84%
2	**1**	3936	668	83%	1214	69%	900	77%
	2	2425	788	67%	1510	38%	1099	55%
	3	4162	843	80%	1466	65%	1088	74%
	4	3579	656	82%	1248	65%	914	74%
3	**1**	4276	304	93%	913	79%	601	86%
	2	2575	730	72%	1974	23%	1299	50%
	3	4224	489	88%	1252	70%	851	80%
	4	3397	641	81%	1765	48%	1166	66%
4	**1**	4301	68	98%	452	89%	227	95%
	2	2598	949	63%	2016	22%	1360	48%
	3	4025	303	92%	864	79%	506	87%
	4	3174	904	72%	1861	41%	1272	60%
5	**1**	4376	1	100%	394	91%	166	96%
	2	2696	966	64%	2105	22%	1480	45%
	3	4224	0	100%	357	92%	158	96%
	4	2931	918	69%	1943	34%	1407	52%

Table G.9: Resultant Forces on anchor groups for Arrangement 3, Load Case 3

Direction	Group	Overall Maximum Tension [kN]	Minimum Resultant Tension [kN]	Reduction	Maximum Resultant Tension [kN]	Reduction	Average Resultant Tension [kN]	Reduction
0	**1**	3158	882	72%	1923	40%	1370	57%
	2	2725	22	99%	306	89%	157	94%
	3	4176	911	78%	2085	50%	1444	65%
	4	4082	0	100%	300	93%	153	96%
1	**1**	3723	682	82%	1579	58%	1135	70%
	2	2541	505	80%	1198	53%	835	67%
	3	4278	773	82%	1775	59%	1265	70%
	4	3824	364	90%	831	78%	594	84%
2	**1**	3936	668	83%	1214	69%	900	77%
	2	2425	788	67%	1510	38%	1099	55%
	3	4162	843	80%	1466	65%	1088	74%
	4	3579	656	82%	1248	65%	914	74%
3	**1**	4276	304	93%	913	79%	601	86%
	2	2575	730	72%	1974	23%	1299	50%
	3	4224	489	88%	1252	70%	851	80%
	4	3397	641	81%	1765	48%	1166	66%
4	**1**	4301	68	98%	452	89%	227	95%
	2	2598	949	63%	2016	22%	1360	48%
	3	4025	303	92%	864	79%	506	87%
	4	3174	904	72%	1861	41%	1272	60%
5	**1**	4376	1	100%	394	91%	166	96%
	2	2696	966	64%	2105	22%	1480	45%
	3	4224	0	100%	357	92%	158	96%
	4	2931	918	69%	1943	34%	1407	52%

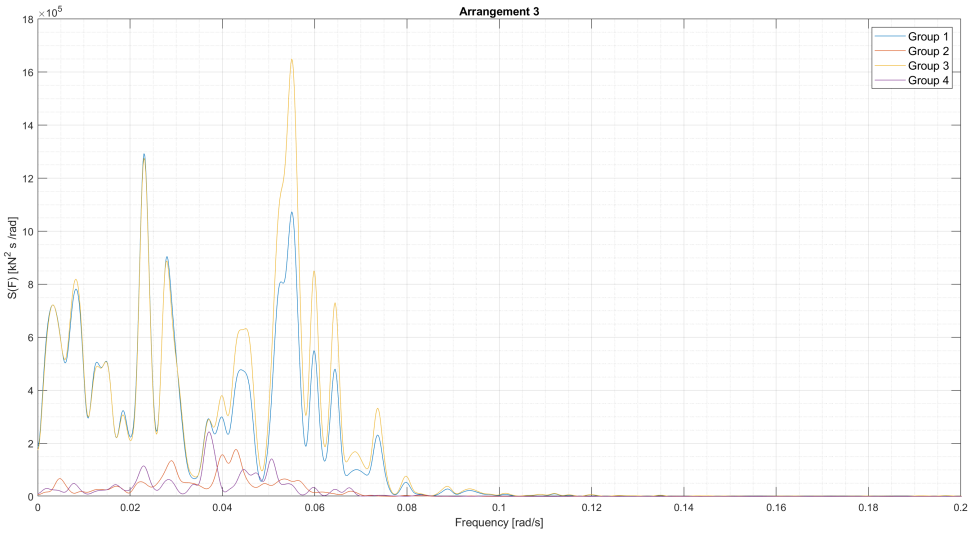

Figure G.7: PSD of resultant anchor forces for Arrangement 3 Load Case 1

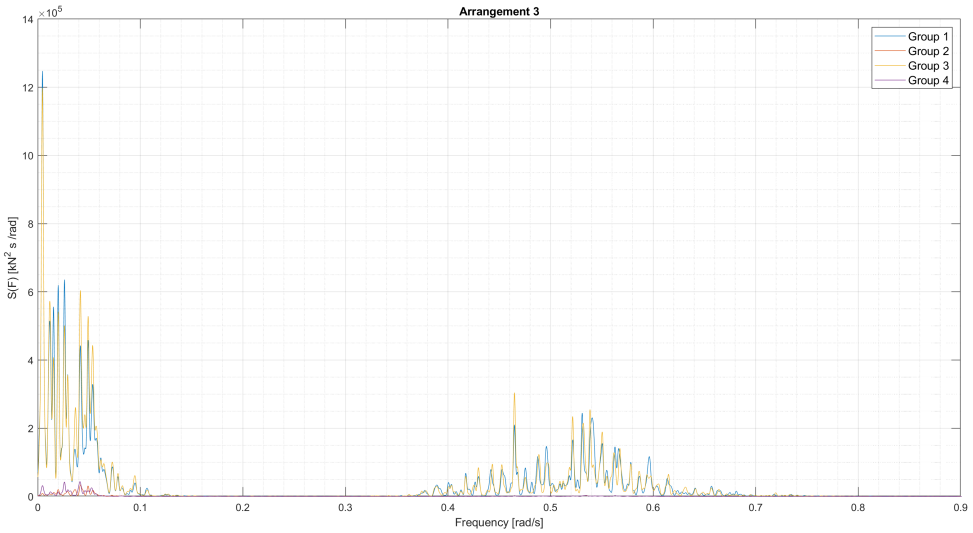

Figure G.8: PSD of resultant anchor forces for Arrangement 3 Load Case 2

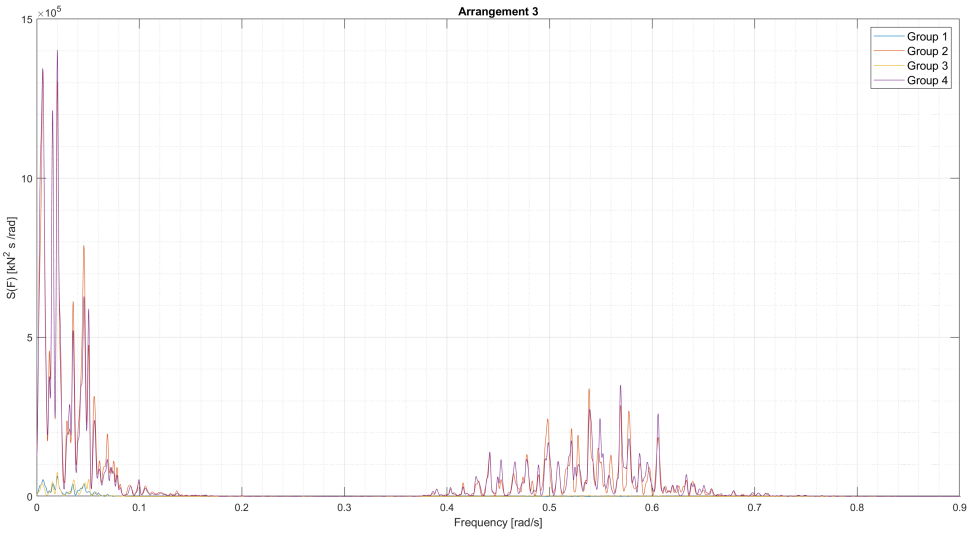

Figure G.9: PSD of resultant anchor forces for Arrangement 3 Load Case 3

APPENDIX H

ULS Checks for Arrangements

The tables for the ULS checks of the the mooring lines of each turbine of the arrangements under environmental loading are presented here.

H.1 Arrangement 1

H.1.1 High Safety Class

Table H.1: ULS Checks for Arrangement 1, Load Case 1 - High Safety Class

Direction Number	Line Number	T1		T2		T3		T4		T5	
		T_d [kN]	$S_c > T_d$	T_d [kN]	$S_c > T_d$	T_d [kN]	$S_c > T_d$	T_d [kN]	$S_c > T_d$	T_d [kN]	$S_c > T_d$
0	**Line 1**	9228	PASS	8834	PASS	8834	PASS	15326	FAIL	15326	FAIL
	Line 2	12969	PASS	13384	PASS	13384	PASS	9897	PASS	9897	PASS
	Line 3	12966	PASS	13368	PASS	13368	PASS	9894	PASS	9894	PASS
1	**Line 1**	9532	PASS	9183	PASS	9195	PASS	14887	FAIL	14865	FAIL
	Line 2	11435	PASS	11566	PASS	11568	PASS	9177	PASS	9179	PASS
	Line 3	14542	FAIL	15104	FAIL	15082	FAIL	11721	PASS	11721	PASS
2	**Line 1**	9677	PASS	9423	PASS	9436	PASS	14287	FAIL	14253	FAIL
	Line 2	10578	PASS	10558	PASS	10562	PASS	8921	PASS	8945	PASS
	Line 3	14793	FAIL	15321	FAIL	15385	FAIL	12650	PASS	12629	PASS
3	**Line 1**	10035	PASS	9881	PASS	9879	PASS	13474	PASS	13479	PASS
	Line 2	10044	PASS	9883	PASS	9887	PASS	8810	PASS	8815	PASS
	Line 3	14938	FAIL	15521	FAIL	15506	FAIL	13457	PASS	13462	PASS
4	**Line 1**	10592	PASS	10590	PASS	10578	PASS	12428	PASS	12424	PASS
	Line 2	9767	PASS	9545	PASS	9496	PASS	9013	PASS	9029	PASS
	Line 3	14392	FAIL	14935	FAIL	14957	FAIL	13956	PASS	13929	PASS
5	**Line 1**	11367	PASS	11508	PASS	11507	PASS	11513	PASS	11522	PASS
	Line 2	9412	PASS	9061	PASS	9064	PASS	9115	PASS	9092	PASS
	Line 3	14267	FAIL	14820	FAIL	14800	FAIL	14744	FAIL	14765	FAIL
6	**Line 1**	12150	PASS	12437	PASS	12439	PASS	10622	PASS	11256	PASS
	Line 2	9273	PASS	9078	PASS	9055	PASS	9484	PASS	9258	PASS
	Line 3	13571	PASS	14057	FAIL	14041	FAIL	14832	FAIL	14548	FAIL
7	**Line 1**	13007	PASS	13565	PASS	13568	PASS	9860	PASS	9869	PASS
	Line 2	9247	PASS	8844	PASS	8833	PASS	9958	PASS	9958	PASS
	Line 3	12980	PASS	13392	PASS	13377	PASS	15485	FAIL	15487	FAIL
8	**Line 1**	13633	PASS	14091	FAIL	14085	FAIL	9430	PASS	9437	PASS
	Line 2	9273	PASS	8885	PASS	8902	PASS	10598	PASS	10598	PASS
	Line 3	12259	PASS	12545	PASS	12541	PASS	15161	FAIL	15145	FAIL
9	**Line 1**	14223	FAIL	14747	FAIL	14766	FAIL	9099	PASS	9065	PASS
	Line 2	9416	PASS	9093	PASS	9096	PASS	11511	PASS	11509	PASS
	Line 3	11454	PASS	11600	PASS	11603	PASS	14838	FAIL	14847	FAIL
10	**Line 1**	14732	FAIL	15238	FAIL	15238	FAIL	8800	PASS	8800	PASS
	Line 2	10039	PASS	9891	PASS	9891	PASS	13280	PASS	13281	PASS
	Line 3	10077	PASS	9926	PASS	9926	PASS	13391	PASS	13391	PASS

Table H.2: ULS Checks for Arrangement 1, Load Case 2 - High Safety Class

Direction Number	Line Number	T1		T2		T3		T4		T5	
		T_d [kN]	$S_c > T_d$	T_d [kN]	$S_c > T_d$	T_d [kN]	$S_c > T_d$	T_d [kN]	$S_c > T_d$	T_d [kN]	$S_c > T_d$
0	**Line 1**	9844	PASS	9574	PASS	9574	PASS	14261	FAIL	14261	FAIL
	Line 2	12519	PASS	12799	PASS	12799	PASS	10402	PASS	10402	PASS
	Line 3	12520	PASS	12806	PASS	12806	PASS	10364	PASS	10365	PASS
1	**Line 1**	9975	PASS	9680	PASS	9709	PASS	13763	PASS	13701	PASS
	Line 2	11379	PASS	11423	PASS	11425	PASS	9739	PASS	9793	PASS
	Line 3	13533	PASS	13762	PASS	13823	PASS	11427	PASS	11421	PASS
2	**Line 1**	10048	PASS	9813	PASS	9843	PASS	13603	PASS	13541	PASS
	Line 2	11230	PASS	11180	PASS	11182	PASS	9681	PASS	9735	PASS
	Line 3	13593	PASS	13820	PASS	13881	PASS	11667	PASS	11661	PASS
3	**Line 1**	10510	PASS	10413	PASS	10386	PASS	12854	PASS	12872	PASS
	Line 2	10469	PASS	10384	PASS	10388	PASS	9606	PASS	9416	PASS
	Line 3	14070	FAIL	14293	FAIL	14396	FAIL	12974	PASS	13016	PASS
4	**Line 1**	10879	PASS	10851	PASS	10892	PASS	12184	PASS	12195	PASS
	Line 2	10056	PASS	10012	PASS	10030	PASS	9647	PASS	9530	PASS
	Line 3	13934	PASS	14129	FAIL	14235	FAIL	13342	PASS	13333	PASS
5	**Line 1**	11464	PASS	11462	PASS	11438	PASS	11448	PASS	11462	PASS
	Line 2	9911	PASS	9640	PASS	9748	PASS	9658	PASS	9750	PASS
	Line 3	13470	PASS	13928	PASS	13736	PASS	13929	PASS	13738	PASS
6	**Line 1**	11893	PASS	12072	PASS	12131	PASS	10869	PASS	10912	PASS
	Line 2	9849	PASS	9521	PASS	9590	PASS	10079	PASS	10038	PASS
	Line 3	13115	PASS	13262	PASS	13424	PASS	14018	FAIL	14050	FAIL
7	**Line 1**	12471	PASS	12714	PASS	12775	PASS	10437	PASS	10456	PASS
	Line 2	9790	PASS	9538	PASS	9539	PASS	10456	PASS	10400	PASS
	Line 3	12565	PASS	12795	PASS	12850	PASS	14200	FAIL	14218	FAIL
8	**Line 1**	12998	PASS	13377	PASS	13356	PASS	10065	PASS	9969	PASS
	Line 2	9855	PASS	9528	PASS	9509	PASS	10871	PASS	10921	PASS
	Line 3	12008	PASS	12112	PASS	12132	PASS	14139	FAIL	14149	FAIL
9	**Line 1**	13639	PASS	14084	FAIL	14046	FAIL	9910	PASS	9667	PASS
	Line 2	9978	PASS	9806	PASS	9783	PASS	11568	PASS	11639	PASS
	Line 3	11455	PASS	11472	PASS	11616	PASS	14180	FAIL	14064	FAIL
10	**Line 1**	14065	FAIL	14567	FAIL	14567	FAIL	9533	PASS	9533	PASS
	Line 2	10490	PASS	10358	PASS	10359	PASS	12993	PASS	12993	PASS
	Line 3	10490	PASS	10358	PASS	10359	PASS	13010	PASS	13010	PASS

Table H.3: ULS Checks for Arrangement 1, Load Case 3 - High Safety Class

Direction Number	Line Number	T1		T2		T3		T4		T5	
		T_d [kN]	$S_c > T_d$	T_d [kN]	$S_c > T_d$	T_d [kN]	$S_c > T_d$	T_d [kN]	$S_c > T_d$	T_d [kN]	$S_c > T_d$
0	**Line 1**	9337	PASS	8948	PASS	8948	PASS	15624	FAIL	15624	FAIL
	Line 2	13299	PASS	13646	PASS	13646	PASS	10164	PASS	10164	PASS
	Line 3	13299	PASS	13646	PASS	13646	PASS	10182	PASS	10182	PASS
1	**Line 1**	9675	PASS	9343	PASS	9373	PASS	14991	FAIL	15091	FAIL
	Line 2	11554	PASS	11754	PASS	11773	PASS	9244	PASS	9299	PASS
	Line 3	14499	FAIL	15042	FAIL	14952	FAIL	11758	PASS	11758	PASS
2	**Line 1**	9893	PASS	9686	PASS	9707	PASS	14652	FAIL	14567	FAIL
	Line 2	10850	PASS	10904	PASS	10855	PASS	9051	PASS	9038	PASS
	Line 3	15094	FAIL	15747	FAIL	15614	FAIL	12915	PASS	12687	PASS
3	**Line 1**	10256	PASS	10218	PASS	10143	PASS	13767	PASS	13758	PASS
	Line 2	10199	PASS	10212	PASS	10120	PASS	8936	PASS	9009	PASS
	Line 3	15184	FAIL	15396	FAIL	15656	FAIL	13793	PASS	13833	PASS
4	**Line 1**	10973	PASS	10903	PASS	11054	PASS	12686	PASS	12693	PASS
	Line 2	9903	PASS	9653	PASS	9654	PASS	9159	PASS	9144	PASS
	Line 3	14765	FAIL	15423	FAIL	15307	FAIL	14372	FAIL	14284	FAIL
5	**Line 1**	11673	PASS	11778	PASS	11825	PASS	11827	PASS	11805	PASS
	Line 2	9458	PASS	9177	PASS	9342	PASS	9171	PASS	9338	PASS
	Line 3	14634	FAIL	15066	FAIL	15096	FAIL	15078	FAIL	15106	FAIL
6	**Line 1**	12388	PASS	12648	PASS	12808	PASS	10889	PASS	10886	PASS
	Line 2	9350	PASS	9046	PASS	8992	PASS	9636	PASS	9752	PASS
	Line 3	14047	FAIL	14377	FAIL	14400	FAIL	15311	FAIL	15284	FAIL
7	**Line 1**	13408	PASS	13774	PASS	13637	PASS	10246	PASS	10276	PASS
	Line 2	9333	PASS	9125	PASS	8981	PASS	10282	PASS	10247	PASS
	Line 3	13503	PASS	13824	PASS	13674	PASS	15703	FAIL	15729	FAIL
8	**Line 1**	13951	PASS	14465	FAIL	14376	FAIL	9668	PASS	9617	PASS
	Line 2	9266	PASS	9070	PASS	9171	PASS	10859	PASS	10858	PASS
	Line 3	12435	PASS	12707	PASS	12685	PASS	15552	FAIL	15577	FAIL
9	**Line 1**	14714	FAIL	15193	FAIL	15140	FAIL	9217	PASS	9185	PASS
	Line 2	9561	PASS	9210	PASS	9156	PASS	11687	PASS	11748	PASS
	Line 3	11765	PASS	11874	PASS	11724	PASS	15010	FAIL	15318	FAIL
10	**Line 1**	15108	FAIL	15426	FAIL	15426	FAIL	9063	PASS	9063	PASS
	Line 2	10222	PASS	10143	PASS	10144	PASS	13604	PASS	13604	PASS
	Line 3	10222	PASS	10143	PASS	10144	PASS	13643	PASS	13643	PASS

H.1.2 Normal Safety Class

Table H.4: ULS Checks for Arrangement 1, Load Case 1 - Normal Safety Class

Direction Number	Line Number	T1		T2		T3		T4		T5	
		T_d [kN]	$S_c > T_d$	T_d [kN]	$S_c > T_d$	T_d [kN]	$S_c > T_d$	T_d [kN]	$S_c > T_d$	T_d [kN]	$S_c > T_d$
0	**Line 1**	7613	PASS	7272	PASS	7272	PASS	12600	PASS	12600	PASS
	Line 2	10654	PASS	11014	PASS	11014	PASS	8151	PASS	8151	PASS
	Line 3	10652	PASS	11000	PASS	11000	PASS	8149	PASS	8149	PASS
1	**Line 1**	7859	PASS	7557	PASS	7567	PASS	12239	PASS	12223	PASS
	Line 2	9408	PASS	9522	PASS	9524	PASS	7552	PASS	7554	PASS
	Line 3	11927	PASS	12412	PASS	12395	PASS	9645	PASS	9645	PASS
2	**Line 1**	7981	PASS	7761	PASS	7771	PASS	11746	PASS	11720	PASS
	Line 2	8714	PASS	8697	PASS	8700	PASS	7344	PASS	7364	PASS
	Line 3	12131	PASS	12589	PASS	12640	PASS	10406	PASS	10390	PASS
3	**Line 1**	8272	PASS	8139	PASS	8137	PASS	11085	PASS	11089	PASS
	Line 2	8279	PASS	8140	PASS	8144	PASS	7253	PASS	7256	PASS
	Line 3	12250	PASS	12754	PASS	12742	PASS	11072	PASS	11076	PASS
4	**Line 1**	8725	PASS	8723	PASS	8714	PASS	10229	PASS	10227	PASS
	Line 2	8052	PASS	7857	PASS	7818	PASS	7418	PASS	7430	PASS
	Line 3	11811	PASS	12282	PASS	12300	PASS	11484	PASS	11462	PASS
5	**Line 1**	9354	PASS	9476	PASS	9475	PASS	9480	PASS	9487	PASS
	Line 2	7764	PASS	7460	PASS	7463	PASS	7503	PASS	7485	PASS
	Line 3	11708	PASS	12187	PASS	12171	PASS	12126	PASS	12143	PASS
6	**Line 1**	9989	PASS	10237	PASS	10239	PASS	8748	PASS	9297	PASS
	Line 2	7641	PASS	7469	PASS	7451	PASS	7809	PASS	7612	PASS
	Line 3	11144	PASS	11564	PASS	11551	PASS	12200	PASS	11955	PASS
7	**Line 1**	10685	PASS	11168	PASS	11170	PASS	8122	PASS	8129	PASS
	Line 2	7629	PASS	7280	PASS	7271	PASS	8200	PASS	8200	PASS
	Line 3	10663	PASS	11020	PASS	11008	PASS	12726	PASS	12727	PASS
8	**Line 1**	11193	PASS	11591	PASS	11586	PASS	7765	PASS	7771	PASS
	Line 2	7651	PASS	7315	PASS	7329	PASS	8729	PASS	8729	PASS
	Line 3	10076	PASS	10323	PASS	10319	PASS	12463	PASS	12450	PASS
9	**Line 1**	11673	PASS	12128	PASS	12144	PASS	7490	PASS	7464	PASS
	Line 2	7767	PASS	7485	PASS	7488	PASS	9478	PASS	9476	PASS
	Line 3	9423	PASS	9549	PASS	9551	PASS	12201	PASS	12208	PASS
10	**Line 1**	12086	PASS	12529	PASS	12529	PASS	7245	PASS	7245	PASS
	Line 2	8275	PASS	8147	PASS	8147	PASS	10931	PASS	10931	PASS
	Line 3	8306	PASS	8175	PASS	8175	PASS	11019	PASS	11019	PASS

Table H.5: ULS Checks for Arrangement 1, Load Case 2 - Normal Safety Class

Direction Number	**Line Number**	**T1**		**T2**		**T3**		**T4**		**T5**	
		T_d [kN]	$S_c > T_d$	T_d [kN]	$S_c > T_d$	T_d [kN]	$S_c > T_d$	T_d [kN]	$S_c > T_d$	T_d [kN]	$S_c > T_d$
0	**Line 1**	8109	PASS	7873	PASS	7873	PASS	11727	PASS	11727	PASS
	Line 2	10291	PASS	10532	PASS	10532	PASS	8559	PASS	8559	PASS
	Line 3	10291	PASS	10538	PASS	10538	PASS	8529	PASS	8529	PASS
1	**Line 1**	8216	PASS	7963	PASS	7987	PASS	11323	PASS	11273	PASS
	Line 2	9361	PASS	9404	PASS	9405	PASS	8010	PASS	8053	PASS
	Line 3	11116	PASS	11322	PASS	11370	PASS	9407	PASS	9402	PASS
2	**Line 1**	8280	PASS	8079	PASS	8102	PASS	11184	PASS	11134	PASS
	Line 2	9232	PASS	9193	PASS	9194	PASS	7960	PASS	8003	PASS
	Line 3	11168	PASS	11372	PASS	11421	PASS	9615	PASS	9610	PASS
3	**Line 1**	8654	PASS	8567	PASS	8546	PASS	10577	PASS	10591	PASS
	Line 2	8617	PASS	8544	PASS	8548	PASS	7898	PASS	7747	PASS
	Line 3	11552	PASS	11753	PASS	11834	PASS	10672	PASS	10706	PASS
4	**Line 1**	8955	PASS	8932	PASS	8964	PASS	10026	PASS	10035	PASS
	Line 2	8283	PASS	8237	PASS	8251	PASS	7933	PASS	7840	PASS
	Line 3	11441	PASS	11618	PASS	11702	PASS	10976	PASS	10970	PASS
5	**Line 1**	9431	PASS	9435	PASS	9416	PASS	9424	PASS	9435	PASS
	Line 2	8161	PASS	7931	PASS	8017	PASS	7946	PASS	8018	PASS
	Line 3	11069	PASS	11454	PASS	11302	PASS	11455	PASS	11303	PASS
6	**Line 1**	9782	PASS	9937	PASS	9984	PASS	8945	PASS	8980	PASS
	Line 2	8110	PASS	7833	PASS	7888	PASS	8290	PASS	8257	PASS
	Line 3	10778	PASS	10913	PASS	11042	PASS	11530	PASS	11555	PASS
7	**Line 1**	10253	PASS	10465	PASS	10514	PASS	8587	PASS	8602	PASS
	Line 2	8062	PASS	7843	PASS	7844	PASS	8602	PASS	8557	PASS
	Line 3	10332	PASS	10529	PASS	10573	PASS	11679	PASS	11693	PASS
8	**Line 1**	10680	PASS	11004	PASS	10988	PASS	8279	PASS	8203	PASS
	Line 2	8116	PASS	7838	PASS	7823	PASS	8947	PASS	8987	PASS
	Line 3	9877	PASS	9969	PASS	9985	PASS	11626	PASS	11634	PASS
9	**Line 1**	11198	PASS	11578	PASS	11548	PASS	8146	PASS	7953	PASS
	Line 2	8217	PASS	8063	PASS	8045	PASS	9518	PASS	9575	PASS
	Line 3	9426	PASS	9443	PASS	9558	PASS	11654	PASS	11562	PASS
10	**Line 1**	11542	PASS	11970	PASS	11970	PASS	7840	PASS	7840	PASS
	Line 2	8638	PASS	8524	PASS	8524	PASS	10687	PASS	10687	PASS
	Line 3	8638	PASS	8524	PASS	8524	PASS	10700	PASS	10700	PASS

Table H.6: ULS Checks for Arrangement 1, Load Case 3 - Normal Safety Class

Direction Number	Line Number	T1		T2		T3		T4		T5	
		T_d [kN]	$S_c > T_d$	T_d [kN]	$S_c > T_d$	T_d [kN]	$S_c > T_d$	T_d [kN]	$S_c > T_d$	T_d [kN]	$S_c > T_d$
0	**Line 1**	7694	PASS	7359	PASS	7359	PASS	12845	PASS	12845	PASS
	Line 2	10926	PASS	11229	PASS	11229	PASS	8363	PASS	8363	PASS
	Line 3	10926	PASS	11229	PASS	11229	PASS	8377	PASS	8377	PASS
1	**Line 1**	7967	PASS	7681	PASS	7705	PASS	12330	PASS	12410	PASS
	Line 2	9503	PASS	9674	PASS	9689	PASS	7602	PASS	7646	PASS
	Line 3	11906	PASS	12371	PASS	12300	PASS	9677	PASS	9677	PASS
2	**Line 1**	8147	PASS	7966	PASS	7983	PASS	12046	PASS	11979	PASS
	Line 2	8929	PASS	8973	PASS	8933	PASS	7443	PASS	7433	PASS
	Line 3	12386	PASS	12938	PASS	12832	PASS	10623	PASS	10442	PASS
3	**Line 1**	8446	PASS	8406	PASS	8346	PASS	11326	PASS	11318	PASS
	Line 2	8398	PASS	8400	PASS	8327	PASS	7349	PASS	7407	PASS
	Line 3	12461	PASS	12664	PASS	12871	PASS	11346	PASS	11378	PASS
4	**Line 1**	9029	PASS	8972	PASS	9093	PASS	10441	PASS	10447	PASS
	Line 2	8153	PASS	7939	PASS	7941	PASS	7529	PASS	7517	PASS
	Line 3	12124	PASS	12681	PASS	12589	PASS	11824	PASS	11754	PASS
5	**Line 1**	9601	PASS	9694	PASS	9731	PASS	9733	PASS	9715	PASS
	Line 2	7791	PASS	7549	PASS	7680	PASS	7544	PASS	7677	PASS
	Line 3	12016	PASS	12391	PASS	12415	PASS	12400	PASS	12423	PASS
6	**Line 1**	10186	PASS	10411	PASS	10539	PASS	8961	PASS	8958	PASS
	Line 2	7702	PASS	7439	PASS	7396	PASS	7926	PASS	8019	PASS
	Line 3	11537	PASS	11828	PASS	11846	PASS	12591	PASS	12570	PASS
7	**Line 1**	11012	PASS	11331	PASS	11223	PASS	8428	PASS	8452	PASS
	Line 2	7688	PASS	7499	PASS	7385	PASS	8456	PASS	8428	PASS
	Line 3	11091	PASS	11371	PASS	11252	PASS	12908	PASS	12928	PASS
8	**Line 1**	11457	PASS	11897	PASS	11827	PASS	7952	PASS	7912	PASS
	Line 2	7636	PASS	7458	PASS	7538	PASS	8937	PASS	8936	PASS
	Line 3	10225	PASS	10458	PASS	10441	PASS	12783	PASS	12803	PASS
9	**Line 1**	12075	PASS	12492	PASS	12449	PASS	7581	PASS	7556	PASS
	Line 2	7874	PASS	7575	PASS	7532	PASS	9621	PASS	9669	PASS
	Line 3	9675	PASS	9770	PASS	9651	PASS	12346	PASS	12591	PASS
10	**Line 1**	12397	PASS	12688	PASS	12688	PASS	7450	PASS	7450	PASS
	Line 2	8418	PASS	8346	PASS	8346	PASS	11195	PASS	11195	PASS
	Line 3	8418	PASS	8346	PASS	8346	PASS	11226	PASS	11226	PASS

H.2 Arrangement 2

H.2.1 High Safety Class

Table H.7: ULS Checks for Arrangement 2, Load Case 1 - High Safety Class

Direction Number	Line Number	T1		T2		T3		T4		T5		T6	
		T_d [kN]	$S_c > T_d$	T_d [kN]	$S_c > T_d$	T_d [kN]	$S_c > T_d$	T_d [kN]	$S_c > T_d$	T_d [kN]	$S_c > T_d$	T_d [kN]	$S_c > T_d$
0	**Line 1**	9228	PASS	15331	FAIL	8829	PASS	15324	FAIL	8821	PASS	15291	FAIL
	Line 2	12969	PASS	9895	PASS	13377	PASS	9890	PASS	13371	PASS	9891	PASS
	Line 3	12966	PASS	9893	PASS	8210	PASS	5972	PASS	8213	PASS	9889	PASS
1	**Line 1**	9370	PASS	14575	FAIL	9046	PASS	14579	FAIL	9037	PASS	14565	FAIL
	Line 2	11423	PASS	11530	PASS	11564	PASS	11518	PASS	11571	PASS	11538	PASS
	Line 3	14066	FAIL	9062	PASS	14630	FAIL	9037	PASS	14601	FAIL	9050	PASS
2	**Line 1**	9731	PASS	14061	FAIL	9484	PASS	14043	FAIL	9469	PASS	14098	FAIL
	Line 2	10631	PASS	12391	PASS	10608	PASS	12386	PASS	10604	PASS	12401	PASS
	Line 3	14529	FAIL	8964	PASS	15075	FAIL	8958	PASS	15061	FAIL	8960	PASS
3	**Line 1**	10048	PASS	13618	PASS	9917	PASS	13645	PASS	9911	PASS	13576	PASS
	Line 2	10023	PASS	13487	PASS	9866	PASS	13460	PASS	9860	PASS	13473	PASS
	Line 3	14866	FAIL	8782	PASS	15421	FAIL	8755	PASS	15414	FAIL	8811	PASS
4	**Line 1**	10623	PASS	12465	PASS	10604	PASS	12467	PASS	10606	PASS	12495	PASS
	Line 2	9747	PASS	14138	FAIL	9465	PASS	14152	FAIL	9468	PASS	14212	FAIL
	Line 3	14629	FAIL	8957	PASS	15164	FAIL	8940	PASS	15194	FAIL	8974	PASS
5	**Line 1**	11448	PASS	11491	PASS	11590	PASS	11480	PASS	11585	PASS	11472	PASS
	Line 2	9401	PASS	14628	FAIL	9039	PASS	14619	FAIL	9066	PASS	14589	FAIL
	Line 3	14095	FAIL	9026	PASS	14650	FAIL	9031	PASS	14632	FAIL	9040	PASS

Table H.8: ULS Checks for Arrangement 2, Load Case 2 - High Safety Class

Direction Number	Line Number	T1		T2		T3		T4		T5		T6	
		T_d [kN]	$S_c > T_d$	T_d [kN]	$S_c > T_d$	T_d [kN]	$S_c > T_d$	T_d [kN]	$S_c > T_d$	T_d [kN]	$S_c > T_d$	T_d [kN]	$S_c > T_d$
0	**Line 1**	9844	PASS	14315	FAIL	9538	PASS	14308	FAIL	9566	PASS	14220	FAIL
	Line 2	12519	PASS	10407	PASS	12809	PASS	10401	PASS	12793	PASS	10360	PASS
	Line 3	12520	PASS	10420	PASS	12810	PASS	10413	PASS	12791	PASS	10416	PASS
1	**Line 1**	9957	PASS	13830	PASS	9840	PASS	13988	FAIL	9750	PASS	13832	PASS
	Line 2	11348	PASS	11481	PASS	11444	PASS	11468	PASS	11400	PASS	11461	PASS
	Line 3	13562	PASS	9737	PASS	14070	FAIL	9818	PASS	13915	PASS	9713	PASS
2	**Line 1**	10432	PASS	13428	PASS	10096	PASS	13380	PASS	10149	PASS	13488	PASS
	Line 2	10877	PASS	12224	PASS	10814	PASS	12230	PASS	10841	PASS	12160	PASS
	Line 3	13835	PASS	9647	PASS	14066	FAIL	9670	PASS	14121	FAIL	9736	PASS
3	**Line 1**	10508	PASS	12835	PASS	10354	PASS	12819	PASS	10348	PASS	12778	PASS
	Line 2	10417	PASS	12849	PASS	10350	PASS	12892	PASS	10344	PASS	12901	PASS
	Line 3	13892	PASS	9410	PASS	14151	FAIL	9423	PASS	14144	FAIL	9413	PASS
4	**Line 1**	10856	PASS	12098	PASS	10843	PASS	12114	PASS	10878	PASS	12187	PASS
	Line 2	10158	PASS	13308	PASS	10036	PASS	13233	PASS	10008	PASS	13530	PASS
	Line 3	13800	PASS	9581	PASS	14087	FAIL	9574	PASS	14160	FAIL	9576	PASS
5	**Line 1**	11439	PASS	11502	PASS	11497	PASS	11451	PASS	11461	PASS	11443	PASS
	Line 2	9939	PASS	14007	FAIL	9687	PASS	13851	PASS	9695	PASS	13967	FAIL
	Line 3	13698	PASS	9730	PASS	13814	PASS	9697	PASS	13869	PASS	9734	PASS

Table H.9: ULS Checks for Arrangement 2, Load Case 3 - High Safety Class

Direction Number	Line Number	T1		T2		T3		T4		T5		T6	
		T_d [kN]	$S_c > T_d$	T_d [kN]	$S_c > T_d$	T_d [kN]	$S_c > T_d$	T_d [kN]	$S_c > T_d$	T_d [kN]	$S_c > T_d$	T_d [kN]	$S_c > T_d$
0	**Line 1**	9337	PASS	15593	FAIL	8983	PASS	15586	FAIL	8989	PASS	15501	FAIL
	Line 2	13299	PASS	10154	PASS	13661	PASS	10150	PASS	13687	PASS	10117	PASS
	Line 3	13270	PASS	10140	PASS	13657	PASS	10135	PASS	13655	PASS	10178	PASS
1	**Line 1**	9658	PASS	15034	FAIL	9354	PASS	15078	FAIL	10348	PASS	15189	FAIL
	Line 2	11608	PASS	11793	PASS	11688	PASS	11738	PASS	12881	PASS	11786	PASS
	Line 3	14732	FAIL	9292	PASS	15091	FAIL	9321	PASS	15073	FAIL	9314	PASS
2	**Line 1**	9823	PASS	14513	FAIL	9595	PASS	14445	FAIL	9589	PASS	14340	FAIL
	Line 2	10758	PASS	12725	PASS	10855	PASS	12674	PASS	10804	PASS	12748	PASS
	Line 3	14851	FAIL	9012	PASS	15250	FAIL	8997	PASS	15367	FAIL	9015	PASS
3	**Line 1**	10289	PASS	13716	PASS	10135	PASS	13744	PASS	10129	PASS	13732	PASS
	Line 2	10176	PASS	13661	PASS	10142	PASS	13803	PASS	10138	PASS	13620	PASS
	Line 3	15063	FAIL	8904	PASS	15609	FAIL	9005	PASS	15602	FAIL	8918	PASS
4	**Line 1**	10858	PASS	12751	PASS	10964	PASS	12627	PASS	10936	PASS	12845	PASS
	Line 2	9779	PASS	14537	FAIL	9627	PASS	14496	FAIL	9648	PASS	14549	FAIL
	Line 3	14998	FAIL	9005	PASS	15249	FAIL	9021	PASS	15447	FAIL	9054	PASS
5	**Line 1**	11618	PASS	11782	PASS	11796	PASS	11900	PASS	11860	PASS	11847	PASS
	Line 2	9438	PASS	14999	FAIL	9281	PASS	14924	FAIL	9278	PASS	15007	FAIL
	Line 3	14521	FAIL	9212	PASS	14915	FAIL	9266	PASS	14936	FAIL	9368	PASS

H.2.2 Normal Safety Class

Table H.10: ULS Checks for Arrangement 2, Load Case 1 - Normal Safety Class

Direction Number	Line Number	T1		T2		T3		T4		T5		T6	
		T_d [kN]	$S_c > T_d$	T_d [kN]	$S_c > T_d$	T_d [kN]	$S_c > T_d$	T_d [kN]	$S_c > T_d$	T_d [kN]	$S_c > T_d$	T_d [kN]	$S_c > T_d$
0	**Line 1**	7613	PASS	12603	PASS	7267	PASS	12598	PASS	7261	PASS	12570	PASS
	Line 2	10654	PASS	8150	PASS	11008	PASS	8146	PASS	11003	PASS	8147	PASS
	Line 3	10652	PASS	8149	PASS	6531	PASS	4750	PASS	6533	PASS	8145	PASS
1	**Line 1**	7730	PASS	11991	PASS	7448	PASS	11994	PASS	7441	PASS	11983	PASS
	Line 2	9398	PASS	9494	PASS	9520	PASS	9484	PASS	9526	PASS	9500	PASS
	Line 3	11549	PASS	7461	PASS	12036	PASS	7441	PASS	12012	PASS	7451	PASS
2	**Line 1**	8023	PASS	11567	PASS	7809	PASS	11553	PASS	7797	PASS	11597	PASS
	Line 2	8757	PASS	10201	PASS	8737	PASS	10196	PASS	8733	PASS	10209	PASS
	Line 3	11920	PASS	7378	PASS	12394	PASS	7374	PASS	12383	PASS	7375	PASS
3	**Line 1**	8282	PASS	11199	PASS	8168	PASS	11221	PASS	8162	PASS	11166	PASS
	Line 2	8263	PASS	11096	PASS	8127	PASS	11074	PASS	8122	PASS	11084	PASS
	Line 3	12193	PASS	7231	PASS	12675	PASS	7209	PASS	12669	PASS	7254	PASS
4	**Line 1**	8750	PASS	10259	PASS	8734	PASS	10260	PASS	8736	PASS	10285	PASS
	Line 2	8036	PASS	11628	PASS	7793	PASS	11639	PASS	7796	PASS	11689	PASS
	Line 3	12000	PASS	7373	PASS	12465	PASS	7359	PASS	12489	PASS	7387	PASS
5	**Line 1**	9418	PASS	9463	PASS	9541	PASS	9454	PASS	9537	PASS	9448	PASS
	Line 2	7755	PASS	12034	PASS	7443	PASS	12027	PASS	7464	PASS	12002	PASS
	Line 3	11572	PASS	7432	PASS	12052	PASS	7436	PASS	12037	PASS	7445	PASS

Table H.11: ULS Checks for Arrangement 2, Load Case 2 - Normal Safety Class

Direction Number	Line Number	T1		T2		T3		T4		T5		T6	
		T_d [kN]	$S_c > T_d$	T_d [kN]	$S_c > T_d$	T_d [kN]	$S_c > T_d$	T_d [kN]	$S_c > T_d$	T_d [kN]	$S_c > T_d$	T_d [kN]	$S_c > T_d$
0	**Line 1**	8109	PASS	11770	PASS	7844	PASS	11764	PASS	7866	PASS	11693	PASS
	Line 2	10291	PASS	8562	PASS	10540	PASS	8557	PASS	10527	PASS	8525	PASS
	Line 3	10291	PASS	8573	PASS	10541	PASS	8567	PASS	10526	PASS	8570	PASS
1	**Line 1**	8202	PASS	11376	PASS	8091	PASS	11502	PASS	8019	PASS	11376	PASS
	Line 2	9336	PASS	9450	PASS	9420	PASS	9439	PASS	9385	PASS	9434	PASS
	Line 3	11139	PASS	8009	PASS	11567	PASS	8073	PASS	11443	PASS	7990	PASS
2	**Line 1**	8586	PASS	11045	PASS	8304	PASS	11006	PASS	8346	PASS	11093	PASS
	Line 2	8951	PASS	10058	PASS	8902	PASS	10063	PASS	8923	PASS	10007	PASS
	Line 3	11361	PASS	7933	PASS	11568	PASS	7951	PASS	11611	PASS	8003	PASS
3	**Line 1**	8652	PASS	10561	PASS	8521	PASS	10549	PASS	8515	PASS	10516	PASS
	Line 2	8575	PASS	10573	PASS	8517	PASS	10607	PASS	8512	PASS	10613	PASS
	Line 3	11410	PASS	7742	PASS	11640	PASS	7752	PASS	11634	PASS	7745	PASS
4	**Line 1**	8938	PASS	9958	PASS	8925	PASS	9971	PASS	8953	PASS	10030	PASS
	Line 2	8363	PASS	10950	PASS	8255	PASS	10889	PASS	8233	PASS	11127	PASS
	Line 3	11334	PASS	7881	PASS	11585	PASS	7874	PASS	11642	PASS	7876	PASS
5	**Line 1**	9412	PASS	9467	PASS	9463	PASS	9426	PASS	9434	PASS	9420	PASS
	Line 2	8184	PASS	11517	PASS	7968	PASS	11393	PASS	7975	PASS	11484	PASS
	Line 3	11250	PASS	8003	PASS	11364	PASS	7977	PASS	11407	PASS	8006	PASS

Table H.12: ULS Checks for Arrangement 2, Load Case 3 - Normal Safety Class

Direction Number	Line Number	T1		T2		T3		T4		T5		T6	
		T_d [kN]	$S_c > T_d$	T_d [kN]	$S_c > T_d$	T_d [kN]	$S_c > T_d$	T_d [kN]	$S_c > T_d$	T_d [kN]	$S_c > T_d$	T_d [kN]	$S_c > T_d$
0	**Line 1**	7694	PASS	12820	PASS	7387	PASS	12815	PASS	7391	PASS	12746	PASS
	Line 2	10926	PASS	8355	PASS	11241	PASS	8351	PASS	11261	PASS	8325	PASS
	Line 3	10902	PASS	8343	PASS	11238	PASS	8339	PASS	11236	PASS	8373	PASS
1	**Line 1**	7953	PASS	12365	PASS	7690	PASS	12400	PASS	8556	PASS	12487	PASS
	Line 2	9547	PASS	9705	PASS	9621	PASS	9661	PASS	10653	PASS	9700	PASS
	Line 3	12091	PASS	7640	PASS	12411	PASS	7664	PASS	12395	PASS	7658	PASS
2	**Line 1**	8091	PASS	11936	PASS	7894	PASS	11882	PASS	7889	PASS	11799	PASS
	Line 2	8855	PASS	10473	PASS	8934	PASS	10432	PASS	8893	PASS	10491	PASS
	Line 3	12192	PASS	7412	PASS	12543	PASS	7400	PASS	12636	PASS	7414	PASS
3	**Line 1**	8471	PASS	11285	PASS	8340	PASS	11307	PASS	8334	PASS	11297	PASS
	Line 2	8379	PASS	11241	PASS	8345	PASS	11354	PASS	8341	PASS	11209	PASS
	Line 3	12365	PASS	7323	PASS	12833	PASS	7404	PASS	12827	PASS	7335	PASS
4	**Line 1**	8937	PASS	10493	PASS	9021	PASS	10394	PASS	8999	PASS	10569	PASS
	Line 2	8053	PASS	11955	PASS	7919	PASS	11922	PASS	7936	PASS	11965	PASS
	Line 3	12310	PASS	7407	PASS	12542	PASS	7419	PASS	12699	PASS	7446	PASS
5	**Line 1**	9557	PASS	9697	PASS	9708	PASS	9791	PASS	9759	PASS	9749	PASS
	Line 2	7775	PASS	12338	PASS	7631	PASS	12278	PASS	7629	PASS	12343	PASS
	Line 3	11926	PASS	7577	PASS	12271	PASS	7619	PASS	12287	PASS	7702	PASS

H.3 Arrangement 3

H.3.1 High Safety Class

Table H.13: ULS Checks for Arrangement 3, Load Case 1 - High Safety Class

Direction Number	Line Number	T1		T2		T3		T4		T5	
		T_d [kN]	$S_c > T_d$	T_d [kN]	$S_c > T_d$	T_d [kN]	$S_c > T_d$	T_d [kN]	$S_c > T_d$	T_d [kN]	$S_c > T_d$
0	**Line 1**	9243	PASS	11496	PASS	15339	FAIL	11536	PASS	14398	FAIL
	Line 2	12956	PASS	9085	PASS	9887	PASS	14787	FAIL	10751	PASS
	Line 3	12966	PASS	14822	FAIL	9894	PASS	9081	PASS	9252	PASS
	Line 4									10739	PASS
1	**Line 1**	9481	PASS	13349	PASS	14648	FAIL	9887	PASS	13659	PASS
	Line 2	11270	PASS	8902	PASS	11566	PASS	15144	FAIL	9875	PASS
	Line 3	14068	FAIL	13261	PASS	9139	PASS	9911	PASS	9436	PASS
	Line 4									12215	PASS
2	**Line 1**	9612	PASS	14029	FAIL	13954	PASS	9358	PASS	12891	PASS
	Line 2	10547	PASS	8803	PASS	12399	PASS	14805	FAIL	9555	PASS
	Line 3	14338	FAIL	12370	PASS	8818	PASS	10594	PASS	9538	PASS
	Line 4									12952	PASS
3	**Line 1**	10065	PASS	14997	FAIL	13465	PASS	9201	PASS	12277	PASS
	Line 2	10070	PASS	9215	PASS	13565	PASS	14879	FAIL	10960	PASS
	Line 3	14983	FAIL	11530	PASS	8952	PASS	11671	PASS	9907	PASS
	Line 4									13939	PASS
4	**Line 1**	10646	PASS	15112	FAIL	12550	PASS	8933	PASS	11521	PASS
	Line 2	9675	PASS	9433	PASS	14017	FAIL	14220	FAIL	9275	PASS
	Line 3	14638	FAIL	10662	PASS	8915	PASS	12492	PASS	10261	PASS
	Line 4									14157	FAIL
5	**Line 1**	11448	PASS	15359	FAIL	11590	PASS	8823	PASS	10753	PASS
	Line 2	9408	PASS	9850	PASS	14881	FAIL	13358	PASS	9210	PASS
	Line 3	14259	FAIL	9872	PASS	9054	PASS	13435	PASS	10787	PASS
	Line 4									14428	FAIL

Table H.14: ULS Checks for Arrangement 3, Load Case 2 - High Safety Class

Direction Number	Line Number	T1		T2		T3		T4		T5	
		T_d [kN]	$S_c > T_d$	T_d [kN]	$S_c > T_d$	T_d [kN]	$S_c > T_d$	T_d [kN]	$S_c > T_d$	T_d [kN]	$S_c > T_d$
0	**Line 1**	9844	PASS	11445	PASS	14186	FAIL	11419	PASS	13635	PASS
	Line 2	12519	PASS	9810	PASS	10373	PASS	13914	PASS	11049	PASS
	Line 3	12520	PASS	13917	PASS	10389	PASS	9788	PASS	9868	PASS
	Line 4									11046	PASS
1	**Line 1**	10077	PASS	12921	PASS	13861	PASS	10374	PASS	13283	PASS
	Line 2	11439	PASS	9538	PASS	11425	PASS	14418	FAIL	10345	PASS
	Line 3	13719	PASS	12858	PASS	9758	PASS	10408	PASS	9952	PASS
	Line 4									12154	PASS
2	**Line 1**	10371	PASS	13322	PASS	13331	PASS	10153	PASS	12601	PASS
	Line 2	10912	PASS	9637	PASS	12156	PASS	14032	FAIL	10108	PASS
	Line 3	13703	PASS	12150	PASS	9636	PASS	10956	PASS	10119	PASS
	Line 4									12663	PASS
3	**Line 1**	10570	PASS	13867	PASS	12768	PASS	9820	PASS	12046	PASS
	Line 2	10451	PASS	9703	PASS	12703	PASS	13986	FAIL	9915	PASS
	Line 3	13819	PASS	11463	PASS	9697	PASS	11561	PASS	10351	PASS
	Line 4									13114	PASS
4	**Line 1**	10934	PASS	14029	FAIL	12157	PASS	9617	PASS	11509	PASS
	Line 2	10190	PASS	10045	PASS	13448	PASS	13391	PASS	9815	PASS
	Line 3	13730	PASS	10832	PASS	9762	PASS	12127	PASS	10719	PASS
	Line 4									13445	PASS
	Line 1	11358	PASS	14132	FAIL	11413	PASS	9514	PASS	11067	PASS
	Line 2	9884	PASS	10374	PASS	13802	PASS	12778	PASS	9789	PASS
	Line 3	13468	PASS	10363	PASS	9701	PASS	12767	PASS	11047	PASS

Table H.15: ULS Checks for Arrangement 3, Load Case 3 - High Safety Class

Direction Number	Line Number	T1		T2		T3		T4		T5	
		T_d [kN]	$S_c > T_d$	T_d [kN]	$S_c > T_d$	T_d [kN]	$S_c > T_d$	T_d [kN]	$S_c > T_d$	T_d [kN]	$S_c > T_d$
0	**Line 1**	9337	PASS	11733	PASS	15647	FAIL	11731	PASS	14883	FAIL
	Line 2	13299	PASS	9260	PASS	10136	PASS	15071	FAIL	11161	PASS
	Line 3	13270	PASS	15090	FAIL	10141	PASS	9268	PASS	9337	PASS
	Line 4									11165	PASS
1	**Line 1**	9558	PASS	13633	PASS	14993	FAIL	10106	PASS	14143	FAIL
	Line 2	11584	PASS	8893	PASS	11745	PASS	15432	FAIL	10153	PASS
	Line 3	14541	FAIL	13571	PASS	9160	PASS	10164	PASS	9524	PASS
	Line 4									12642	PASS
2	**Line 1**	9955	PASS	14395	FAIL	14431	FAIL	9681	PASS	13414	PASS
	Line 2	10742	PASS	9011	PASS	12739	PASS	15488	FAIL	9797	PASS
	Line 3	15015	FAIL	12720	PASS	9006	PASS	10888	PASS	9804	PASS
	Line 4									13501	PASS
3	**Line 1**	10386	PASS	15113	FAIL	13605	PASS	9175	PASS	12552	PASS
	Line 2	10272	PASS	9247	PASS	13616	PASS	15200	FAIL	9527	PASS
	Line 3	15247	FAIL	11784	PASS	8927	PASS	11799	PASS	10177	PASS
	Line 4									14106	FAIL
4	**Line 1**	10889	PASS	15514	FAIL	12737	PASS	8978	PASS	11805	PASS
	Line 2	9862	PASS	11196	PASS	14692	FAIL	14578	FAIL	9356	PASS
	Line 3	15144	FAIL	11049	PASS	9059	PASS	12806	PASS	10643	PASS
	Line 4									14789	FAIL
5	**Line 1**	11663	PASS	15798	FAIL	11798	PASS	8924	PASS	11130	PASS
	Line 2	9477	PASS	10216	PASS	15356	FAIL	13806	PASS	9325	PASS
	Line 3	14925	FAIL	10198	PASS	9241	PASS	13825	PASS	11147	PASS
	Line 4									15122	FAIL

H.3.2 Normal Safety Class

Table H.16: ULS Checks for Arrangement 3, Load Case 1 - Normal Safety Class

Direction Number	Line Number	T1		T2		T3		T4		T5	
		T_d [kN]	$S_c > T_d$	T_d [kN]	$S_c > T_d$	T_d [kN]	$S_c > T_d$	T_d [kN]	$S_c > T_d$	T_d [kN]	$S_c > T_d$
0	**Line 1**	7626	PASS	9466	PASS	12610	PASS	9498	PASS	11839	PASS
	Line 2	10643	PASS	7480	PASS	8144	PASS	12160	PASS	8859	PASS
	Line 3	10652	PASS	12189	PASS	8149	PASS	7476	PASS	7618	PASS
	Line 4									8849	PASS
1	**Line 1**	7819	PASS	10985	PASS	12050	PASS	8143	PASS	11239	PASS
	Line 2	9277	PASS	7326	PASS	9522	PASS	12455	PASS	8134	PASS
	Line 3	11550	PASS	10915	PASS	7522	PASS	8163	PASS	7769	PASS
	Line 4									10059	PASS
2	**Line 1**	7929	PASS	11542	PASS	11482	PASS	7709	PASS	10612	PASS
	Line 2	8690	PASS	7250	PASS	10207	PASS	12179	PASS	7871	PASS
	Line 3	11769	PASS	10184	PASS	7262	PASS	8726	PASS	7858	PASS
	Line 4									10661	PASS
3	**Line 1**	8296	PASS	12328	PASS	11077	PASS	7572	PASS	10107	PASS
	Line 2	8300	PASS	7583	PASS	11158	PASS	12234	PASS	9089	PASS
	Line 3	12286	PASS	9493	PASS	7366	PASS	9606	PASS	8160	PASS
	Line 4									11462	PASS
4	**Line 1**	8768	PASS	12423	PASS	10327	PASS	7354	PASS	9488	PASS
	Line 2	7979	PASS	7768	PASS	11532	PASS	11694	PASS	7638	PASS
	Line 3	12007	PASS	8780	PASS	7339	PASS	10281	PASS	8454	PASS
	Line 4									11641	PASS
5	**Line 1**	9418	PASS	12626	PASS	9541	PASS	7263	PASS	8860	PASS
	Line 2	7761	PASS	8114	PASS	12235	PASS	10993	PASS	7585	PASS
	Line 3	11702	PASS	8132	PASS	7455	PASS	11054	PASS	8887	PASS
	Line 4									11863	PASS

Table H.17: ULS Checks for Arrangement 3, Load Case 2 - Normal Safety Class

Direction Number	Line Number	T1		T2		T3		T4		T5	
		T_d [kN]	$S_c > T_d$	T_d [kN]	$S_c > T_d$	T_d [kN]	$S_c > T_d$	T_d [kN]	$S_c > T_d$	T_d [kN]	$S_c > T_d$
0	**Line 1**	8109	PASS	9421	PASS	11667	PASS	9400	PASS	11212	PASS
	Line 2	10291	PASS	8067	PASS	8535	PASS	11443	PASS	9096	PASS
	Line 3	10291	PASS	11445	PASS	8549	PASS	8049	PASS	8115	PASS
	Line 4									9094	PASS
1	**Line 1**	8297	PASS	10630	PASS	11401	PASS	8536	PASS	10923	PASS
	Line 2	9408	PASS	7843	PASS	9405	PASS	11852	PASS	8513	PASS
	Line 3	11264	PASS	10579	PASS	8025	PASS	8564	PASS	8187	PASS
	Line 4									10001	PASS
2	**Line 1**	8537	PASS	10960	PASS	10967	PASS	8349	PASS	10368	PASS
	Line 2	8979	PASS	7925	PASS	10004	PASS	11541	PASS	8318	PASS
	Line 3	11256	PASS	9999	PASS	7924	PASS	9015	PASS	8327	PASS
	Line 4									10418	PASS
3	**Line 1**	8701	PASS	11405	PASS	10508	PASS	8074	PASS	9915	PASS
	Line 2	8603	PASS	7981	PASS	10457	PASS	11500	PASS	8158	PASS
	Line 3	11351	PASS	9436	PASS	7970	PASS	9514	PASS	8519	PASS
	Line 4									10788	PASS
4	**Line 1**	9000	PASS	11539	PASS	10005	PASS	7909	PASS	9474	PASS
	Line 2	8389	PASS	8264	PASS	11061	PASS	11015	PASS	8075	PASS
	Line 3	11278	PASS	8916	PASS	8024	PASS	9981	PASS	8822	PASS
	Line 4									11058	PASS
5	**Line 1**	9347	PASS	11625	PASS	9396	PASS	7825	PASS	9111	PASS
	Line 2	8140	PASS	8536	PASS	11354	PASS	10516	PASS	8052	PASS
	Line 3	11067	PASS	8527	PASS	7980	PASS	10508	PASS	9095	PASS
	Line 4									11073	PASS

Table H.18: ULS Checks for Arrangement 3, Load Case 3 - Normal Safety Class

Direction Number	Line Number	T1		T2		T3		T4		T5	
		T_d [kN]	$S_c > T_d$	T_d [kN]	$S_c > T_d$	T_d [kN]	$S_c > T_d$	T_d [kN]	$S_c > T_d$	T_d [kN]	$S_c > T_d$
0	**Line 1**	7694	PASS	9657	PASS	12863	PASS	9656	PASS	12238	PASS
	Line 2	10926	PASS	7615	PASS	8340	PASS	12395	PASS	9189	PASS
	Line 3	10902	PASS	12409	PASS	8344	PASS	7621	PASS	7680	PASS
	Line 4									9192	PASS
1	**Line 1**	7873	PASS	11218	PASS	12332	PASS	8316	PASS	11633	PASS
	Line 2	9528	PASS	7315	PASS	9667	PASS	12692	PASS	8355	PASS
	Line 3	11939	PASS	11170	PASS	7536	PASS	8363	PASS	7834	PASS
	Line 4									10400	PASS
2	**Line 1**	8197	PASS	11842	PASS	11870	PASS	7962	PASS	11035	PASS
	Line 2	8842	PASS	7412	PASS	10483	PASS	12732	PASS	8060	PASS
	Line 3	12323	PASS	10468	PASS	7408	PASS	8960	PASS	8066	PASS
	Line 4									11104	PASS
3	**Line 1**	8548	PASS	12428	PASS	11196	PASS	7547	PASS	10332	PASS
	Line 2	8455	PASS	7605	PASS	11206	PASS	12497	PASS	7836	PASS
	Line 3	12512	PASS	9698	PASS	7341	PASS	9710	PASS	8374	PASS
	Line 4									11605	PASS
4	**Line 1**	8962	PASS	12753	PASS	10482	PASS	7385	PASS	9718	PASS
	Line 2	8120	PASS	9274	PASS	12079	PASS	11988	PASS	7696	PASS
	Line 3	12427	PASS	9088	PASS	7450	PASS	10537	PASS	8761	PASS
	Line 4									12157	PASS
5	**Line 1**	9593	PASS	12984	PASS	9709	PASS	7340	PASS	9164	PASS
	Line 2	7806	PASS	8404	PASS	12621	PASS	11357	PASS	7670	PASS
	Line 3	12247	PASS	8390	PASS	7600	PASS	11372	PASS	9178	PASS
	Line 4									12428	PASS

BIBLIOGRAPHY

[1] 4C OFFSHORE, *Hywind scotland pilot park offshore wind farm*. http://www.4coffshore.com/windfarms/hywind-scotland-pilot-park-united-kingdom-uk76.html, 2017.

[2] C. BAK, F. ZAHLE, R. BITSCHE, T. KIM, A. YDE, L. C. HENRIKSEN, M. H. HANSEN, AND A. NATARAJAN, *Description of the DTU 10 MW reference wind turbine*, tech. rep., DTU Vindenergi, 2013.

[3] W. BIERBOOMS, *Lecture Slides for OE5662 Offshore Wind Farm Design: Lecture 4b Offshore Wind Farm Aspects*, 2017.

[4] H. BREDMOSE, *Lecture Slides for 46211 Offshore Wind Energy: Lecture 9 Wind-wave climates, Simple wind forcing model*, 2016.

[5] K. S. CHAKRABARTI, *Handbook of Offshore Engineering Volume II*, Elsevier, Plainfield, IL, 1st ed., 2005.

[6] B. D. DIAZ, M. RASULO, C. AUBENY, C. FONTANA, S. R. ARWADE, D. J. DEGROOT, AND M. LANDON, *Multiline anchors for floating offshore wind towers*, 09 2016.

[7] DNV, *DNV-OS-E301 Position Mooring*, 2010.

[8] ——, *DNV-RP-C205 Environmental Conditions and Environmental Loads*, 2010.

[9] ——, *DNV-OS-J101 Design of Offshore Wind Turbine Structures*, 2013.

[10] ——, *DNV-OS-J103 Design of Floating Wind Turbine Structures*, 2013.

[11] C. FONTANA, S. T. HALLOWELL, S. R. ARWADE, D. J. DEGROOT, M. E. LANDON, C. AUBENY, B. DIAZ, A. T. MYERS, AND S. OZMUTLU, *Multiline anchor force dynamics in floating offshore wind turbines*, (2018).

[12] C. FONTANA, S. R. ARWADE, D. J. DEGROOT, A. T. MYERS, M. E. LANDON, AND C. AUBENY, *Efficient Multiline Anchor Systems for Floating Offshore Wind Turbines*, no. OMAE2016-54476, OMAE, 2016.

[13] FUGRO GEOS, *Wind and wave frequency distributions for sites around the British Isles*, tech. rep., Fugro GEOS, 2001.

[14] F. GONZALEZ-LONGATT, P. WALL, AND V. TERZIJA, *Wake effect in Wind Farm Performance: Steady-State and Dynamic Behaviour*, 39 (2012), p. 329–338.

[15] M. GRECO, *Lecture Notes to TMR 4215: Sea Loads, year = 2017, publisher = Norwegian University of Science and Technology, Department of Marine Technology*.

[16] M. HALL AND P. CONNOLLY, *Coupled Dynamics Modelling of a Floating Wind Farm With Shared Mooring Lines*, no. OMAE2018-78489, OMAE, 2018.

[17] S. T. HALLOWELL, S. R. ARWADE, C. M. FONTANA, D. J. DEGROOT, B. D. DIAZ, AND M. E. LANDON, *Reliability of Mooring Lines and Shared Anchors of Floating Offshore Wind Turbines*, no. ISOPE-I-17-441, International Society of Offshore and Polar Engineers, 2017.

[18] M. HERDUIN, C. GAUDIN, M. J. CASSIDY, C. O'LOUGHLIN, AND J. HAMBLETON, *Multi-Directional Load Cases on Shared Anchors for Arrays of Floating Structures*, Asian Wave and Tidal Energy Conference, 2016.

[19] K. B. HOLE, *Design of Mooring Systems for Large Floating Wind Turbines in Shallow Water*, Norwegian University of Science and Technology, Department of Marine Technology, 2018.

[20] W. HSU, K. THIAGARAJAN, AND L. MANUEL, *Snap loads on mooring lines of a floating offshore wind turbine structure*, no. OMAE2014-23587, OMAE, 2014.

[21] INTERNATIONAL ELECTROTECHNICAL COMMISSION, *IEC 61400-1 International Standard Wind turbines – Part 1: Design requirements* , 2005.

[22] N. O. JENSEN, *A Note on Wind Generator Interaction*, tech. rep., Risø National Laboratory, Roskilde, Denmark, 1983.

[23] T. JIMENEZ, D. KEYSER, AND S. TEGEN, *Floating Offshore Wind in Hawaii: Potential for Jobs and Economic Impacts from Two Future Scenarios* , tech. rep., NREL, 2016.

[24] K. JOHANNESSEN, T. STOKKA MELING, AND S. HAVER, *Joint distribution for wind and waves in the northern north sea*, 12 (2002).

[25] J. M. J. JOURNÉE, W. W. MASSIE, AND R. H. M. HUIJSMANS, *Offshore hydromechanics*, tech. rep., Delft University of Technology, 2015.

[26] G. KATSOURIS AND A. MARINA, *Cost Modelling of Floating Wind Farms*, tech. rep., ECN, 2016.

[27] N. KELLEY AND B. J. JONKMAN, *Overview of the TurbSim Stochastic Inflow Turbulence Simulator*, tech. rep., NREL, 2007.

[28] L. LI, Z. GAO, AND T. MOAN, *Joint environmental data at five european offshore sites for design of combined wind and wave energy devices*, 137 (2013).

[29] Y. LIU, *2.019 Design of Ocean Systems: Mooring Dynamics (II)*, MIT OpenCourseWare.

[30] J. F. MANWELL, J. G. MCGOWAN, AND A. L. ROGERS, *WIND ENERGY EXPLAINED: Theory, Design and Application*, Wiley, 2nd ed., 2005.

[31] S. OCEAN, *SIMA User Guide*, tech. rep., SINTEF Ocean, 2017.

[32] M. RANDOLPH AND S. GOURVENEC, *Offshore Geotechnical Engineering*, Spon Press, University of Western Australia, 2011.

[33] J. RINGSBERG, H. JANSSON, M. ÖRGÅRD, S.-H. YANG, AND E. JOHNSON, *Comparison of Mooring Solutions and Array Systems for Point Absorbing Wave Energy Devices*, no. OMAE2018-77062, OMAE, 06 2018.

[34] K. ROSCOE, S. CAIRES, F. DIERMANSE, AND J. GROENEWEG, *Extreme offshore wave statistics in the North Sea*, vol. 133, 05 2010, pp. 47–58.

[35] R. SNELL, R. V. AHILAN, AND T. VERSAVEL, *Reliability of Mooring Systems: Application to Polyester Moorings*, no. OTC 10777, OTC, 05 1989.

[36] STATOIL ASA, *World's first floating wind farm has started production*.
`https://www.statoil.com/en/news/worlds-first-floating-wind-farm-started-production.html`, 2017.
Accessed: 2017-10-12.

[37] S. WELLER, P. DAVIES, A. VICKERS, AND L. JOHANNING, *Synthetic rope responses in the context of load history: The influence of aging.*, 96 (2015).

[38] WINDEUROPE, *Wind in power: 2016 European statistics*, 2017.

[39] ——, *EU agrees 32% renewable energy target for 2030*, 2018.

[40] ——, *The European offshore wind industry: Key trends and statistics 2017*, 2018.

[41] W. XUE, *Design, numerical modelling and analysis of a spar floater supporting the DTU10MW wind turbine*, 2016.